Research Square

Preprints are preliminary reports that have not undergone peer review.
They should not be considered conclusive, used to inform clinical practice,
or referenced by the media as validated information.

Identification of marker genes and signaling pathways associated with amyotrophic lateral sclerosis using bioinformatics analysis of RNA sequencing data

Basavaraj Mallikarjunayya Vastrad
Nesmatrix Private Limited, Gadag, 582101, Karanataka, India https://orcid.org/0000-0003-2202-7637
Shivaling Pattanashetti
Nesmatrix Private Limited, Gadag, 582101, Karanataka, India https://orcid.org/0009-0003-9246-1604
Siddalingeshwar Patil
Nesmatrix Private Limited, Gadag, 582101, Karanataka, India https://orcid.org/0009-0000-2685-2760
Chanabasayya Vastrad
channu.vastrad@gmail.com

Biostatistics and Bioinformatics, Chanabasava Nilaya, Bharthinagar, Dharwad 580001, Karnataka, India.
https://orcid.org/0000-0003-3615-4450

Research Article

Keywords: Bioinformatics analysis, Biomarker, Differentially expressed genes, Amyotrophic lateral sclerosis, protein-protein interaction network

Posted Date: June 18th, 2026

DOI: https://doi.org/10.21203/rs.3.rs-10064327/v1

License: This work is licensed under a Creative Commons Attribution 4.0 International License.
Read Full License

Additional Declarations: The authors declare no competing interests.

Identification of marker genes and signaling pathways associated with amyotrophic lateral sclerosis using bioinformatics analysis of RNA sequencing data

Basavaraj Vastrad[1], Shivaling Pattanashetti[1], Siddalingeshwar Patil[1], Chanabasayya Vastrad*[2]

1, Nesmatrix Private Limited, Gadag, 582101, Karanataka, India

2. Biostatistics and Bioinformatics, Chanabasava Nilaya, Bharthinagar, Dharwad 580001, Karnataka, India.

* Chanabasayya Vastrad

channu.vastrad@gmail.com

Ph: +919480073398

Chanabasava Nilaya, Bharthinagar,

Dharwad 580001 , Karanataka, India

Abstract

Amyotrophic lateral sclerosis (ALS), is a global disease that is a leading cause of neurodegenerative condition that affects motor neurons. However, the etiology of ALS remains poorly understood. The genes responsible for the pathogenesis of ALS have not been fully identified. The present study aimed to explore new genes of ALS by mining the ALS RNA sequencing data. RNA sequencing data (GSE277709) in the Gene Expression Omnibus (GEO) database were analysed to identify the differentially expressed genes (DEGs) (ALS vs. normal control) using bioinformatics methods. The DEGs were subjected to Gene Ontology (GO) functional enrichment and REACTOME pathway enrichment, and the protein-protein interaction (PPI) networks and functional modules were constructed to screen the hub genes. Then, the microRNAs (miRNAs) and transcription factors (TF) in ALS were screened out from the the miRNet and NetworkAnalyst database. Potential drug targets for ALS were obtained from the DrugBank database. MiRNA-hub gene regulatory network, TF-hub gene regulatory network and drug-hub gene interaction network were constructed by Cytoscape software. Finally, receiver operating characteristic (ROC) curve assess the diagnostic value of hub genes. There exist strong correlations among samples of ALS and normal control group. There was a total of 958 DEGs, including 479 up-regulated genes and 479 down-regulated genes. GO were significantly enriched in multicellular organismal process, primary metabolic process, cell periphery, intracellular membraneless organelle, signaling receptor and transmembrane transporter activity. Enrichment Analysis of REACTOME indicated that the top pathways were extracellular matrix organization and sensory perception. Hub genes EGFR, FN1, CAV1, BCAR1, YAP1, POU5F1, TTYH1, ACTA1, GPR17 and TF were identified form PPI network and modules. The MiRNA-hub gene regulatory network and TF-hub gene regulatory network showed that hsa-miR-6874-5p, hsa-miR-561-5p, GATA2 and SRF might play an important role in the ALS. By analyzing drug-hub gene interaction network, we pridicted drug molecules such as Lormetazepam and Medazepam for ALS treatment. These hub demonstrated strong diagnostic values. The study highlights the potential impact of EGFR, FN1, CAV1, BCAR1, YAP1, POU5F1, TTYH1, ACTA1, GPR17 and TF on the

development and progression of ALS, supporting their role as potential biomarkers.

Keywords: Bioinformatics analysis; Biomarker; Differentially expressed genes; Amyotrophic lateral sclerosis; protein-protein interaction network

Introduction

Amyotrophic lateral sclerosis (ALS), also called Lou Gehrig's disease is a neurodegenerative condition that affects motor neurons [Rizea et al. 2024]. ALS is the major causes of muscle weakness and muscle twitching that affect your ability to walk independently, reach for objects, chew food and talk [Grad et al. 2017]. ALS is estimated to affect worldwide around 223,000 in 2015 and are forecasted to reach 377,000 by 2040 [Arthur et al. 2016]. The etiology of ALS is multifactorial, and involves sports with a high incidence of concussions, military jobs, smoking, exposure to heavy metals (lead, manganese), pesticides, neurotoxins (cyanobacteria), and electromagnetic fields [Quinn et al. 2020]. Research points in ALS include genetic mutations, oxidative stress, excitotoxicity, mitochondrial and proteasomal dysfunctions, altered synaptic function, disturbed axonal transport, and neuroinflammation [Tzeplaeff et al. 2023]. Risk factors include obesity [Li et al. 2021], diabetes mellitus [Zhang et al. 2022], hypertension [Moreau et al. 2012], hyperlipidemia [Dedic et al. 2012], cardiovascular diseases [Abdel Magid et al. 2022], inflammation [Batty et al. 2023], oxidative stress [Motataianu et al. 2022], anxiety and depression [Larsson et al. 2023], cognitive dysfunction [Jellinger, 2023], respiratory failure [Niedermeyer et al. 2019] and stroke [Kwon et al. 2025]. However, the pathophysiologic mechanism underlying many ALS cases remains unclear, resulting in a lack of effective treatment [Ilieva et al. 2023]. Therefore, exploring the underlying molecular mechanism of ALS and searching for potential genes and signaling pathways involved in ALS are of great significance to human health.

Previous studies revealed that genes and signaling pathways are involved in ALS. Some genes and signaling pathways, such as C9ORF72 [van den Berg et al. 2024], SOD1 [Huang et al. 2024], TDP43 [Chong and Souayah, 2025], FUS [Moens et al. 2025], UBQLN2 [Thumbadoo et al. 2025], WNT signaling pathway [Jiang et al. 2021]. HMGB1 signaling pathway [Paudel et al. 2020], mitogen-

activated protein kinase signalingpathway [Sahana and Zhang, 2021], estrogen signaling pathway [Chowdhury et al. 2025] and PI3K/AKT signaling pathway [Qi et al. 2022] have been suggested to cause ALS. Notably, a substantial proportion of heritability is still lacking. One potential interpretation is that unidentified genes might partially link to the missing heritability. Therefore, there are still many related biomarkers and signaling pathways to be identified, which will help us better understand the molecular pathogenesis of ALS and facilitate the discovery of novel diagnostic biomarkers or therapeutic target.

RNA sequencing data analyses are important techniques in disease research and have been widely used to identify novel biomarkers and signaling pathways and improve the diagnosis and treatment of various diseases [Joshi et al. 2021; Prashanth et al. 2021]. Therefore, it is an important approach to explore and identify novel biomarkers and signaling pathways associated with ALS by screening for genes related to the onset and progression of ALS.

In this study, we analyzed the RNA sequencing data of GSE277709 [Kõks et al. 2021] from Gene Expression Omnibus (GEO) (available online: https://www.ncbi.nlm.nih.gov/geo) [Clough and Barrett, 2016] was downloaded to explore the molecular mechanism of ALS at both the gene expression level and expression regulation level. Differentially expressed genes (DEGs) were identified between ALS and normal control samples. In addition, the Gene Ontology (GO), REACTOME pathway enrichment analysis, protein-protein interaction (PPI) network, miRNA-hub gene regulatory network, TF-hub gene regulatory network, drug-hub gene interaction network and receiver operating characteristic (ROC) curve analysis were implemented to analyze the key differentially expressed genes, and the related molecular mechanisms were illuminated by this investigation. We aimed to explore new molecular biomarkers or potential therapeutic targets for ALS.

Materials and Methods

RNA-sequencing data source

We downloaded the RNA sequencing data GSE277709 [Kõks et al. 2021]from the GEO database with its platform as GPL24676 Illumina NovaSeq 6000 (Homo sapiens). A total of 84 samples were available, including 42 ALS samples from

whole blood of ALS patients and 42 normal control samples from whole blood of healthy controls.

Identification of DEGs

To assess DEGs, using the 'DESeq2' package [Love et al. 2014] of R software. The Benjamini and Hochberg (BH) method was performed to adjust P value to decrease the false positive error [Solari et al. 2017]. A gene was defined as a DEG between the ALS and normal control samples, when the adjust P value was < 0.05, and the gene expression fold change (FC) value was > 0.822 for up-regulated genes and the gene expression fold change (FC) value was < -1.379 for down-regulated genes, which were visualized as volcano plot and heat map. ggplot2 and gplot packages in R software was applied to generate volcano plot and heat map.

GO and pathway enrichment analyses of DEGs

The Gene Ontology (GO) (http://www.geneontology.org) [Thomas, 2017] is a bioinformatics tool providing a framework and set of concepts for describing the functions of gene products from all organisms. GO explains the three main categories: biological processes (BP), cell components (CC), and molecular functions (MF). REACTOME (https://reactome.org/) [Fabregat et al. 2018] is a database resource integrated the information of genomes, biological pathways, diseases and chemicals. To better understand the biological function and characteristics, g:Profiler (http://biit.cs.ut.ee/gprofiler/) [Reimand et al. 2007] was used to perform enrichment analysis. GO terms and REACTOME maps of biological functions associated with an adjusted P value < 0.05.

Construction of the PPI network and module analysis

All DEGs were analyzed using the online tool HIPPIE (Human Integrated Protein-Protein Interaction rEference) interactome (https://cbdm-01.zdv.uni-mainz.de/~mschaefer/hippie/network.php) [Alanis-Lobato et al. 2020]. The interaction information of all DEGs was downloaded and further modified by Cytoscaple software (http://www.cytoscape.org/) (v3.10.4) for better visualization [Ono et al. 2025]. Network Analyzer plugin is commonly used for significant gene identification (hub genes), and the hub genes in the PPI network were determined by four algorithms, namely, node degree [Luo et al. 2017], betweenness [Li et al.

2017], stress [Gilbert et al. 2021] and closeness [Li et al. 2020]. The significant gene modules were identified by PEWCC Cytoscape plug-in [Zaki et al. 2013].

Construction of the miRNA-hub gene regulatory network

The target miRNAs of the hub genes were predicted by miRNet database (https://www.mirnet.ca/) [Fan et al 2018]. MiRNAs that were found in databases (TarBase, miRTarBase, miRecords, miRanda (S mansoni only), miR2Disease, HMDD, PhenomiR, SM2miR, PharmacomiR, EpimiR, starBase, TransmiR, ADmiRE, and TAM 2.0) were selected as the target miRNAs, and a visual miRNA-hub gene regulatory network was constructed according to the targeting relationship between the hub genes and miRNAs using Cytoscape software [Ono et al. 2025].

Construction of the TF-hub gene regulatory network The target TFs of the hub genes were predicted by NetworkAnalyst database (https://www.networkanalyst.ca/) [Zhou et al 2019]. TFs that were found in database (JASPAR) were selected as the target TFs, and a visual TF-hub gene regulatory network was constructed according to the targeting relationship between the hub genes and TFs using Cytoscape software [Ono et al. 2025].

Construction of the drug-hub gene interaction network

The drug molecules of the hub genes were predicted by NetworkAnalyst database (https://www.networkanalyst.ca/) [Zhou et al 2019]. Drug molecules that were found in database (DrugBank) were selected as the target drug molecules, and a visual drug-hub gene interaction network was constructed according to the targeting relationship between the hub genes and drug molecules using Cytoscape software [Ono et al. 2025].

Receiver operating characteristic (ROC) curves analysis

Validation dataset was retrieved from GEO database to verify hub gene expression differences in ALS and normal control samples. The ROC curves were constructed using the pROC package [Robin et al. 2011], with area under the curve (AUC) values determined to evaluate diagnostic performance of hub genes. Higher AUC indicates better diagnostic performance of hub genes. Usually, an AUC value of >0.8 indicated excellent diagnostic value.

Results

Identification of DEGs

A total of 958 DEGs were screened from the GSE277709 RNA sequencing dataset with fold change (FC) value was > 0.822 for up-regulated genes and the gene expression fold change (FC) value was < -1.379 for down-regulated genes, and adj $P < 0.05$), including 479 up-regulated and 479 down-regulated genes (Table 1). Fig. 1 shows the volcano plots of the DEGs. In Fig. 2, the heatmap displayed the DEGs that were up-and down-regulated between ALS group and the normal control group.

GO and pathway enrichment analyses of DEGs

To elucidate the biological significance of the DEGs, we performed comprehensive functional enrichment analyses. The GO enrichment analysis revealed that these genes were significantly enriched BP: multicellular organismal process, response to stimulus, primary metabolic process and biosynthetic process (Table 2). The CC analysis revealed predominant associations with cell periphery, plasma membrane, intracellular membraneless organelle and organelle lumen (Table 2). The MF analysis identified key roles in signaling receptor binding, cell adhesion molecule binding, transmembrane transporter activity and metal ion transmembrane transporter activity (Table 2). The enriched terms for each GO category are visually summarized in Fig.3 - Fig.4. The REACTOME pathway enrichment analysis further indicated significant enrichment in major pathways: extracellular matrix organization, ECM proteoglycans, sensory perception and neuronal system (Table 3). Fig.3 - Fig.4 illustrates the five most statistically significant enriched pathways based on adj p-values.

Construction of the PPI network and module analysis

A total of 958 DEGs were subjected to PPI network analysis using the HIPPIE database. The analysis was performed with default parameters, yielding a network comprising 8576 interconnected nodes and 19922 edges after excluding unconnected protein nodes. In the HIPPIE -generated PPI network, nodes represent genes, while edges indicate functional interactions between them. The PPI network was subsequently visualized and analyzed using Cytoscape software (Fig. 5). The

hub genes were identified using the cytoHubba plugin in Cytoscape, employing four algorithms: node degree, betweenness, stress and closeness. Integrating these results identified hub genes: EGFR, FN1, CAV1, BCAR1, YAP1, POU5F1, TTYH1, ACTA1, GPR17 and TF (Table 4). We further used the PEWCC plugin to identify the gene cluster modules according to the filter criteria, and the results showed that two significant modules were identified. Module 1 had 79 nodes and 119 edges (Fig. 6). GO term and pathway enrichment analysis showed that the genes in this module was extracellular matrix organization, diseases of glycosylation, axon guidance, ECM proteoglycans, regulation of insulin-like growth factor (IGF) transport and uptake by insulin-like growth factor Binding proteins (IGFBPs), signal transduction, multicellular organismal process, response to stimulus and cell periphery (Fig. 7). Module 2 had 61 nodes and 77 edges (Fig. 8). GO term and pathway enrichment analysis showed that the genes in this module was neuronal system and transmission across chemical synapses (Fig. 9).

Construction of the miRNA-hub gene regulatory network

MiRNAs have been reported to control gene levels by binding to the target mRNA and play a key role in disease progression [Cheng et al. 2023]. We constructed a regulatory network of hub genes and miRNAs by Cytoscape, which comprised 2753 nodes [hub gene:407, miRNA: 2346] and 40543 edges (Fig. 10). CCND1 was predicted to be regulated by 543 miRNAs (ex; hsa-miR-6874-5p), FN1 was predicted to be regulated by 366 miRNAs (ex; hsa-miR-1307-3p), TJP1 was predicted to be regulated by 346 miRNAs (ex; hsa-miR-153-3p), YAP1 was predicted to be regulated by 315 miRNAs (ex; hsa-miR-92b-3p), IGF2BP1 was predicted to be regulated by 295 miRNAs (ex; hsa-miR-7160-3p), NCAPG was predicted to be regulated by 172 miRNAs (ex; hsa-miR-561-5p), TMEM132A was predicted to be regulated by 122 miRNAs (ex; hsa-miR-23a-3p), ACTN2 was predicted to be regulated by 117 miRNAs (ex; hsa-miR-6887-3p), HNRNPA1L2 was predicted to be regulated by 112 miRNAs (ex; hsa-miR-7157-3p) and TF was predicted to be regulated by 110 miRNAs (ex; hsa-miR-152-3p) (Table 5).

Construction of the TF-hub gene regulatory network

TFs have been reported to control gene levels by binding to the target gene and play a key role in disease progression [Morimoto et al. 2012]. We constructed a

regulatory network of hub genes and TFs by Cytoscape, which comprised 478 nodes [hub gene: 82, TF: 396] and 3042 edges (Fig. 11). BCAR1 was predicted to be regulated by 28 TFs (ex; GATA2), CAV1 was predicted to be regulated by 16 TFs (ex; SREBF1), FN1 was predicted to be regulated by 14 TFs (ex; RELA), FLNC was predicted to be regulated by 12 TFs (ex; GATA3), IGF2BP1 was predicted to be regulated by 12 TFs (ex; MAX), SLC6A15 was predicted to be regulated by 16 TFs (ex; SRF), POU5F1 was predicted to be regulated by 11 TFs (ex; IRF2), HNRNPA1L2 was predicted to be regulated by 11 TFs (ex; MEF2A), ACTN2 was predicted to be regulated by 11 TFs (ex; USF2) and CTNNA3 was predicted to be regulated by 10 TFs (ex; YY1) (Table 5).

Construction of the drug-hub gene interaction network

Drug molecules have been reported to control protein levels by binding to the target protein [Morimoto et al. 2012]. We constructed a regulatory network of hub genes and drug molecules by Cytoscape (Fig.12 and Fig.13). Up-regulated genes such as GABRE was predicted to be targeted by 76 drug molecules (ex; Lormetazepam), F10 was predicted to be targeted by 70 drug molecules (ex; Lonoctocog alfa), MET was predicted to be targeted by 34 drug molecules (ex; Capmatinib), PDGFRB was predicted to be targeted by 28 drug molecules (ex; Becaplermin), GRIA1 was predicted to be targeted by 19 drug molecules (ex; Perampanel) (Table 6), while down-regulated genes such as GABRG2 was predicted to be targeted by 86 drug molecules (ex; Medazepam), DRD4 was predicted to be targeted by 40 drug molecules (ex; Cabergoline), GRIN2B was predicted to be targeted by 39 drug molecules (ex; Taurine), CHRNB2 was predicted to be targeted by 26 drug molecules (ex; Physostigmine) and TF was predicted to be targeted by 17 drug molecules (ex; Ferrous succinate) (Table 6).

Receiver operating characteristic (ROC) curves analysis

The ROC curve was used to measure the diagnostic value of hub genes. The diagnostic value of hub genes in recognizing ALS from normal control presented excellent diagnostic value with AUC of 0.891 in EGFR, AUC of 0. 913 in FN1, AUC of 0. 908 in CAV1, AUC of 0. 898 in BCAR1, AUC of 0. 894 in YAP1, AUC of 0. 890 in POU5F1, AUC of 0. 907 in TTYH1, AUC of 0. 917 in ACTA1, AUC of 0. 916 in GPR17 and AUC of 0. 895 in TF (Fig.14).

Discussion

ALS still is a severe disease which is hard to diagnosed and continuously makes patients and social suffering. The rapid advancement of RNA sequencing technology and bioinformatics could provide more references for finding diagnostic biomarkers and prognostic suggestions for diseases.

In our investigation, GSE277709, a RNA sequencing data which downloaded from the NCBI-GEO database, was used to explore potential biomarkers and molecular mechanisms of ALS. Firstly, 958 DEGs (479 up-regulated genes and 479 down-regulated genes) between ALS groups and normal control groups were screened out. IGFBP5 [Albrethsen et al. 2025] and MMP2 [Fang et al. 2010] might involve in the pathogenesis of ALS. Studies have shown that COL1A2 [Pan et al. 2010], GREM1 [Atak et al. 2026], DCN (decorin) [Bolton et al. 2008], MMP2 [Belo et al. 2015] and RSC1A1 [Osswald et al. 2005] are altered expressed in patients with obesity. GREM1 [Mitroi et al. 2022], DCN (decorin) [Chen et al. 2020], STC2 [Gude et al. 2023], MMP2 [Arreguin-Cano et al. 2019] and TNFRSF11B [Biscetti et al. 2014] were a risk factors for the pathogenesis of diabetes mellitus. Altered expression of IGFBP5 [Lee et al. 2013], COL1A2 [Tian et al. 2016], GREM1 [Meng et al. 2020], THBS2 [Oguri et al. 2009] and MMP2 [Wu et al. 2019] promotes the occurrence of hypertension. The expression level of MMP2 [Giricz et al. 2006] was related to the severity of hyperlipidemia. Studies have shown that IGFBP5 [Zhu et al. 2024], COL1A2 [Huang et al. 2022], GREM1 [Kuprytė et al. 2024], DCN (decorin) [Vu et al. 2018], STC2 [Gude et al. 2023], THBS2 [Hsu et al. 2021], MMP2 [Wang et al. 2022] and RNY [Repetto et al. 2015] are related to the pathogenesis of cardiovascular diseases. IGFBP5 [Lang et al. 2006], COL1A2 [Xu et al. 2024], GREM1 [Qu et al. 2020], DCN (decorin) [Liu et al. 2018], THBS2 [Zhao et al. 2020], MMP2 [de Jager and Hoefer, 2017], TNFRSF11B [Zhang et al. 2023] and RNY1 [Saffold et al. 2025] can be used as a biomarkers in the diagnosis of inflammation. DCN (decorin) [Xie et al. 2022], STC2 [Qie et al. 2024] and MMP2 [Gong et al. 2018] are associated with oxidative stress. Altered expression of IGFBP5 [Capuano et al. 2019], COL1A2 [Huang et al. 2022] and MMP2 [Bobińska et al. 2016] might promote anxiety and depression. IGFBP5 [Capuano et al. 2019], DCN (decorin) [Jiang et al. 2022] and MMP2 [Li et al. 2025] might serve as a biomarkers for the pathogenetic activity of cognitive dysfunction.

IGFBP5 [Chen et al. 2025], GREM1 [Aoshima et al. 2021], DCN (decorin) [Kehlet et al. 2017], COL12A1 [Huang et al. 2025], THBS2 [Yu et al. 2025] and MMP2 [D Avila-Mesquita et al. 2021] have been reported to be very important in respiratory failure. Previous studies have reported that the expression changes of COL1A2 [Lindahl et al. 2009], DCN (decorin) [Xu et al. 2012], STC2 [Bermejo et al. 2025], THBS2 [Luo et al. 2026], MMP2 [Kreisel et al. 2016], TNFRSF11B [Biscetti et al. 2013] and RSC1A1 [Sebastiani et al. 2018] are potent risk factors for stroke. These might be pivotal genes involved in the pathophysiological process of ALS

Then, GO and REACTOME pathway enrichment analysis were conducted to gain more insights into the function of these DEGs in ALS. Signaling pathways include Regulation of Insulin-like Growth Factor (IGF) transport and uptake by insulin-like growth factor binding proteins (IGFBPs) [Hosback et al. 2007], diseases of glycosylation [Nakamura et al. 2024], axon guidance [Kim et al. 2023], signal transduction [Medinas et al. 2017], sensory perception [Kleinerova et al. 2025], neuronal system [Gentile et al. 2019], transmission across chemical synapses [Gulino et al. 2023] and transport of small molecules [Magrané and Manfredi, 2009] are involved in the ALS. GJA1 [Vicario et al. 2022], WNT5A [Liu et al. 2022], EGFR (epidermal growth factor receptor) [Wang et al. 2023], CCN2 [Gonzalez et al. 2018], STMN2 [Liu et al. 2024], CRYAB (crystallin alpha B) [Lu et al. 2019], FGF1 [Cassina et al. 2005], TIMP3 [Lee et al. 2008], YAP1 [Li et al. 2025], LOX (lysyl oxidase) [Li et al. 2004], GPNMB (glycoprotein nmb) [Clarke et al. 2024], HAND2 [Rodrigues et al. 2021], CAV1 [Adey et al. 2023], PIEZO2 [Sonkod et al. 2025], LRP4 [Rivner et al. 2017], GDNF (glial cell derived neurotrophic factor) [Mòdol-Caballero et al. 2021], NDNF (neuron derived neurotrophic factor) [Cheng et al. 2023], HECW1 [Haouari et al. 2023], HTR2B [Arnoux et al. 2021], LGR5 [Song et al. 2015], CXCL12 [Mullick et al. 2026], MAP1B [Strohm et al. 2022], UCHL1 [Li et al. 2020], DPYSL3 [Blasco et al. 2013], AXL (AXL receptor tyrosine kinase) [Spatafora et al. 2026], CRMP1 [Kawamoto et al. 2022], FGF2 [Petri et al. 2009], IGFBP3 [Albrethsen et al. 2025], TYRO3 [Fujita et al. 2018], L1CAM [Dunlop et al. 2023], SELENOP (selenoprotein P) [Urbano et al. 2022], SCD (stearoyl-CoA desaturase) [Vinknes et al. 2013], GPM6A [Nakamura et al. 2025], CORO2B [Wu et al. 2024], PLS3 [Wadman et al. 2019], CCL2 [Nógrádi et al. 2025], PDK4 [Pradhan et al. 2025]

ETS1 [Scoles et al. 2012], OSMR (oncostatin M receptor) [Chen et al. 2024], MMP1 [Łukaszewicz-Zając et al. 2014], BRCA1 [Noristani et al. 2015], HTRA1 [Zhang et al. 2025], PHLDA3 [Szebényi et al. 2024], IGFBP4 [Albrethsen et al. 2025], PLG (plasminogen) [Glas et al. 2007], FGF8 [Imaizumi et al. 2018], DLL4 [Mora et al. 2024], MT-ND4 [Berardo et al. 2020], PRKCG (protein kinase C gamma) [Seki et al. 2007], NDST3 [Tang et al. 2022], GAD1 [Romano et al. 2021], CHRNB2 [Jalaiei et al. 2025] and ABCC9 [Dugan et al. 2021] have been demonstrated to play important roles in ALS.

The studies suggested COL1A1 [Pan et al. 2010], COL3A1 [Wang et al. 2024], LUM (lumican) [Strieder-Barboza et al. 2022], THY1 [Al-Ameri et al. 2024], TNC (tenascin C) [Benbow et al. 2016], PAPPA (pappalysin 1) [Martín-Rivada et al. 2025], WNT5A [Koutaki et al. 2021], LAMA4 [Hagemann et al. 2023], SOD3 [Gao et al. 2020] and EGFR (epidermal growth factor receptor) [Cao et al. 2022] could be potential diagnostic biomarkers for obesity. Previous studies demonstrated that COL1A1 [Lin et al. 2021], CCN1 [Xiang et al. 2023], COL3A1 [Gaikwad et al. 2010], LUM (lumican) [Strieder-Barboza et al. 2022], THY1 [Aparicio et al. 1990], TNC (tenascin C) [Li et al. 2022], FN1 [Liu et al. 2025], WNT5A [Liu et al. 2023], SOD3 [Kuo et al. 2019] and EGFR (epidermal growth factor receptor) [Li et al. 2018] are associated with diabetes mellitus. COL1A1 [Castoldi et al. 2012], CCN1 [Liu et al. 2023], COL3A1 [Samokhin et al. 2018], SULF1 [Cha et al. 2018], WNT5A [Kawarazaki et al. 2020], KCNK2 [Shima et al. 2024], SOD3 [Chi et al. 2025], EGFR (epidermal growth factor receptor) [Rafikova et al. 2016], FST (follistatin) [Kuganathan et al. 2024] and AMOTL2 [Deng et al. 2024] might play a role in the pathogenesis of hypertension. COL1A1 [Chen et al. 2024], CCN1 [Yao et al. 2022], WNT5A [Awan et al. 2022], SOD3 [Cui et al. 2014], EGFR (epidermal growth factor receptor) [Fang et al. 2016], CCN2 [Tejera-Muñoz et al. 2022], FGF1 [Li et al. 2026], SNAI2 [Liu et al. 2025], DKK1 [Di et al. 2021] and CACNA2D1 [Xiong et al. 2021] might be involved in the pathogenesis of hyperlipidemia. COL1A1 [Luo et al. 2025], COL8A1 [Alzhrani et al. 2024], CCN1 [Yang et al. 2021], COL3A1 [Norgan Radler et al. 2025], SVEP1 [Osawa et al. 2025], GJA1 [Yi et al. 2024], CDH11 [Cao et al. 2021], LUM (lumican) [Su et al. 2026], THY1 [Li et al. 2020] and TNC (tenascin C) [Li et al. 2022] can be used as clinical prognostic as well as diagnostic biomarkers for cardiovascular diseases. COL1A1 [Shi et al. 2020], COL8A1 [Li et

al. 2025], CCN1 [Jiang et al. 2022], GJA1 [Vicario et al. 2022], CDH11 [Tang et al. 2025], LUM (lumican) [Lohr et al. 2012], THY1 [Schubert et al. 2011], TNC (tenascin C) [Imanaka-Yoshida et al. 2021], SULF1 [Zhu et al. 2026] and FN1 [Yu et al. 2024] can be used as a prognostic, diagnostic and therapeutic target in inflammation. COL1A1 [Fu et al. 2019], CCN1 [Yoshida et al. 2007], LUM (lumican) [Li et al. 2025], THY1 [Chen et al. 2019], TNC (tenascin C) [Hasanzadeh et al. 2021], ITGA11 [Liu et al. 2026], WNT5A [Zhao et al. 2015], SOD3 [Wert et al. 2018], EGFR (epidermal growth factor receptor) [Chen et al. 2017] and CCN2 [Valentijn et al. 2021] can be used as a biomarkers of oxidative stress. GJA1 [Kaut et al. 2017], TNC (tenascin C) [Peng et al. 2022], WNT5A [Ortiz-Matamoros and Arias, 2018], KCNK2 [Congiu et al. 2015], EGFR (epidermal growth factor receptor) [McFarland et al. 2015], FGF1 [Deng et al. 2019], SLIT3 [Jiang et al. 2026], ABI3BP [Kari et al. 2023], STC1 [Chao et al. 2021] and DKK1 [Ortiz-Matamoros and Arias, 2018] were identified as a crucial genes in anxiety and depression. CCN1 [Huo et al. 2026], GJA1 [Kajiwara et al. 2018], THY1 [Magen et al. 2015], TNC (tenascin C) [Hasanzadeh et al. 2021], FN1 [Fei et al. 2026], WNT5A [Ding et al. 2017], EGFR (epidermal growth factor receptor) [Chen et al. 2016], CCN2 [Liu et al. 2025], STMN2 [Pulukuri et al. 2025] and EFEMP1 [Zhang et al. 2020] might play an important role in regulating the genetic network related to the occurrence and development of cognitive dysfunction. The abnormal expression of COL1A1 [Tsitoura et al. 2021], CCN1 [Morrell et al. 2020], COL3A1 [Wan et al. 2020], THY1 [Zhou et al. 2016], TNC (tenascin C) [Donovan et al. 2023], SULF1 [Tu et al. 2024], FN1 [Wang et al. 2025], WNT5A [Huang et al. 2025] and EGFR (epidermal growth factor receptor) [Venkataraman et al. 2017] might be related to the progression of respiratory failure. The abnormal expression of COL1A1 [Feng et al. 2021], CCN1 [Lee et al. 2025], COL3A1 [Lv et al. 2014], GJA1 [Li et al. 2025], THY1 [Wang et al. 2001], TNC (tenascin C) [Chelluboina et al. 2022], ITGA11 [Hou et al. 2025], SOD3 [Mai et al. 2019], EGFR (epidermal growth factor receptor) [Nakano et al. 2023], and CRYAB (crystallin alpha B) [Arac et al. 2011] contributes to the stroke. Therefore, in this study, we obtained a functional overview of the complex gene expression changes in ALS by focusing on signaling pathway and GO terms. Novel biomarkers for ALS are listed in Table 7.

Further, we constructed a PPI network via the HIPPIE database and Cytoscape software and screened out hub genes (EGFR, FN1, CAV1, BCAR1, YAP1, POU5F1, TTYH1, ACTA1, GPR17, TF, COL6A3, COL12A1, THBS2, COL6A1, CXCL12, IGFBP3, MMP2, TIMP3, COL1A1, LOX, COL5A1, DCN6 , MMP14, PRKCG, ACTN2 and GRIN2B) from the PPI network and modules. EGFR (epidermal growth factor receptor) is implicated in the pathogenesis of ALS, particularly via its role in neuroinflammation and glial cell dysfunction [Le Pichon et al. 2013]. FN1 is implicated in the pathogenesis of ALS primarily through dysregulation of the extracellular matrix (ECM), neuroinflammation, and fibrotic remodelling around motor neuron [Lin et al. 2020]. CAV1 is implicated in ALS pathogenesis mainly via its role in membrane lipid-raft organization, neurotrophic signalling, and neuronal survival [Adey et al. 2023]. BCAR1 biology as a focal-adhesion and mechanosensing scaffold protein suggests it might involved indirectly to ALS pathogenesis through altered signaling at the neuron–extracellular matrix (ECM) interface, neuroinflammation, and survival pathways [Camacho Leal Mdel et al. 2015]. YAP1 appears to be associated in ALS mainly as a protective regulator of TDP-43 pathology and astrocyte-mediated support rather than as a classic causative ALS gene [Zhang et al. 2025]. GPR17 contributes to ALS pathogenesis by promoting an immature, dysfunctional oligodendrocyte state that weakens metabolic and structural support for motor neurons [Bonfanti et al. 2020]. Transferrin (TF) is involved in ALS mainly through iron transport and iron-homeostasis disturbance [Mizuno et al. 2006]. CXCL12 participates in ALS pathogenesis mainly through the CXCL12/CXCR4/CXCR7 chemokine axis, which affects neuroinflammation, glial signaling, and motor-neuron/axon preservation [Mullick et al. 2026]. IGFBP3 is associated in ALS mainly through the IGF signaling axis, where it regulates how much insulin-like growth factor-1 is available to motor neurons and muscle [Sakowski et al. 2009]. MMP2 is associated in ALS mainly as part of the extracellular-matrix remodeling and neuroinflammation axis [Łukaszewicz-Zając et al. 2014]. TIMP3 can promote motor-neuron apoptosis and might act upstream of Fas/caspase signaling in ALS models [Lee et al. 2008]. COL1A1 might be involved in ALS indirectly through extracellular-matrix remodeling, focal adhesion signaling, and stress responses in motor neurons and spinal cord tissue [Rasà et al. 2025]. LOX expression and activity are associated in SOD1^G93A^ ALS models and in vulnerable CNS regions, suggesting association with disease advancement [Li et al. 2004]. MMP14

is associated in ALS mainly as a matrix-remodeling and neurodegeneration-associated protease [Sánchez-Torres et al. 2020]. PRKCG is relevant to ALS biology as a kinase that can influence neuronal survival pathways, synaptic function, and stress signaling [Guo et al. 2020]. Current evidence suggests at most an ACTN2 play role in ALS through muscle and cytoskeletal pathology rather than direct motor-neuron [Shtilbans et al. 2011]. POU5F1, TTYH1, ACTA1, COL6A3, COL12A1, THBS2, COL6A1, COL5A1, DCN6 and GRIN2B does not currently have strong direct evidence as an ALS-causing or ALS-risk genes.

To explore the molecular mechanism of ALS, miRNA-hub gene regulatory network and TF-hub gene regulatory network were also constructed. We identified miRNA and TFs, all of which can regulate the expression of hub genes and provide more evidences for the elucidation of the mechanism of ALS progression. Hsa-miR-23a-3p [Liu et al. 2023], hsa-miR-152-3p [Zhu et al. 2023], SREBF1 [Yuan et al. 2018], RELA [Schiaffino et al. 2018], SRF [Song et al. 2023] and YY1 [Chen et al. 2023] serving as biomarkers in ALS. Hsa-miR-6874-5p, hsa-miR-1307-3p, hsa-miR-153-3p, hsa-miR-92b-3p, hsa-miR-7160-3p, hsa-miR-561-5p, hsa-miR-6887-3p, hsa-miR-7157-3p, GATA2, GATA3, IRF2, MEF2A and USF2 might be a novel targets for the treatment of ALS.

Next, the candidate drug targeting hub genes with ALS were screened out via the DrugBank database. The drug-hub gene interaction network analysis identified several potential therapeutic compounds, such as Lormetazepam, Lonoctocog alfa, Capmatinib, Becaplermin, Perampanel, Medazepam, Cabergoline, Taurine, Physostigmine and Ferrous succinate, which might target these senescence-related genes, offering promising candidates for future ALS treatment strategies. Drug molecules such as Perampanel [Turalde et al. 2022], Taurine [Nakazato et al. 2022] and Physostigmine [Norris et al. 1993] exhibits significant therapeutic potential as a treatment for ALS.

Finally, we performed ROC analysis to investigate the sensitivity and specificity of hub gene diagnosis of ALS, and the results showed that the expression of hub genes was related to the diagnosis of ALS.

In conclusion, this study identified novel biomarkers and signaling pathways through integrative bioinformatics analysis, providing new insights into ALS

pathogenesis. Taken above, our bioinformatics analysis identified 958 DEGs of ALS. Among them, EGFR, FN1, CAV1, BCAR1, YAP1, POU5F1, TTYH1, ACTA1, GPR17 and TF were verified and considered as hub genes were associated with disease prognosis, which could be predictive and therapeutic targets.

Declarations

Acknowledgement

I thanks very much to Kõks S, Rallmann K, Muldmaa M, Price J, Pfaff AL, Taba P, Murdoch University, Centre for Molecular Medicine and Innovative Therapeutics, Perth, Australia, the authors who deposited their RNA- sequencing dataset GSE277709, into the public GEO database.

Funding

The authors received no financial support for the research

Conflict of interest

The authors declare that they have no conflict of interest.

Ethical approval

Not applicable

Consent to participate

Not applicable

Written Consent for publication

Not applicable

Clinical trial number

Not applicable

Availability of data and materials

The datasets supporting the conclusions of this article are available in the GEO (Gene Expression Omnibus) (https://www.ncbi.nlm.nih.gov/geo/) repository. [(GSE277709) https://www.ncbi.nlm.nih.gov/geo/query/acc.cgi?acc=GSE277709]

Code availability

Not applicable

Author Contributions

B. V. - Writing original draft, and review and editing

S.P. - Formal analysis and validation

S.P. - Software and validation

C. V. - Software and investigation

Authors

Basavaraj Vastrad ORCID ID: 0000-0003-2202-7637

Shivaling Pattanashetti ORCID ID: 0009-0003-9246-1604

Siddalingeshwar Patil ORCID ID: 0009-0000-2685-2760

Chanabasayya Vastrad ORCID ID: 0000-0003-3615-4450

References

Rizea RE, Corlatescu AD, Costin HP, Dumitru A, Ciurea AV. Understanding Amyotrophic Lateral Sclerosis: Pathophysiology, Diagnosis, and Therapeutic Advances. Int J Mol Sci. 2024;25(18):9966. doi:10.3390/ijms25189966

Grad LI, Rouleau GA, Ravits J, Cashman NR. Clinical Spectrum of Amyotrophic Lateral Sclerosis (ALS). Cold Spring Harb Perspect Med. 2017;7(8):a024117.. doi:10.1101/cshperspect.a024117

Arthur KC, Calvo A, Price TR, Geiger JT, Chiò A, Traynor BJ. Projected increase in amyotrophic lateral sclerosis from 2015 to 2040. Nat Commun. 2016;7:12408. doi:10.1038/ncomms12408

Quinn C, Elman L. Amyotrophic Lateral Sclerosis and Other Motor Neuron Diseases. Continuum (Minneap Minn). 2020;26(5):1323-1347. doi:10.1212/CON.0000000000000911

Tzeplaeff L, Wilfling S, Requardt MV, Herdick M. Current State and Future Directions in the Therapy of ALS. Cells. 2023;12(11):1523. doi:10.3390/cells12111523

Li C, Ou R, Wei Q, Shang H. Shared genetic links between amyotrophic lateral sclerosis and obesity-related traits: a genome-wide association study. Neurobiol Aging. 2021;102:211.e1-211.e9. doi:10.1016/j.neurobiolaging.2021.01.023

Zhang L, Tang L, Huang T, Fan D. Association between type 2 diabetes and amyotrophic lateral sclerosis. Sci Rep. 2022;12(1):2544. doi:10.1038/s41598-022-06463-6

Moreau C, Brunaud-Danel V, Dallongeville J, Duhamel A, Laurier-Grymonprez L, de Reuck J, Wiart AC, Perez T, Richard F, Amouyel P, et al. Modifying effect of arterial hypertension on amyotrophic lateral sclerosis. Amyotroph Lateral Scler. 2012;13(2):194-201. doi:10.3109/17482968.2011.610110

Dedic SI, Stevic Z, Dedic V, Stojanovic VR, Milicev M, Lavrnic D. Is hyperlipidemia correlated with longer survival in patients with amyotrophic lateral sclerosis?. Neurol Res. 2012;34(6):576-580. doi:10.1179/1743132812Y.0000000049

Abdel Magid HS, Topol B, McGuire V, Hinman JA, Kasarskis EJ, Nelson LM. Cardiovascular Diseases, Medications, and ALS: A Population-Based Case-Control Study. Neuroepidemiology. 2022;56(6):423-432. doi:10.1159/000526982

Batty GD, Kivimäki M, Frank P, Gale CR, Wright L. Systemic inflammation and subsequent risk of amyotrophic lateral sclerosis: Prospective cohort study. Brain Behav Immun. 2023;114:46-51. doi:10.1016/j.bbi.2023.07.026

Motataianu A, Serban G, Barcutean L, Balasa R. Oxidative Stress in Amyotrophic Lateral Sclerosis: Synergy of Genetic and Environmental Factors. Int J Mol Sci. 2022;23(16):9339. doi:10.3390/ijms23169339

Larsson BJ, Nordin K, Nygren I. Symptoms of anxiety and depression in patients with amyotrophic lateral sclerosis and their relatives during the disease trajectory. J Neurol Sci. 2023;455:122780. doi:10.1016/j.jns.2023.122780

Jellinger KA. The Spectrum of Cognitive Dysfunction in Amyotrophic Lateral Sclerosis: An Update. Int J Mol Sci. 2023;24(19):14647. doi:10.3390/ijms241914647

Kotchoubey B, Lang S, Winter S, Birbaumer N. Cognitive processing in completely paralyzed patients with amyotrophic lateral sclerosis. Eur J Neurol. 2003;10(5):551-558. doi:10.1046/j.1468-1331.2003.00647.x

Kwon S, Kim B, Han KD, Jung W, Cho EB, Shin DW, Min JH. Increased risk of ischemic stroke in amyotrophic lateral sclerosis: a nationwide cohort study in South Korea. Neurol Sci. 2025;46(6):2687-2695. doi:10.1007/s10072-025-08074-1

Niedermeyer S, Murn M, Choi PJ. Respiratory Failure in Amyotrophic Lateral Sclerosis. Chest. 2019;155(2):401-408. doi:10.1016/j.chest.2018.06.035

Ilieva H, Vullaganti M, Kwan J. Advances in molecular pathology, diagnosis, and treatment of amyotrophic lateral sclerosis. BMJ. 2023;383:e075037. doi:10.1136/bmj-2023-075037

van den Berg LH, Rothstein JD, Shaw PJ, Babu S, Benatar M, Bucelli RC, Genge A, Glass JD, Hardiman O, Libri V, et al. Safety, tolerability, and pharmacokinetics of antisense oligonucleotide BIIB078 in adults with C9orf72-associated amyotrophic lateral sclerosis: a phase 1, randomised, double blinded, placebo-controlled, multiple ascending dose study. Lancet Neurol. 2024;23(9):901-912. doi:10.1016/S1474-4422(24)00216-3

Huang M, Liu YU, Yao X, Qin D, Su H. Variability in SOD1-associated amyotrophic lateral sclerosis: geographic patterns, clinical heterogeneity, molecular alterations, and therapeutic implications. Transl Neurodegener. 2024;13(1):28. doi:10.1186/s40035-024-00416-x

Chong ZZ, Souayah N. Pathogenic TDP-43 in amyotrophic lateral sclerosis. Drug Discov Today. 2025;30(5):104351. doi:10.1016/j.drudis.2025.104351

Moens TG, Da Cruz S, Neumann M, Shelkovnikova TA, Shneider NA, Van Den Bosch L. Amyotrophic lateral sclerosis caused by FUS mutations: advances with broad implications. Lancet Neurol. 2025;24(2):166-178. doi:10.1016/S1474-4422(24)00517-9

Thumbadoo KM, Nementzik LR, Swanson MEV, Dieriks BV, Dragunow M, Faull RLM, Curtis MA, Blair IP, Nicholson GA, Williams KL, et al. A meta-analysis of genetic variant pathogenicity and sex differences in UBQLN2-linked amyotrophic lateral sclerosis and frontotemporal dementia. Neurobiol Dis. 2025;216:107127. doi:10.1016/j.nbd.2025.107127

Jiang X, Guan Y, Zhao Z, Meng F, Wang X, Gao X, Liu J, Chen Y, Zhou F, Zhou S, et al. Potential Roles of the WNT Signaling Pathway in Amyotrophic Lateral Sclerosis. Cells. 2021;10(4):839. doi:10.3390/cells10040839

Paudel YN, Angelopoulou E, Piperi C, Othman I, Shaikh MF. Implication of HMGB1 signaling pathways in Amyotrophic lateral sclerosis (ALS): From molecular mechanisms to pre-clinical results. Pharmacol Res. 2020;156:104792. doi:10.1016/j.phrs.2020.104792

Sahana TG, Zhang K. Mitogen-Activated Protein Kinase Pathway in Amyotrophic Lateral Sclerosis. Biomedicines. 2021;9(8):969. doi:10.3390/biomedicines9080969

Chowdhury MR, Reddy RVS, Nampoothiri NK, Erva RR, Vijaykumar SD. Exploring bioactive natural products for treating neurodegenerative diseases: a computational network medicine approach targeting the estrogen signaling pathway in amyotrophic lateral sclerosis and Parkinson's disease. Metab Brain Dis. 2025;40(4):169. doi:10.1007/s11011-025-01585-y

Qi Y, Yang C, Zhao H, Deng Z, Xu J, Liang W, Sun Z, Nieland JDV. Neuroprotective Effect of Sonic Hedgehog Mediated PI3K/AKT Pathway in Amyotrophic Lateral Sclerosis Model Mice. Mol Neurobiol. 2022;59(11):6971-6982. doi:10.1007/s12035-022-03013-z

Joshi H, Vastrad B, Joshi N, Vastrad C, Tengli A, Kottursheti I. Identification of Key Pathways and Genes in Obesity Using Bioinformatics Analysis and Molecular Docking Studies. Front Endocrinol (Lausanne). 2021;12:628907. doi:10.3389/fendo.2021.628907

Prashanth G, Vastrad B, Tengli A, Vastrad C, Kottursheti I. Investigation of candidate genes and mechanisms underlying obesity associated type 2 diabetes mellitus using bioinformatics analysis and screening of small drug molecules. BMC Endocr Disord. 2021;21(1):80. doi:10.1186/s12902-021-00718-5

Kõks S, Rallmann K, Muldmaa M, Price J, Pfaff AL, Taba P. Whole blood transcriptome profile identifies motor neurone disease RNA biomarker signatures. Exp Biol Med (Maywood). 2025;249:10401. doi:10.3389/ebm.2024.10401

Clough E, Barrett T. The Gene Expression Omnibus Database. Methods Mol Biol. 2016;1418:93-110. doi:10.1007/978-1-4939-3578-9_5

Love MI, Huber W, Anders S. Moderated estimation of fold change and dispersion for RNA-seq data with DESeq2. Genome Biol. 2014;15(12):550. doi:10.1186/s13059-014-0550-8

Solari A, Goeman JJ. Minimally adaptive BH: A tiny but uniform improvement of the procedure of Benjamini and Hochberg. Biom J. 2017;59(4):776-780. doi:10.1002/bimj.201500253

Reimand J, Kull M, Peterson H, Hansen J, Vilo J. g:Profiler--a web-based toolset for functional profiling of gene lists from large-scale experiments. Nucleic Acids Res. 2007;35(Web Server issue):W193-W200. doi:10.1093/nar/gkm226

Thomas PD. The Gene Ontology and the Meaning of Biological Function. Methods Mol Biol. 2017;1446:15-24. doi:10.1007/978-1-4939-3743-1_2

Fabregat A, Jupe S, Matthews L, Sidiropoulos K, Gillespie M, Garapati P, Haw R, Jassal B, Korninger F, May B et al The Reactome Pathway Knowledgebase. Nucleic Acids Res. 2018;46(D1):D649–D655. doi:10.1093/nar/gkx1132

Alanis-Lobato G, Schaefer MH. Generation and Interpretation of Context-Specific Human Protein-Protein Interaction Networks with HIPPIE. Methods Mol Biol. 2020;2074:135-144. doi:10.1007/978-1-4939-9873-9_11

Ono K, Fong D, Gao C, Churas C, Pillich R, Lenkiewicz J, Pratt D, Pico AR, Hanspers K, Xin Y, et al. Cytoscape Web: bringing network biology to the browser. Nucleic Acids Res. 2025;53(W1):W203-W212. doi:10.1093/nar/gkaf365

Luo X, Guo L, Dai XJ, Wang Q, Zhu W, Miao X, Gong H. Abnormal intrinsic functional hubs in alcohol dependence: evidence from a voxelwise degree centrality analysis. Neuropsychiatr Dis Treat. 2017;13:2011-2020. doi:10.2147/NDT.S142742

Li Y, Li W, Tan Y, Liu F, Cao Y, Lee KY. Hierarchical Decomposition for Betweenness Centrality Measure of Complex Networks. Sci Rep. 2017;7:46491.. doi:10.1038/srep46491

Gilbert M, Li Z, Wu XN, Rohr L, Gombos S, Harter K, Schulze WX. Comparison of path-based centrality measures in protein-protein interaction networks revealed proteins with phenotypic relevance during adaptation to changing nitrogen environments. J Proteomics. 2021;235:104114. doi:10.1016/j.jprot.2021.104114

Li G, Li M, Wang J, Li Y, Pan Y. United Neighborhood Closeness Centrality and Orthology for Predicting Essential Proteins. IEEE/ACM Trans Comput Biol Bioinform. 2020;17(4):1451-1458. doi:10.1109/TCBB.2018.2889978

Zaki N, Efimov D, Berengueres J. Protein complex detection using interaction reliability assessment and weighted clustering coefficient. BMC Bioinformatics. 2013;14:163. doi:10.1186/1471-2105-14

Asli NS, Pitulescu ME, Kessel M. MicroRNAs in organogenesis and disease. Curr Mol Med. 2008;8(8):698-710. doi:10.2174/156652408786733739

Fan Y, Xia J. miRNet-Functional Analysis and Visual Exploration of miRNA-Target Interactions in a Network Context. Methods Mol Biol. 2018; 1819:215-233. doi:10.1007/978-1-4939-8618-7_10

Engelkamp D, van Heyningen V. Transcription factors in disease. Curr Opin Genet Dev. 1996;6(3):334-342. doi:10.1016/s0959-437x(96)80011-6

Zhou G, Soufan O, Ewald J, Hancock REW, Basu N, Xia J. NetworkAnalyst 3.0: a visual analytics platform for comprehensive gene expression profiling and meta-analysis. Nucleic Acids Res. 2019;47:W234-W241. doi:10.1093/nar/gkz240

Robin X, Turck N, Hainard A, Tiberti N, Lisacek F, Sanchez JC, Müller M. pROC: an open-source package for R and S+ to analyze and compare ROC curves. BMC Bioinformatics 2011;12:77. doi:10.1186/1471-2105-12-77

Cheng J, Ho WK, Wu BT, Liu HP, Lin WY. miRNA profiling as a complementary diagnostic tool for amyotrophic lateral sclerosis. Sci Rep. 2023;13(1):13805. doi:10.1038/s41598-023-40879-y

Morimoto N, Miyazaki K, Kurata T, et al. Effect of mitochondrial transcription factor a overexpression on motor neurons in amyotrophic lateral sclerosis model mice. J Neurosci Res. 2012;90(6):1200-1208. doi:10.1002/jnr.23000

Albrethsen J, Drici L, Slot Vilmann LM, Holmboe SA, Thomsen CE, Rogaczewska Groendahl VL, Ottenheijm ME, Nielsen AB, Christoffersen C, et al. Targeted proteomics of serum IGF-I, -II, IGFBP-2, -3, -4, -5, -6 and ALS. Clin Chem Lab Med. 2025;63(8):1528-1537. doi:10.1515/cclm-2024-1428

Fang L, Teuchert M, Huber-Abel F, Schattauer D, Hendrich C, Dorst J, Zettlmeissel H, Wlaschek M, Scharffetter-Kochanek K, et al. MMP-2 and MMP-9 are elevated in spinal cord and skin in a mouse model of ALS. J Neurol Sci. 2010;294(1-2):51-56. doi:10.1016/j.jns.2010.04.005

Atak M, Kılıç H, Şen B, Arpa M. Functional Food Potential of White Tea from East Black Sea Region: Targeting GREM1 Expression and Metabolic Dysregulation in Obesity. Int J Mol Sci. 2026;27(2):929. doi:10.3390/ijms27020929

Bolton K, Segal D, McMillan J, Jowett J, Heilbronn L, Abberton K, Zimmet P, Chisholm D, Collier G, Walder K. Decorin is a secreted protein associated with obesity and type 2 diabetes. Int J Obes (Lond). 2008;32(7):1113-1121. doi:10.1038/ijo.2008.41

Belo VA, Lacchini R, Miranda JA, Lanna CM, Souza-Costa DC, Tanus-Santos JE. Increased activity of MMP-2 in hypertensive obese children is associated with hypoadiponectinemia. Obesity (Silver Spring). 2015;23(1):177-182. doi:10.1002/oby.20939

Osswald C, Baumgarten K, Stümpel F, Gorboulev V, Akimjanova M, Knobeloch KP, Horak I, Kluge R, Joost HG, Koepsell H. Mice without the regulator gene Rsc1A1 exhibit increased Na+-D-glucose cotransport in small intestine and develop obesity. Mol Cell Biol. 2005;25(1):78-87. doi:10.1128/MCB.25.1.78-87.2005

Mitroi AF, Leopa N, Dumitru E, Brînzan C, Tocia C, Dumitru A, Popescu RC. Association of TCF7L2, CASC8 and GREM1 Polymorphisms in Patients with Colorectal Cancer and Type II Diabetes Mellitus. Genes (Basel). 2022;13(8):1297. doi:10.3390/genes13081297

Chen F, Lai J, Zhu Y, He M, Hou H, Wang J, Chen C, Wang DW, Tang J. Cardioprotective Effect of Decorin in Type 2 Diabetes. Front Endocrinol (Lausanne). 2020;11:479258. doi:10.3389/fendo.2020.479258

Gude MF, Hjortebjerg R, Bjerre M, Charles MH, Witte DR, Sandbæk A, Frystyk J. The STC2-PAPP-A-IGFBP4-IGF1 axis and its associations to mortality and CVD in T2D. Endocr Connect. 2023;12(3):e220451. doi:10.1530/EC-22-0451

Arreguin-Cano JA, Ayerdi-Nájera B, Tacuba-Saavedra A, Navarro-Tito N, Dávalos-Martínez A, Emigdio-Vargas A, Barrera-Rodríguez E, Blanco-García N, Gutiérrez-Venegas G, Ventura-Molina E, et al. MMP-2 salivary activity in type 2 diabetes mellitus patients. Diabetol Metab Syndr. 2019;11:113. doi:10.1186/s13098-019-0510-2

Biscetti F, Porreca CF, Bertucci F, Straface G, Santoliquido A, Tondi P, Angelini F, Pitocco D, Santoro L, Gasbarrini A, et al. TNFRSF11B gene polymorphisms increased risk of peripheral arterial occlusive disease and critical limb ischemia in patients with type 2 diabetes. Acta Diabetol. 2014;51(6):1025-1032. doi:10.1007/s00592-014-0664-1

Lee DH, Kim JE, Kang YJ. Insulin Like Growth Factor Binding Protein-5 Regulates Excessive Vascular Smooth Muscle Cell Proliferation in Spontaneously Hypertensive Rats via ERK 1/2 Phosphorylation. Korean J Physiol Pharmacol. 2013;17(2):157-162. doi:10.4196/kjpp.2013.17.2.157

Tian DZ, Wei W, Dong YJ. Influence of COL1A2 gene variants on the incidence of hypertensive intracerebral hemorrhage in a Chinese population. Genet Mol Res. 2016;15(1):10.4238/gmr.15017369. doi:10.4238/gmr.15017369

Meng L, Teng X, Liu Y, Yang C, Wang S, Yuan W, Meng J, Chi H, Duan L, Liu X. Vital Roles of Gremlin-1 in Pulmonary Arterial Hypertension Induced by Systemic-to-Pulmonary Shunts. J Am Heart Assoc. 2020;9(15):e016586. doi:10.1161/JAHA.120.016586

Oguri M, Kato K, Yokoi K, Watanabe S, Metoki N, Yoshida H, Satoh K, Aoyagi Y, Nishigaki Y, Yoshida H, et al. Association of polymorphisms of THBS2 and HSPA8 with hypertension in Japanese individuals with chronic kidney disease. Mol Med Rep. 2009;2(2):205-211. doi:10.3892/mmr_00000085

Wu W, Liu D, Jiang S, Zhang K, Zhou H, Lu Q. Polymorphisms in gene MMP-2 modify the association of cadmium exposure with hypertension risk. Environ Int. 2019;124:441-447. doi:10.1016/j.envint.2019.01.041

Giricz Z, Lalu MM, Csonka C, Bencsik P, Schulz R, Ferdinandy P. Hyperlipidemia attenuates the infarct size-limiting effect of ischemic preconditioning: role of matrix metalloproteinase-2 inhibition. J Pharmacol Exp Ther. 2006;316(1):154-161. doi:10.1124/jpet.105.091140

Zhu Q, Cheang I, Guo Q, Lu X, Li Y, Yao W, Zhang H, Li X. Serum IGFBP5 as a predictor of major adverse cardiac events in patients with acute myocardial infarction. Int J Cardiol. 2024;411:132268. doi:10.1016/j.ijcard.2024.132268

Huang K, Zhang X, Duan J, Wang R, Wu Z, Yang C, Yang L. STAT4 and COL1A2 are potential diagnostic biomarkers and therapeutic targets for heart failure comorbided with depression. Brain Res Bull. 2022;184:68-75. doi:10.1016/j.brainresbull.2022.03.014

Kuprytė M, Lesauskaitė V, Siratavičiūtė V, Utkienė L, Jusienė L, Pangonytė D. Expression of Osteopontin and Gremlin 1 Proteins in Cardiomyocytes in Ischemic Heart Failure. Int J Mol Sci. 2024;25(15):8240. doi:10.3390/ijms25158240

Vu TT, Marquez J, Le LT, Nguyen ATT, Kim HK, Han J. The role of decorin in cardiovascular diseases: more than just a decoration. Free Radic Res. 2018;52(11-12):1210-1219. doi:10.1080/10715762.2018.1516285

Hsu CH, Liu IF, Kuo HF, Li CY, Lian WS, Chang CY, Chen YH, Liu WL, Lu CY, Liu YR, et al. miR-29a-3p/THBS2 Axis Regulates PAH-Induced Cardiac Fibrosis. Int J Mol Sci. 2021;22(19):10574. doi:10.3390/ijms221910574

Wang LY, Tan CS, Lai MKP, Hilal S. Factors Associated with RANTES, EMMPIRIN, MMP2 and MMP9, and the Association of These Biomarkers with Cardiovascular Disease in a Multi-Ethnic Population. J Clin Med. 2022;11(24):7281. doi:10.3390/jcm11247281

Repetto E, Lichtenstein L, Hizir Z, Tekaya N, Benahmed M, Ruidavets JB, Zaragosi LE, Perret B, Bouchareychas L, Genoux A, et al. RNY-derived small RNAs as a signature of coronary artery disease. BMC Med. 2015;13:259. doi:10.1186/s12916-015-0489-y

Lang CH, Krawiec BJ, Huber D, McCoy JM, Frost RA. Sepsis and inflammatory insults downregulate IGFBP-5, but not IGFBP-4, in skeletal muscle via a TNF-dependent mechanism. Am J Physiol Regul Integr Comp Physiol. 2006;290(4):R963-R972. doi:10.1152/ajpregu.00684.2005

Xu J, Zhou K, Gu H, Zhang Y, Wu L, Bian C, Huang Z, Chen G, Cheng X, Yin X. Exosome miR-4738-3p-mediated regulation of COL1A2 through the NF-κB and inflammation signaling pathway alleviates osteoarthritis low-grade inflammation symptoms. Biomol Biomed. 2024;24(3):520-536. doi:10.17305/bb.2023.9921

Qu S, Liu Z, Wang B. Down-regulation of Gremlin1 inhibits inflammatory response and vascular permeability in chronic idiopathic urticaria through suppression of TGF-β signaling pathway. Gene. 2020;756:144916. doi:10.1016/j.gene.2020.144916

Liu D, Kong F, Yuan Y, Seth P, Xu W, Wang H, Xiao F, Wang L, Zhang Q, Yang Y, et al. Decorin-Modified Umbilical Cord Mesenchymal Stem Cells (MSCs) Attenuate Radiation-Induced Lung Injuries via Regulating Inflammation, Fibrotic Factors, and Immune Responses. Int J Radiat Oncol Biol Phys. 2018;101(4):945-956. doi:10.1016/j.ijrobp.2018.04.007

Zhao F, Dong J, Guo J, Bi L. Inhibiting role of long non-coding RNA LINC01197 in inflammation in rheumatoid arthritis through the microRNA-150/THBS2 axis. Exp Cell Res. 2020;394(2):112136. doi:10.1016/j.yexcr.2020.112136

de Jager SCA, Hoefer IE. Beyond the matrix: MMP2 as critical regulator of inflammation-mediated vascular dysfunction. Cardiovasc Res. 2017;113(14):1705-1707. doi:10.1093/cvr/cvx202

Zhang D, Xu C, Zhang J, Zeng R, Qi Q, Xu J, Pan Y, Liu X, Shi S, Zhang J, et al. Plasma TNFRSF11B as a New Predictive Inflammatory Marker of Sepsis-ARDS with Endothelial Dysfunction. J Proteome Res. 2023;22(11):3640-3651. doi:10.1021/acs.jproteome.3c00576

Saffold CE, Richardson AC, Pua HH. RNY1 partitions into extracellular vesicles and ribonucleoprotein particles during airway inflammation to regulate macrophage programming. Preprint. bioRxiv. 2025;2025.12.04.691704. doi:10.64898/2025.12.04.691704

Xie X, Li D, Cui Y, Xie T, Cai J, Yao Y. Decorin Protects Retinal Pigment Epithelium Cells from Oxidative Stress and Apoptosis via AMPK-mTOR-Regulated Autophagy. Oxid Med Cell Longev. 2022;2022:3955748. doi:10.1155/2022/3955748

Qie S, Xiong H, Liu Y, Yan C, Wang Y, Tian L, Wang C, Sang N. Stanniocalcin 2 governs cancer cell adaptation to nutrient insufficiency through alleviation of oxidative stress. Cell Death Dis. 2024;15(8):567. doi:10.1038/s41419-024-06961-7

Gong W, Ma Y, Li A, Shi H, Nie S. Trimetazidine suppresses oxidative stress, inhibits MMP-2 and MMP-9 expression, and prevents cardiac rupture in mice with myocardial infarction. Cardiovasc Ther. 2018;36(5):e12460. doi:10.1111/1755-5922.12460

Capuano AW, Wilson RS, Honer WG, Petyuk VA, Leurgans SE, Yu L, Gatchel JR, Arnold S, Bennett DA, Arvanitakis Z. Brain IGFBP-5 modifies the relation of depressive symptoms to decline in cognition in older persons. J Affect Disord. 2019;250:313-318. doi:10.1016/j.jad.2019.03.051

Bobińska K, Szemraj J, Czarny P, Gałecki P. Role of MMP-2, MMP-7, MMP-9 and TIMP-2 in the development of recurrent depressive disorder. J Affect Disord. 2016;205:119-129. doi:10.1016/j.jad.2016.03.068

Jiang R, Smailovic U, Haytural H, Tijms BM, Li H, Haret RM, Shevchenko G, Chen G, Abelein A, Gobom J, et al. Increased CSF-decorin predicts brain pathological changes driven by Alzheimer's Aβ amyloidosis. Acta Neuropathol Commun. 2022;10(1):96. doi:10.1186/s40478-022-01398-5

Li X, Ding W, Zhang X, Tang X, Zheng Y, Ma Y, Bao X, Kang X, Zhu S. Caveolin-1-Mediated Blood-Brain Barrier Disruption via MMP2/9 Contributes to Postoperative Cognitive Dysfunction. Neurochem Res. 2025;50(4):210. doi:10.1007/s11064-025-04458-z

Chen N, Qi Y, Ma W, Zhu X, Li X. Role and mechanism of IGFBP5 in the real-ambient particulate matter exposure-induced chronic lung injury. Front Pharmacol. 2025;16:1604301. doi:10.3389/fphar.2025.1604301

Aoshima Y, Enomoto Y, Muto S, Meguro S, Kawasaki H, Kosugi I, Fujisawa T, Enomoto N, Inui N, Nakamura Y, et al. Gremlin-1 for the Differential Diagnosis of Idiopathic Pulmonary Fibrosis Versus Other Interstitial Lung Diseases: A Clinical and Pathophysiological Analysis. Lung. 2021;199(3):289-298. doi:10.1007/s00408-021-00440-y

Kehlet SN, Bager CL, Willumsen N, Dasgupta B, Brodmerkel C, Curran M, Brix S, Leeming DJ, Karsdal MA. Cathepsin-S degraded decorin are elevated in fibrotic lung disorders - development and biological validation of a new serum biomarker. BMC Pulm Med. 2017;17(1):110. doi:10.1186/s12890-017-0455-x

Huang H, Deng L, Zhang Y, Wang Y, Yan D, Lin X, Wang Y, Wang Y, Hu X. Novel variant of COL12A1 gene causing neonatal hypotonia and respiratory failure. Neurol Sci. 2025;46(6):2847-2854. doi:10.1007/s10072-025-08028-7

Yu L, Wang R, Hou Q, Yang F, Liu Y, Peng M, Dong Y, Liu Y, Cheng Z. Enhanced THBS2 promotes collagen synthesis and inflammatory secretome of fibroblasts in idiopathic pulmonary fibrosis. Sci Rep. 2025;15(1):25926. doi:10.1038/s41598-025-09318-y

D Avila-Mesquita C, Couto AES, Campos LCB, Vasconcelos TF, Michelon-Barbosa J, Corsi CAC, Mestriner F, Petroski-Moraes BC, Garbellini-Diab MJ, Couto DMS, et al. MMP-2 and MMP-9 levels in plasma are altered and associated with mortality in COVID-19 patients. Biomed Pharmacother. 2021;142:112067. doi:10.1016/j.biopha.2021.112067

Lindahl K, Rubin CJ, Brändström H, Karlsson MK, Holmberg A, Ohlsson C, Mellström D, Orwoll E, Mallmin H, Kindmark A, et al. Heterozygosity for a coding SNP in COL1A2 confers a lower BMD and an increased stroke risk. Biochem Biophys Res Commun. 2009;384(4):501-505. doi:10.1016/j.bbrc.2009.05.006

Xu YZ, Zhao KJ, Yang ZG, Zhang YH, Zhang YW, Hong B, Liu JM. Decreased plasma decorin levels following acute ischemic stroke: correlation with MMP-2 and differential expression in TOAST subtypes. Mol Med Rep. 2012;6(6):1319-1324. doi:10.3892/mmr.2012.1108

Bermejo N, López JJ, Berna-Erro A, Fernández E, Corbacho AJ, Vázquez MT, Granados MP, Redondo PC. Stanniocalcin2, A Promising New Target for Identifying Patients with Stroke/Ictus. Int J Mol Sci. 2025;26(20):9999. doi:10.3390/ijms26209999

Luo S, Zhang Y, Li B, Li X, Wang Y, Hu C, Wu C, Wu Y, Wang Z, Tang C. Artesunate protects against ischemic stroke through THBS2/CD36/TLR4 pathway. Int Immunopharmacol. 2026;178:116562. doi:10.1016/j.intimp.2026.116562

Kreisel SH, Stroick M, Griebe M, Alonso A, Reuter B, Hennerici MG, Fatar M. True Effects or Bias? MMP-2 and MMP-9 Serum Concentrations after Acute Stroke. Cerebrovasc Dis. 2016;42(5-6):352-360. doi:10.1159/000446405

Biscetti F, Straface G, Giovannini S, Santoliquido A, Angelini F, Santoro L, Porreca CF, Pecorini G, Ghirlanda G, Flex A. Association between TNFRSF11B gene polymorphisms and history of ischemic stroke in Italian diabetic patients. Hum Genet. 2013;132(1):49-55. doi:10.1007/s00439-012-1224-9

Sebastiani A, Greve F, Gölz C, Förster CY, Koepsell H, Thal SC. RS1 (Rsc1A1) deficiency limits cerebral SGLT1 expression and delays brain damage after

experimental traumatic brain injury. J Neurochem. 2018;147(2):190-203. doi:10.1111/jnc.14551

Hosback S, Hardiman O, Nolan CM, Doyle MA, Gorman G, Lynch C, O'Toole O, Jakeman P. Circulating insulin-like growth factors and related binding proteins are selectively altered in amyotrophic lateral sclerosis and multiple sclerosis. Growth Horm IGF Res. 2007;17(6):472-479. doi:10.1016/j.ghir.2007.06.002.

Nakamura K, Fujita K, Suzuki M, Kunugi A, Hirozane Y, Kunikata T, Takahashi B, Narazaki G, Kondo H, Haji S, et al. Neuroinflammation and glycosylation-related cerebrospinal fluid proteins for predicting functional decline in amyotrophic lateral sclerosis: a proteomic study. Front Neurol. 2024;15:1418320.. doi:10.3389/fneur.2024.1418320

Kim SH, Nichols KD, Anderson EN, Liu Y, Ramesh N, Jia W, Kuerbis CJ, Scalf M, Smith LM, Pandey UB, et al. Axon guidance genes modulate neurotoxicity of ALS-associated UBQLN2. Elife. 2023;12:e84382. doi:10.7554/eLife.84382

Medinas DB, González JV, Falcon P, Hetz C. Fine-Tuning ER Stress Signal Transducers to Treat Amyotrophic Lateral Sclerosis. Front Mol Neurosci. 2017;10:216. doi:10.3389/fnmol.2017.00216

Kleinerova J, Chipika RH, Tan EL, Yunusova Y, Marchand-Pauvert V, Kassubek J, Pradat PF, Bede P. Sensory Dysfunction in ALS and Other Motor Neuron Diseases: Clinical Relevance, Histopathology, Neurophysiology, and Insights from Neuroimaging. Biomedicines. 2025;13(3):559. doi:10.3390/biomedicines13030559

Gentile F, Scarlino S, Falzone YM, Lunetta C, Tremolizzo L, Quattrini A, Riva N. The Peripheral Nervous System in Amyotrophic Lateral Sclerosis: Opportunities for Translational Research. Front Neurosci. 2019;13:601. doi:10.3389/fnins.2019.00601

Gulino R. Synaptic Dysfunction and Plasticity in Amyotrophic Lateral Sclerosis. Int J Mol Sci. 2023;24(5):4613. doi:10.3390/ijms24054613

Magrané J, Manfredi G. Mitochondrial function, morphology, and axonal transport in amyotrophic lateral sclerosis. Antioxid Redox Signal. 2009;11(7):1615-1626. doi:10.1089/ARS.2009.2604

Vicario N, Castrogiovanni P, Imbesi R, Giallongo S, Mannino G, Furno DL, Giuffrida R, Zappalà A, Li Volti G, Tibullo D, et al. GJA1/CX43 High Expression Levels in the Cervical Spinal Cord of ALS Patients Correlate to Microglia-Mediated Neuroinflammatory Profile. Biomedicines. 2022;10(9):2246. doi:10.3390/biomedicines10092246

Liu J, Zhou F, Chen Y, Guan Y, Meng F, Zhao Z, Wang X, Gao X, Jiang X, Zhang H, et al. Wnt5a protects motor neurons in amyotrophic lateral sclerosis by regulating the Wnt/Ca2+ signaling pathway. Am J Transl Res. 2022;14(8):5343-5362.

Wang Y, Liang W, Wang T, Zhang C, Yang Y, Cong C, Wang X, Wang S, Wang D, Huo D, et al. Researches of calcium-activated chloride channel ANO1 intervening amyotrophic lateral sclerosis progression by activating EGFR and CaMKII signaling. Brain Res Bull. 2023;204:110792. doi:10.1016/j.brainresbull.2023.110792

Gonzalez D, Rebolledo DL, Correa LM, Court FA, Cerpa W, Lipson KE, van Zundert B, Brandan E. The inhibition of CTGF/CCN2 activity improves muscle and locomotor function in a murine ALS model. Hum Mol Genet. 2018;27(16):2913-2926. doi:10.1093/hmg/ddy204

Liu Y, Yan D, Yang L, Chen X, Hu C, Chen M. Stathmin 2 is a potential treatment target for TDP-43 proteinopathy in amyotrophic lateral sclerosis. Transl Neurodegener. 2024;13(1):20. doi:10.1186/s40035-024-00413-0

Lu SZ, Guo YS, Liang PZ, Zhang SZ, Yin S, Yin YQ, Wang XM, Ding F, Gu XS, Zhou JW. Suppression of astrocytic autophagy by αB-crystallin contributes to α-synuclein inclusion formation. Transl Neurodegener. 2019;8:3. doi:10.1186/s40035-018-0143-7

Cassina P, Pehar M, Vargas MR, Castellanos R, Barbeito AG, Estévez AG, Thompson JA, Beckman JS, Barbeito L. Astrocyte activation by fibroblast growth factor-1 and motor neuron apoptosis: implications for amyotrophic lateral sclerosis. J Neurochem. 2005;93(1):38-46. doi:10.1111/j.1471-4159.2004.02984.x

Lee JK, Shin JH, Suh J, Choi IS, Ryu KS, Gwag BJ. Tissue inhibitor of metalloproteinases-3 (TIMP-3) expression is increased during serum deprivation-

induced neuronal apoptosis in vitro and in the G93A mouse model of amyotrophic lateral sclerosis: a potential modulator of Fas-mediated apoptosis. Neurobiol Dis. 2008;30(2):174-185. doi:10.1016/j.nbd.2008.01.004

Li D, Wei Y, Yang R, Luo X, Liu Y, Zhao W, Yang H, Wu Y, Wang Y, Huang Z. An unrecognized mechanism of self-protection in degenerating neurons mediated by astrocytic YAP through Wnts/β-catenin/EAAT2 signaling in C9orf72-poly-GA mice. Theranostics. 2025;15(16):8176-8201. doi:10.7150/thno.113599

Li PA, He Q, Cao T, Yong G, Szauter KM, Fong KS, Karlsson J, Keep MF, Csiszar K. Up-regulation and altered distribution of lysyl oxidase in the central nervous system of mutant SOD1 transgenic mouse model of amyotrophic lateral sclerosis. Brain Res Mol Brain Res. 2004;120(2):115-122. doi:10.1016/j.molbrainres.2003.10.013

Clarke BE, Ziff OJ, Tyzack G, Petrić Howe M, Wang Y, Klein P, Smith CA, Hall CA, Helmy A, Howell M, et al. Human VCP mutant ALS/FTD microglia display immune and lysosomal phenotypes independently of GPNMB. Mol Neurodegener. 2024;19(1):90. doi:10.1186/s13024-024-00773-1

Rodrigues ACZ, Wang ZM, Messi ML, Bonilla HJ, Liu L, Freeman WM, Delbono O. Heart and neural crest derivative 2-induced preservation of sympathetic neurons attenuates sarcopenia with aging. J Cachexia Sarcopenia Muscle. 2021;12(1):91-108. doi:10.1002/jcsm.12644

Adey BN, Cooper-Knock J, Al Khleifat A, Fogh I, van Damme P, Corcia P, Couratier P, Hardiman O, McLaughlin R, Gotkine M, et al. Large-scale analyses of CAV1 and CAV2 suggest their expression is higher in post-mortem ALS brain tissue and affects survival. Front Cell Neurosci. 2023;17:1112405. doi:10.3389/fncel.2023.1112405

Sonkodi B, Nagy ZF, Keller-Pintér A, Klivényi P, Molnár MJ, Széll M. Genetic Variants in SDC3, KCNA2, KCNK1, KCNK16, and Heat Shock Transcription Factor-1 Genes: An Exploratory Analysis Supporting the Piezo2 Channelopathy Hypothesis in Amyotrophic Lateral Sclerosis Onset. Int J Mol Sci. 2025;26(20):10218. doi:10.3390/ijms262010218

Rivner MH, Liu S, Quarles B, Fleenor B, Shen C, Pan J, Mei L. Agrin and low-density lipoprotein-related receptor protein 4 antibodies in amyotrophic lateral sclerosis patients. Muscle Nerve. 2017;55(3):430-432. doi:10.1002/mus.25438

Mòdol-Caballero G, García-Lareu B, Herrando-Grabulosa M, Verdés S, López-Vales R, Pagès G, Chillón M, Navarro X, Bosch A. Specific Expression of Glial-Derived Neurotrophic Factor in Muscles as Gene Therapy Strategy for Amyotrophic Lateral Sclerosis. Neurotherapeutics. 2021;18(2):1113-1126. doi:10.1007/s13311-021-01025-6

Cheng W, Huang J, Fu XQ, Tian WY, Zeng PM, Li Y, Luo ZG. Intrathecal delivery of AAV-NDNF ameliorates disease progression of ALS mice. Mol Ther. 2023;31(11):3277-3289. doi:10.1016/j.ymthe.2023.09.018

Haouari S, Andres CR, Lanznaster D, Marouillat S, Brulard C, Dangoumau A, Ung D, Veyrat-Durebex C, Laumonnier F, Blasco H, et al. Study of Ubiquitin Pathway Genes in a French Population with Amyotrophic Lateral Sclerosis: Focus on HECW1 Encoding the E3 Ligase NEDL1. Int J Mol Sci. 2023;24(2):1268. doi:10.3390/ijms24021268

Arnoux A, Ayme-Dietrich E, Dieterle S, Goy MA, Schann S, Frauli M, Monassier L, Dupuis L. Evaluation of a 5-HT2B receptor agonist in a murine model of amyotrophic lateral sclerosis. Sci Rep. 2021;11(1):23582. doi:10.1038/s41598-021-02900-0

Song SJ, Mao XG, Wang C, Han AG, Yan M, Xue XY. LGR5/GPR49 is implicated in motor neuron specification in nervous system. Neurosci Lett. 2015;584:135-140. doi:10.1016/j.neulet.2014.09.056

Mullick S, Chakraborty A, Porel P, Nath R, Chaudhary P, Islam A, Das J, Pramanik S, Panigrahy UP, Sridhar SB, et al. Decoding Neuroinflammatory Pathways: The Role of the CXCL12-CXCR4/CXCR7 Axis in ALS-Related Cognitive Impairment. Mol Neurobiol. 2026;63(1):513. doi:10.1007/s12035-026-05807-x

Strohm L, Hu Z, Suk Y, Rühmkorf A, Sternburg E, Gattringer V, Riemenschneider H, Berutti R, Graf E, Weishaupt JH, et al. Multi-omics profiling identifies a

deregulated FUS-MAP1B axis in ALS/FTD-associated UBQLN2 mutants. Life Sci Alliance. 2022;5(11):e202101327. doi:10.26508/lsa.202101327

Apostolo D, Ferreira LL, D'Onghia D, Vincenzi F, Vercellino N, Perazzi M, Pirisi M, Cantello R, Minisini R, Mazzini L, et al. Lower Circulating Gas6 Levels Are Associated with Bulbar Phenotype and Faster Disease Progression in Amyotrophic Lateral Sclerosis Patients. Mol Neurobiol. 2025;62(5):6273-6282. doi:10.1007/s12035-024-04671-

Li R, Wang J, Xie W, Liu J, Wang C. UCHL1 from serum and CSF is a candidate biomarker for amyotrophic lateral sclerosis. Ann Clin Transl Neurol. 2020;7(8):1420-1428. doi:10.1002/acn3.51141

Blasco H, Bernard-Marissal N, Vourc'h P, Guettard YO, Sunyach C, Augereau O, Khederchah J, Mouzat K, Antar C, Gordon PH, et al. A rare motor neuron deleterious missense mutation in the DPYSL3 (CRMP4) gene is associated with ALS. Hum Mutat. 2013;34(7):953-960. doi:10.1002/humu.22329

Spatafora MG, Dubin J, Domi T, Lombardi R, Cabras P, Dalla Bella E, Consonni M, Quattrini A, Verri M, Lauria G, et al. Increased CSF levels of soluble AXL at diagnosis correlate with poor prognosis in patients affected by amyotrophic lateral sclerosis. Brain Commun. 2026;8(2):fcag086. doi:10.1093/braincomms/fcag086

Kawamoto Y, Tada M, Asano T, Nakamura H, Jitsuki-Takahashi A, Makihara H, Kubota S, Hashiguchi S, Kunii M, Ohshima T, et al. Phosphorylated CRMP1, axon guidance protein, is a component of spheroids and is involved in axonal pathology in amyotrophic lateral sclerosis. Front Neurol. 2022;13:994676. doi:10.3389/fneur.2022.994676

Petri S, Krampfl K, Kuhlemann K, Dengler R, Grothe C. Preserved expression of fibroblast growth factor (FGF)-2 and FGF receptor 1 in brain and spinal cord of amyotrophic lateral sclerosis patients. Histochem Cell Biol. 2009;131(4):509-519. doi:10.1007/s00418-008-0549-x

Fujita K, Chen X, Homma H, Tagawa K, Amano M, Saito A, Imoto S, Akatsu H, Hashizume Y, Kaibuchi K, et al. Targeting Tyro3 ameliorates a model of PGRN-mutant FTLD-TDP via tau-mediated synaptic pathology. Nat Commun. 2018;9(1):433. doi:10.1038/s41467-018-02821-z

Dunlop RA, Banack SA, Cox PA. L1CAM immunocapture generates a unique extracellular vesicle population with a reproducible miRNA fingerprint. RNA Biol. 2023;20(1):140-148. doi:10.1080/15476286.2023.2198805

Urbano T, Vinceti M, Mandrioli J, Chiari A, Filippini T, Bedin R, Tondelli M, Simonini C, Zamboni G, Shimizu M, et al. Selenoprotein P Concentrations in the Cerebrospinal Fluid and Serum of Individuals Affected by Amyotrophic Lateral Sclerosis, Mild Cognitive Impairment and Alzheimer's Dementia. Int J Mol Sci. 2022;23(17):9865. doi:10.3390/ijms23179865

Vinknes KJ, Elshorbagy AK, Nurk E, Drevon CA, Gjesdal CG, Tell GS, Nygård O, Vollset SE, Refsum H. Plasma stearoyl-CoA desaturase indices: association with lifestyle, diet, and body composition. Obesity (Silver Spring). 2013;21(3):E294-E302. doi:10.1002/oby.20011

Nakamura R, Tohnai G, Atsuta N, Matsuda Y, Morimoto S, Ito D, Katsuno M, Izumi Y, Morita M, Iwata I, et al. A genome-wide association study identifies the GPM6A locus associated with age at onset in ALS. Commun Biol. 2025;8(1):1720. doi:10.1038/s42003-025-09168-4

Wu H, Yang Y, Yi W, Qiu Y, Ma S, Xu J, Fan Y, Chen Y, Chen Y. Coronin 2B deficiency induces nucleolar stress and neuronal apoptosis. Cell Death Dis. 2024;15(6):457. doi:10.1038/s41419-024-06852-x

Wadman RI, Jansen MD, Curial CAD, Groen EJN, Stam M, Wijngaarde CA, Medic J, Sodaar P, van Eijk KR, Huibers MMH, et al. Analysis of FUS, PFN2, TDP-43, and PLS3 as potential disease severity modifiers in spinal muscular atrophy. Neurol Genet. 2019;6(1):e386. doi:10.1212/NXG.0000000000000386

Nógrádi B, Molnár K, Kristóf R, Horváth O, Huang YT, Ridgway Z, Elicegui A, Fuertes-Alvarez S, Alonso-Martin S, Szebeni GJ, et al. The CCL2-CCR2 axis drives neuromuscular denervation in amyotrophic lateral sclerosis. Nat Commun. 2025;16(1):7053. doi:10.1038/s41467-025-62351-3

Pradhan S, Mito T, Khan NA, Olander S, Zhaivoron A, McWilliams TG, Suomalainen A. PDK4 and nutrient responses explain muscle specific manifestation in mitochondrial disease. Clin Transl Med. 2025;15(7):e70404. doi:10.1002/ctm2.70404

Scoles DR, Pflieger LT, Thai KK, Hansen ST, Dansithong W, Pulst SM. ETS1 regulates the expression of ATXN2. Hum Mol Genet. 2012;21(23):5048-5065. doi:10.1093/hmg/dds349

Chen W, Jiang S, Li S, Li C, Xu R. OSMR is a potential driver of inflammation in amyotrophic lateral sclerosis. Neural Regen Res. 2024;19(11):2513-2521. doi:10.4103/1673-5374.391309

Łukaszewicz-Zając M, Mroczko B, Słowik A. Matrix metalloproteinases (MMPs) and their tissue inhibitors (TIMPs) in amyotrophic lateral sclerosis (ALS). J Neural Transm (Vienna). 2014;121(11):1387-1397. doi:10.1007/s00702-014-1205-3

Noristani HN, Sabourin JC, Gerber YN, Teigell M, Sommacal A, Vivanco Md, Weber M, Perrin FE. Brca1 is expressed in human microglia and is dysregulated in human and animal model of ALS. Mol Neurodegener. 2015;10:34. doi:10.1186/s13024-015-0023-x

Zhang PW, Wan ZH, Liu S, Wang J, Sripathi S, Li W, Ahn J, Li S, Fan L, Berlinicke CA, et al. HTRA1-AS1, an ARMS2-region long non-coding RNA, is downregulated in retinas of age-related macular degeneration patients. Preprint. medRxiv. 2025;2025.10.29.25338834. doi:10.1101/2025.10.29.25338834

Szebényi K, Vargová I, Petrova V, Turečková J, Gibbons GM, Řehořová M, Abdelgawad M, Sándor A, Marekova D, Kwok JCF, et al. Inhibition of PHLDA3 expression in human superoxide dismutase 1-mutant amyotrophic lateral sclerosis astrocytes protects against neurotoxicity. Brain Commun. 2024;6(4):fcae244. doi:10.1093/braincomms/fcae244

Glas M, Popp B, Angele B, Koedel U, Chahli C, Schmalix WA, Anneser JM, Pfister HW, Lorenzl S. A role for the urokinase-type plasminogen activator system in amyotrophic lateral sclerosis. Exp Neurol. 2007;207(2):350-356. doi:10.1016/j.expneurol.2007.07.007

Imaizumi K, Fujimori K, Ishii S, Otomo A, Hosoi Y, Miyajima H, Warita H, Aoki M, Hadano S, Akamatsu W, et al. Rostrocaudal Areal Patterning of Human PSC-Derived Cortical Neurons by FGF8 Signaling. eNeuro. 2018;5(2):ENEURO.0368-17.2018. doi:10.1523/ENEURO.0368-17.2018

Mora P, Laisné M, Bourguignon C, Rouault P, Jaspard-Vinassa B, Maître M, Gadeau AP, Renault MA, Horng S, et al. Astrocytic DLL4-NOTCH1 signaling pathway promotes neuroinflammation via the IL-6-STAT3 axis. J Neuroinflammation. 2024;21(1):258. doi:10.1186/s12974-024-03246-w

Berardo A, Emmanuele V, Vargas W, Tanji K, Naini A, Hirano M. Leber hereditary optic neuropathy plus dystonia, and transverse myelitis due to double mutations in MT-ND4 and MT-ND6. J Neurol. 2020;267(3):823-829. doi:10.1007/s00415-019-09619-z

Seki T, Takahashi H, Adachi N, et al. Aggregate formation of mutant protein kinase C gamma found in spinocerebellar ataxia type 14 impairs ubiquitin-proteasome system and induces endoplasmic reticulum stress. Eur J Neurosci. 2007;26(11):3126-3140. doi:10.1111/j.1460-9568.2007.05933.x

Tang Q, Li X, Wang J. Tubulin deacetylase NDST3 modulates lysosomal acidification: Implications in neurological diseases. Bioessays. 2022;44(11):e2200110. doi:10.1002/bies.202200110

Romano G, Holodkov N, Klima R, Feiguin F. TDP-43 regulates GAD1 mRNA splicing and GABA signaling in Drosophila CNS. Sci Rep. 2021;11(1):18761. doi:10.1038/s41598-021-98241-z

Jalaiei A, Asadi MR, Daneshmandpour Y, Rezazadeh M, Ghafouri-Fard S. Clinical, molecular, physiologic, and therapeutic feature of patients with CHRNA4 and CHRNB2 deficiency: A systematic review. J Neurochem. 2025;169(1):e16200. doi:10.1111/jnc.16200

Dugan AJ, Nelson PT, Katsumata Y, Shade LMP, Boehme KL, Teylan MA, Cykowski MD, Mukherjee S, Kauwe JSK, Hohman TJ, et al. Analysis of genes (TMEM106B, GRN, ABCC9, KCNMB2, and APOE) implicated in risk for LATE-NC and hippocampal sclerosis provides pathogenetic insights: a retrospective genetic association study. Acta Neuropathol Commun. 2021;9(1):152. doi:10.1186/s40478-021-01250-2

Andrés-Benito P, Povedano M, Torres P, Portero-Otín M, Ferrer I. Altered Dynein Axonemal Assembly Factor 1 Expression in C-Boutons in Bulbar and Spinal Cord

Motor-Neurons in Sporadic Amyotrophic Lateral Sclerosis. J Neuropathol Exp Neurol. 2019;78(5):416-425. doi:10.1093/jnen/nlz019

Wang Y, Wang X, Niu X, Han K, Ru N, Xiang J, Linghu E. Identification of COL3A1 as a candidate protein involved in the crosstalk between obesity and diarrhea using quantitative proteomics and machine learning. Eur J Pharmacol. 2024;981:176881. doi:10.1016/j.ejphar.2024.176881

Strieder-Barboza C, Flesher CG, Geletka LM, Eichler T, Akinleye O, Ky A, Ehlers AP, Lumeng CN, O'Rourke RW. Lumican modulates adipocyte function in obesity-associated type 2 diabetes. Adipocyte. 2022;11(1):665-675. doi:10.1080/21623945.2022.2154112

Al-Ameri HW, Shetty S, Rahman B, Gopalakrishnan ARK, Ismail AA, Acharya AB. Evaluation of salivary Thy-1 in health, periodontitis, and obesity. Oral Dis. 2024;30(4):2670-2677. doi:10.1111/odi.14652

Benbow JH, Thompson KJ, Cope HL, Brandon-Warner E, Culberson CR, Bossi KL, Li T, Russo MW, Gersin KS, McKillop IH, deLemos AS, et al. Diet-Induced Obesity Enhances Progression of Hepatocellular Carcinoma through Tenascin-C/Toll-Like Receptor 4 Signaling. Am J Pathol. 2016;186(1):145-158. doi:10.1016/j.ajpath.2015.09.015

Martín-Rivada Á, Martos-Moreno GÁ, Guerra-Cantera S, Campillo-Calatayud A, Oxvig C, Frystyk J, Chowen JA, Barrios V, Argente J. Prepubertal Children With Obesity Have High Free IGF-1 Levels and Accelerated Growth Despite Reduced Pappalysin Levels. J Clin Endocrinol Metab. 2025;110(3):e622-e629. doi:10.1210/clinem/dgae288

Koutaki D, Michos A, Bacopoulou F, Charmandari E. The Emerging Role of Sfrp5 and Wnt5a in the Pathogenesis of Obesity: Implications for a Healthy Diet and Lifestyle. Nutrients. 2021;13(7):2459. doi:10.3390/nu13072459

Hagemann T, Czechowski P, Ghosh A, Sun W, Dong H, Noé F, Wolfrum C, Blüher M, Hoffmann A. Laminin α4 Expression in Human Adipose Tissue Depots and Its Association with Obesity and Obesity Related Traits. Biomedicines. 2023;11(10):2806. doi:10.3390/biomedicines11102806

Gao D, Hu S, Zheng X, Lin W, Gao J, Chang K, Zhao D, Wang X, Zhou J, Lu S, et al. SOD3 Is Secreted by Adipocytes and Mitigates High-Fat Diet-Induced Obesity, Inflammation, and Insulin Resistance. Antioxid Redox Signal. 2020;32(3):193-212. doi:10.1089/ars.2018.7628

Cao S, Pan Y, Tang J, Terker AS, Arroyo Ornelas JP, Jin GN, Wang Y, Niu A, Fan X, Wang S, et al. EGFR-mediated activation of adipose tissue macrophages promotes obesity and insulin resistance. Nat Commun. 2022;13(1):4684. doi:10.1038/s41467-022-32348-3

Lin G, Wan X, Liu D, Wen Y, Yang C, Zhao C. COL1A1 as a potential new biomarker and therapeutic target for type 2 diabetes. Pharmacol Res. 2021;165:105436. doi:10.1016/j.phrs.2021.105436

Xiang ZY, Chen SL, Qin XR, Lin SL, Xu Y, Lu LN, Zou HD. Changes and related factors of blood CCN1 levels in diabetic patients. Front Endocrinol (Lausanne). 2023;14:1131993. doi:10.3389/fendo.2023.1131993

Gaikwad AB, Gupta J, Tikoo K. Epigenetic changes and alteration of Fbn1 and Col3A1 gene expression under hyperglycaemic and hyperinsulinaemic conditions. Biochem J. 2010;432(2):333-341. doi:10.1042/BJ20100414

Aparicio JM, Wakisaka A, Takada A, Matsuura N, Yoshiki T. Non-HLA genetic factors and insulin dependent diabetes mellitus in the Japanese: TCRA, TCRB and TCRG, INS, THY1, CD3D and ETS1. Dis Markers. 1990;8(5):283-294.

Li M, Wu M, Zhu H, Hua Y, Ma Z, Yao J, Feng B, Shi B. Serum Tenascin-C and Alarin Levels Are Associated with Cardiovascular Diseases in Type 2 Diabetes Mellitus. Int J Endocrinol. 2022;2022:2009724. doi:10.1155/2022/2009724

Liu X, Xiao D, Zhang D, Pan Y, Guo J, Zhang Y, Li S, Tang Q, Jin X, Sun T. Neutrophil extracellular traps promote bone loss in type 1 diabetes via suppression of the FN1-PI3K/Akt signaling axis. Int Immunopharmacol. 2025;166:115629. doi:10.1016/j.intimp.2025.115629

Liu XK, Qiu QQ, Yu TP, Wang LY, Shi L, Wang B, Sang YQ, Geng HF, Zhang Y, Zhang X, et al. Effect of metformin on Wnt5a in individuals new-onset type 2 diabetes with different body mass indexes: The evidences from the real word

research. J Diabetes Metab Disord. 2023;22(2):1561-1570. doi:10.1007/s40200-023-01286-2

Kuo CW, Chen HL, Tu MY, Chen CM. Serum and urinary SOD3 in patients with type 2 diabetes: comparison with early chronic kidney disease patients and association with development of diabetic nephropathy. Am J Physiol Renal Physiol. 2019;316(1):F32-F41. doi:10.1152/ajprenal.00401.2017

Li Z, Li Y, Overstreet JM, Chung S, Niu A, Fan X, Wang S, Wang Y, Zhang MZ, Harris RC. Inhibition of Epidermal Growth Factor Receptor Activation Is Associated With Improved Diabetic Nephropathy and Insulin Resistance in Type 2 Diabetes. Diabetes. 2018;67(9):1847-1857. doi:10.2337/db17-1513

Castoldi G, Di Gioia CR, Bombardi C, Catalucci D, Corradi B, Gualazzi MG, Leopizzi M, Mancini M, Zerbini G, Condorelli G, et al. MiR-133a regulates collagen 1A1: potential role of miR-133a in myocardial fibrosis in angiotensin II-dependent hypertension. J Cell Physiol. 2012;227(2):850-856. doi:10.1002/jcp.22939

Liu Y, Tang BL, Lu ML, Wang HX. Astragaloside IV improves pulmonary arterial hypertension by increasing the expression of CCN1 and activating the ERK1/2 pathway. J Cell Mol Med. 2023;27(5):622-633. doi:10.1111/jcmm.17681

Samokhin AO, Stephens T, Wertheim BM, Wang RS, Vargas SO, Yung LM, Cao M, Brown M, Arons E, Dieffenbach PB, et al. NEDD9 targets COL3A1 to promote endothelial fibrosis and pulmonary arterial hypertension. Sci Transl Med. 2018;10(445):eaap7294. doi:10.1126/scitranslmed.aap7294

Cha HJ, Kim HY, Kim HS. Sulfatase 1 mediates the attenuation of Ang II-induced hypertensive effects by CCL5 in vascular smooth muscle cells from spontaneously hypertensive rats. Cytokine. 2018;110:1-8. doi:10.1016/j.cyto.2017.12.027

Kawarazaki W, Mizuno R, Nishimoto M, Ayuzawa N, Hirohama D, Ueda K, Kawakami-Mori F, Oba S, Marumo T, Fujita T. Salt causes aging-associated hypertension via vascular Wnt5a under Klotho deficiency. J Clin Invest. 2020;130(8):4152-4166. doi:10.1172/JCI134431

Shima N, Yamamura A, Fujiwara M, Amano T, Matsumoto K, Sekine T, Okano H, Kondo R, Suzuki Y, Yamamura H. Up-regulated expression of two-pore domain K+ channels, KCNK1 and KCNK2, is involved in the proliferation and migration of pulmonary arterial smooth muscle cells in pulmonary arterial hypertension. Front Cardiovasc Med. 2024;11:1343804. doi:10.3389/fcvm.2024.1343804

Chi Z, Do VQ, Kausar R, Kim HK, Nguyen NTT, Le TPH, Lee J, Baek IJ, Lee SW, Kim JH, et al. HDAC6 inhibition upregulates endothelial SOD3 expression via Sp1 acetylation and attenuates angiotensin II-induced hypertension. FEBS J. 2025;292(10):2624-2644. doi:10.1111/febs.70026

Rafikova O, Rafikov R, Kangath A, Qu N, Aggarwal S, Sharma S, Desai J, Fields T, Ludewig B, Yuan JX, et al. Redox regulation of epidermal growth factor receptor signaling during the development of pulmonary hypertension. Free Radic Biol Med. 2016;95:96-111. doi:10.1016/j.freeradbiomed.2016.02.029

Kuganathan A, Leal M, Mehta N, Lu V, Gao B, MacDonald M, Dickhout J, Krepinsky JC. Follistatin lowers blood pressure and improves vascular structure and function in essential and secondary hypertension. Hypertens Res. 2024;47(11):3158-3172. doi:10.1038/s41440-024-01872-8

Deng J, Yang G, Zhong N, Liang L, Chen H. Upregulation of Angiomotin-Like 2 Ameliorates Experimental Pulmonary Arterial Hypertension by Inactivating YAP1 Signaling. J Cardiovasc Pharmacol. 2024;84(3):356-369. doi:10.1097/FJC.0000000000001606

Chen W, Wu X, Hu J, Liu X, Guo Z, Wu J, Shao Y, Hao M, Zhang S, Hu W, et al. The translational potential of miR-26 in atherosclerosis and development of agents for its target genes ACC1/2, COL1A1, CPT1A, FBP1, DGAT2, and SMAD7. Cardiovasc Diabetol. 2024;23(1):21. doi:10.1186/s12933-024-02119-z

Yao Q, Liu J, Cui Q, Jiang T, Xie X, Du X, Zhao Z, Lai B, Xiao L, Wang N. CCN1/Integrin α5β1 Instigates Free Fatty Acid-Induced Hepatocyte Lipid Accumulation and Pyroptosis through NLRP3 Inflammasome Activation. Nutrients. 2022;14(18):3871. doi:10.3390/nu14183871

Awan S, Lambert M, Imtiaz A, Alpy F, Tomasetto C, Oulad-Abdelghani M, Schaeffer C, Moritz C, Julien-David D, Najib S, et al. Wnt5a Promotes Lysosomal Cholesterol Egress and Protects Against Atherosclerosis. Circ Res. 2022;130(2):184-199. doi:10.1161/CIRCRESAHA.121.318881

Cui R, Gao M, Qu S, Liu D. Overexpression of superoxide dismutase 3 gene blocks high-fat diet-induced obesity, fatty liver and insulin resistance. Gene Ther. 2014;21(9):840-848. doi:10.1038/gt.2014.64

Fang Q, Zou C, Zhong P, Lin F, Li W, Wang L, Zhang Y, Zheng C, Wang Y, Li X, et al. EGFR mediates hyperlipidemia-induced renal injury via regulating inflammation and oxidative stress: the detrimental role and mechanism of EGFR activation. Oncotarget. 2016;7(17):24361-24373. doi:10.18632/oncotarget.8222

Tejera-Muñoz A, Rodríguez I, Del Río-García Á, Mohamedi Y, Martín M, Chiminazzo V, Suárez-Álvarez B, López-Larrea C, Ruiz-Ortega M, Rodrigues-Díez RR. The CCN2 Polymorphism rs12526196 Is a Risk Factor for Ascending Thoracic Aortic Aneurysm. Int J Mol Sci. 2022;23(23):15406. doi:10.3390/ijms232315406

Li YJ, Ge HY, Zhang GG, Chen HY, Xi YJ, Wang K, Huang YL, Zhang C, Fan X, Yan XQ. Fibroblast growth factor 1 alleviates diabetic nephropathy by reducing renal lipid accumulation in diabetic kidney. World J Diabetes. 2026;17(2):112475. doi:10.4239/wjd.v17.i2.112475

Liu Z, Wang Y, Li L, Liu L, Li Y, Li Z, Xie Y, Yu F. SNAI2, a potential crossing point between cancer and cardiovascular disease. FASEB J. 2025;39(5):e70459. doi:10.1096/fj.202500198R

Di M, Zhang Y, Zeng R, Liu X, Chen W, Zhang M, Zhang C, Li M, Zhang M. The pro-angiogenesis effect of miR33a-5p/Ets-1/DKK1 signaling in ox-LDL induced HUVECs. Int J Biol Sci. 2021;17(15):4122-4139. doi:10.7150/ijbs.60302

Xiong X, Zhang L, Li Y, Guo S, Chen W, Huang L, Luo Y. Calcium Channel Subunit α2δ-1 as a Potential Biomarker Reflecting Illness Severity and Neuroinflammation in Patients with Acute Ischemic Stroke. J Stroke Cerebrovasc Dis. 2021;30(8):105874. doi:10.1016/j.jstrokecerebrovasdis.2021.105874

Luo C, Tan B, Chu L, Chen L, Zhong X, Jiang Y, Yan Y, Mo F, Wang H, Yang F. Enhanced fibrotic potential of COL1A1hiNR4A1low fibroblasts in ischemic heart revealed by transcriptional dynamics heterogeneity analysis at both bulk and single-cell levels. Front Cardiovasc Med. 2025;11:1460813. doi:10.3389/fcvm.2024.1460813

Alzhrani AA, Rasool M, Karim S, Alhejin A, Haque A, Morsi M, Alama MN, Pushparaj PN. KDM3A knockdown regulates COMP, LOX, COL8A1 and ACOT1 genes in myocardial fibrosis. Bioinformation. 2024;20(4):305-313. doi:10.6026/973206300200305

Yang W, Bai J, Song X, Zhang S, Chen N, You T, Yi K, Li Z, Xie D, Xie X. CCN1 gene polymorphisms associated with congenital heart disease susceptibility in Northwest Chinese population from different high-altitude areas. Environ Sci Pollut Res Int. 2021;28(40):56927-56937. doi:10.1007/s11356-021-14428-x

Norgan Radler C, Ku K, Hodge A, Wang T, Moore P, Sathyamoorthy M. The Novel Association of a Single Nucleotide Variant in the COL3A1 Gene with Diffuse Coronary Aneurysms. Curr Issues Mol Biol. 2025;47(2):82. doi:10.3390/cimb47020082

Osawa I, Akita K, Hasegawa K, Fifer MA, Tower-Rader A, Reilly MP, Maurer MS, Stitziel NO, Javaheri A, Shimada YJ. et al. Plasma SVEP1 Levels Predict Cardiovascular Events in Hypertrophic Cardiomyopathy Beyond Conventional Clinical Risk Models Including NT-proBNP. Circ Heart Fail. 2025;18(2):e012343. doi:10.1161/CIRCHEARTFAILURE.124.012343

Yi J, Chen K, Cao Y, Wen C, An L, Tong R, Wu X, Gao H. Up-regulated novel-miR-17 promotes hypothermic reperfusion arrhythmias by negatively targeting Gja1 and mediating activation of the PKC/c-Jun signaling pathway. J Mol Cell Cardiol. 2024;193:1-10. doi:10.1016/j.yjmcc.2024.05.009

Cao W, Song S, Fang G, Li Y, Wang Y, Wang QS. Cadherin-11 Deficiency Attenuates Ang-II-Induced Atrial Fibrosis and Susceptibility to Atrial Fibrillation. J Inflamm Res. 2021;14:2897-2911. doi:10.2147/JIR.S306073

Su T, Luo T, Lin Y, Liu J, Lai B, Xiao Z. Targeting LUM-mediated inflammatory cell communication and fibroblast apoptosis with SFI in Heart Failure. SLAS Technol. 2026;37:100399. doi:10.1016/j.slast.2026.100399

Li Y, Song D, Mao L, Abraham DM, Bursac N. Lack of Thy1 defines a pathogenic fraction of cardiac fibroblasts in heart failure. Biomaterials. 2020;236:119824. doi:10.1016/j.biomaterials.2020.119824

Shi W, Sun H, Yao Q, Liu H, Zhang L, Han W. Phellodendrine ameliorates intestinal inflammation and protects mucosal barrier via modulating COL1A1, VCAM1 and IL-17 a. Int Immunopharmacol. 2025;152:114403. doi:10.1016/j.intimp.2025.114403

Li Q, Ye L, Talapaneni S, Meng Y, Wang CR, Kalindjian K, Phan J, Chen Y, Demer LL, Tintut Y, et al. COL8A1 regulates endothelial phenotype in inflammatory endothelial-to-mesenchymal transition. Am J Physiol Heart Circ Physiol. 2025;329(5):H1331-H1346. doi:10.1152/ajpheart.00339.2025

Jiang R, Tang J, Zhang X, He Y, Yu Z, Chen S, Xia J, Lin J, Ou Q. CCN1 Promotes Inflammation by Inducing IL-6 Production via α6β1/PI3K/Akt/NF-κB Pathway in Autoimmune Hepatitis. Front Immunol. 2022;13:810671. doi:10.3389/fimmu.2022.810671

Tang H, Fu L, Yang C, Chen L, Wu X, Sun J, Chen Z, Xiong J, Li S, Yang L, et al. CDH11 Contributes to Airway Neutrophilic Inflammation in Severe Asthma via FGFR1. FASEB J. 2025;39(23):e71303. doi:10.1096/fj.202501899RR

Lohr K, Sardana H, Lee S, Wu F, Huso DL, Hamad AR, Chakravarti S. Extracellular matrix protein lumican regulates inflammation in a mouse model of colitis. Inflamm Bowel Dis. 2012;18(1):143-151. doi:10.1002/ibd.21713

Schubert K, Polte T, Bönisch U, Schader S, Holtappels R, Hildebrandt G, Lehmann J, Simon JC, Anderegg U, Saalbach A. Thy-1 (CD90) regulates the extravasation of leukocytes during inflammation. Eur J Immunol. 2011;41(3):645-656. doi:10.1002/eji.201041117

Imanaka-Yoshida K. Tenascin-C in Heart Diseases-The Role of Inflammation. Int J Mol Sci. 2021;22(11):5828. doi:10.3390/ijms22115828

Zhu H, Xu X, Zhu X, Huang J, Cai L, Gao B, Yang C, Wang S, Chen Q, Fang X, et al. SULF1 and EPB41L3: Potential Biomarkers of Acute Myocardial Infarction and the Vascular Inflammatory Milieu. J Inflamm Res. 2026;19:594275. doi:10.2147/JIR.S594275

Yu W, Ye H, Li Y, Bao X, Ni Y, Chen X, Sun Y, Chen A, Zhou W, Li J. Pneumocystis carinii infection drives upregulation of Fn1 expression that causes pulmonary fibrosis with an inflammatory response. Rev Iberoam Micol. 2024;41(1):17-26. doi:10.1016/j.riam.2024.04.002

Fu XH, Chen CZ, Wang Y, Peng YX, Wang WH, Yuan B, Gao Y, Jiang H, Zhang JB. COL1A1 affects apoptosis by regulating oxidative stress and autophagy in bovine cumulus cells. Theriogenology. 2019;139:81-89. doi:10.1016/j.theriogenology.2019.07.024

Yoshida Y, Togi K, Matsumae H, Nakashima Y, Kojima Y, Yamamoto H, Ono K, Nakamura T, Kita T, Tanaka M. CCN1 protects cardiac myocytes from oxidative stress via beta1 integrin-Akt pathway. Biochem Biophys Res Commun. 2007;355(3):611-618. doi:10.1016/j.bbrc.2007.01.195

Li C, Hao R, Li C, Liu L, Ding Z. Integration of single-cell and bulk RNA sequencing data using machine learning identifies oxidative stress-related genes LUM and PCOLCE2 as potential biomarkers for heart failure. Int J Biol Macromol. 2025;300:140793. doi:10.1016/j.ijbiomac.2025.140793

Chen J, Li HY, Wang D, Guo XZ. Delphinidin protects β2m-/Thy1+ bone marrow-derived hepatocyte stem cells against TGF-β1-induced oxidative stress and apoptosis through the PI3K/Akt pathway in vitro. Chem Biol Interact. 2019;297:109-118. doi:10.1016/j.cbi.2018.10.019

Hasanzadeh Z, Nourazarian A, Nikanfar M, Laghousi D, Vatankhah AM, Sadrirad S. Evaluation of the Serum Dkk-1, Tenascin-C, Oxidative Stress Markers Levels and Wnt Signaling Pathway Genes Expression in Patients with Alzheimer's Disease. J Mol Neurosci. 2021;71(4):879-887. doi:10.1007/s12031-020-01710-9

Liu S, Xie K, Zhao H, Sun Y, Song X, Xu L, Yan Y, Wang T, Nyoja S, Gao J, et al. Aflatoxin B1 accelerates diabetic nephropathy progression via ITGA11/LTBP1-dependent oxidative and fibrotic pathways: Evidence from multi-

omics and molecular simulations. Chem Biol Interact. 2026;430:111974. doi:10.1016/j.cbi.2026.111974

Zhao Y, Zhang C, Huang Y, Yu Y, Li R, Li M, Liu N, Liu P, Qiao J. Up-regulated expression of WNT5a increases inflammation and oxidative stress via PI3K/AKT/NF-κB signaling in the granulosa cells of PCOS patients. J Clin Endocrinol Metab. 2015;100(1):201-211. doi:10.1210/jc.2014-2419

Wert KJ, Velez G, Cross MR, Wagner BA, Teoh-Fitzgerald ML, Buettner GR, McAnany JJ, Olivier A, Tsang SH, Harper MM, et al. Extracellular superoxide dismutase (SOD3) regulates oxidative stress at the vitreoretinal interface. Free Radic Biol Med. 2018;124:408-419. doi:10.1016/j.freeradbiomed.2018.06.024

Chen XD, Su MY, Chen TT, Hong HY, Han AD, Li WS. Oxidative stress affects retinal pigment epithelial cell survival through epidermal growth factor receptor/AKT signaling pathway. Int J Ophthalmol. 2017;10(4):507-514. doi:10.18240/ijo.2017.04.02

Valentijn FA, Knoppert SN, Pissas G, Rodrigues-Diez RR, Marquez-Exposito L, Broekhuizen R, Mokry M, Kester LA, Falke LL, Goldschmeding R, et al. CCN2 Aggravates the Immediate Oxidative Stress-DNA Damage Response following Renal Ischemia-Reperfusion Injury. Antioxidants (Basel). 2021;10(12):2020. doi:10.3390/antiox10122020

Kaut O, Sharma A, Schmitt I, Hurlemann R, Wüllner U. DNA methylation of DLG4 and GJA-1 of human hippocampus and prefrontal cortex in major depression is unchanged in comparison to healthy individuals. J Clin Neurosci. 2017;43:261-263. doi:10.1016/j.jocn.2017.05.030

Peng R, Li D, Li Y. Relationships Between Circulating Tenascin-C Levels and Gonadal Hormones in Male Patients with Depressive Disorder: A Retrospective, Cross-Sectional Study. Lab Med. 2022;53(3):273-277. doi:10.1093/labmed/lmab094

Ortiz-Matamoros A, Arias C. Chronic infusion of Wnt7a, Wnt5a and Dkk-1 in the adult hippocampus induces structural synaptic changes and modifies anxiety and memory performance. Brain Res Bull. 2018;139:243-255. doi:10.1016/j.brainresbull.2018.03.008

Congiu C, Minelli A, Bonvicini C, Bortolomasi M, Sartori R, Maj C, Scassellati C, Maina G, Trabucchi L, Segala M, et al. The role of the potassium channel gene KCNK2 in major depressive disorder. Psychiatry Res. 2015;225(3):489-492. doi:10.1016/j.psychres.2014.11.061

McFarland DC, Jutagir DR, Rosenfeld B, Pirl W, Miller AH, Breitbart W, Nelson C. Depression and inflammation among epidermal growth factor receptor (EGFR) mutant nonsmall cell lung cancer patients. Psychooncology. 2019;28(7):1461-1469. doi:10.1002/pon.5097

Deng Z, Deng S, Zhang MR, Tang MM. Fibroblast Growth Factors in Depression. Front Pharmacol. 2019;10:60. doi:10.3389/fphar.2019.00060

Jiang YH, Zhai CY, Ying JN, Wu S, Liu JG, Xu C. Identification and validation of Slit3 as a depression biomarker modulating dynorphinergic neurons in the hypothalamic paraventricular nucleus. Neuropharmacology. 2026;283:110765. doi:10.1016/j.neuropharm.2025.110765

Kari D, Mijiti P, Zou S, Zhang P. Study on the correlation between suicidal ideation and ABI3BP gene、DPYSL2 gene methylation in pediatric bipolar disorder with depressive episode. Heliyon. 2023;10(1):e23680. doi:10.1016/j.heliyon.2023.e23680

Chao B, Zhang L, Pan J, Zhang Y, Chen Y, Xu M, Huang S. Stanniocalcin-1 Overexpression Prevents Depression-Like Behaviors Through Inhibition of the ROS/NF-κB Signaling Pathway. Front Psychiatry. 2021;12:644383. doi:10.3389/fpsyt.2021.644383

Huo X, Wu Z, Zhou X, Zhou Y, Liu J, Li H, Wu Y, Huang Y, Feng G, Hu X, et al. Diminazene Aceturate Ameliorates Hypertension-Induced Cognitive Impairment by Disrupting the CCN1-Integrin αvβ6-TGF-β Axis and Preserving Mitochondrial Integrity. FASEB J. 2026;40(6):e71682. doi:10.1096/fj.202503973R

Kajiwara Y, Wang E, Wang M, Sin WC, Brennand KJ, Schadt E, Naus CC, Buxbaum J, Zhang B. GJA1 (connexin43) is a key regulator of Alzheimer's disease pathogenesis. Acta Neuropathol Commun. 2018;6(1):144. doi:10.1186/s40478-018-0642-x

Magen I, Torres ER, Dinh D, Chung A, Masliah E, Chesselet MF. Social Cognition Impairments in Mice Overexpressing Alpha-Synuclein Under the Thy1 Promoter, a Model of Pre-manifest Parkinson's Disease. J Parkinsons Dis. 2015;5(3):669-680. doi:10.3233/JPD-140503

Hasanzadeh Z, Nourazarian A, Nikanfar M, Laghousi D, Vatankhah AM, Sadrirad S. Evaluation of the Serum Dkk-1, Tenascin-C, Oxidative Stress Markers Levels and Wnt Signaling Pathway Genes Expression in Patients with Alzheimer's Disease. J Mol Neurosci. 2021;71(4):879-887. doi:10.1007/s12031-020-01710-9

Fei F, Shi J, Xi J, Xu Y, Ying S, Fan X, Lu W, Li Z, Li M, Wang Y, et al. Fibronectin1-Expressing Subicular Circuits Selectively Govern the Retrieval of Novel Object Recognition. Adv Sci (Weinh). 2026. doi:10.1002/advs.202516399

Ding S, Xu Z, Yang J, Liu L, Huang X, Wang X, Zhuge Q. The Involvement of the Decrease of Astrocytic Wnt5a in the Cognitive Decline in Minimal Hepatic Encephalopathy. Mol Neurobiol. 2017;54(10):7949-7963. doi:10.1007/s12035-016-0216-5

Chen J, Zeng F, Forrester SJ, Eguchi S, Zhang MZ, Harris RC. Expression and Function of the Epidermal Growth Factor Receptor in Physiology and Disease. Physiol Rev. 2016;96(3):1025-1069. doi:10.1152/physrev.00030.2015

Liu H, Zheng N, Zhang Z, Wu S, Yu S, Wang Y, Dong Z, Zong S, Wang X, Lu Z. Methionine restriction inhibits the TGF-β1/CCN2/NF-κB pathway to attenuate astrocyte inflammation and cognitive impairment in the APP/PS1 mice. Int Immunopharmacol. 2025;166:115498. doi:10.1016/j.intimp.2025.115498

Pulukuri SV, Spurlock EE, Tuz-Zahra F, Tripodis Y, Sampani K, Nicks R, Meng G, Alvarez VE, McKee AC, Xia W, et al. Vitreous STMN2 levels reflect TDP-43-associated neurodegeneration in postmortem eyes and brains. J Alzheimers Dis Rep. 2025;9:25424823251392553. doi:10.1177/25424823251392553

Zhang N, Liao Z, Wu P, Fang H, Cai G. Hypermethylation of EFEMP1 in the Hippocampus May Be Related to the Deficit in Spatial Memory of Rat Neonates Triggered by Repeated Administration of Propofol. Biomed Res Int. 2020;2020:8851480. doi:10.1155/2020/8851480

Tsitoura E, Trachalaki A, Vasarmidi E, Mastrodemou S, Margaritopoulos GA, Kokosi M, Fanidis D, Galaris A, Aidinis V, Renzoni E, et al. Collagen 1a1 Expression by Airway Macrophages Increases In Fibrotic ILDs and Is Associated With FVC Decline and Increased Mortality. Front Immunol. 2021;12:645548. doi:10.3389/fimmu.2021.645548

Morrell ED, Grazioli S, Hung C, Kajikawa O, Kosamo S, Stapleton RD, Gharib SA, Amado-Rodríguez L, Albaiceta G, Wurfel MM, et al. Alveolar CCN1 is associated with mechanical stretch and acute respiratory distress syndrome severity. Am J Physiol Lung Cell Mol Physiol. 2020;319(5):L825-L832. doi:10.1152/ajplung.00073.2020

Wan T, Ye J, Wu P, Cheng M, Jiang B, Wang H, Li J, Ma J, Wang L, Huang X. Recurrent pneumothorax and intrapulmonary cavitary lesions in a male patient with vascular Ehlers-Danlos syndrome and a novel missense mutation in the COL3A1 gene: a case report. BMC Pulm Med. 2020;20(1):149. doi:10.1186/s12890-020-1164-4

Zhou WQ, Wang P, Shao QP, Wang J. Lipopolysaccharide promotes pulmonary fibrosis in acute respiratory distress syndrome (ARDS) via lincRNA-p21 induced inhibition of Thy-1 expression. Mol Cell Biochem. 2016;419(1-2):19-28. doi:10.1007/s11010-016-2745-7

Donovan C, Bai X, Chan YL, Feng M, Ho KF, Guo H, Chen H, Oliver BG. Tenascin C in Lung Diseases. Biology (Basel). 2023;12(2):199. doi:10.3390/biology12020199

Tu M, Lu C, Jia H, Chen S, Wang Y, Li J, Cheng J, Yang M, Zhang G. SULF1 expression is increased and promotes fibrosis through the TGF-β1/SMAD pathway in idiopathic pulmonary fibrosis. J Transl Med. 2024;22(1):885. doi:10.1186/s12967-024-05698-3

Wang F, Zhang J, Yuan Y, Zhou J, Pang S, Li X, Qiu A. Study on the role of FN1 in chronic obstructive pulmonary disease. Gene. 2025;963:149551. doi:10.1016/j.gene.2025.149551

Huang J, Li X, Huang L, Liu H, Tang J. Mechanistic Insights and Therapeutic Potential of Wnt5a Signaling in Alveolar Epithelial Cell Development and

Bronchopulmonary Dysplasia. Stem Cell Rev Rep. 2025;21(8):2372-2385. doi:10.1007/s12015-025-10951-3

Abouhashem AS, Singh K, Azzazy HME, Sen CK. Is Low Alveolar Type II Cell SOD3 in the Lungs of Elderly Linked to the Observed Severity of COVID-19?. Antioxid Redox Signal. 2020;33(2):59-65. doi:10.1089/ars.2020.8111

Venkataraman T, Frieman MB. The role of epidermal growth factor receptor (EGFR) signaling in SARS coronavirus-induced pulmonary fibrosis. Antiviral Res. 2017;143:142-150. doi:10.1016/j.antiviral.2017.03.022

Feng L, Li M, Ren J, Li Y, Wang Q, Zhang P, Zhang X, Wang T, Li Y. Proteomic Analysis Reveals that Di Dang Decoction Protects Against Acute Intracerebral Hemorrhage Stroke in Rats by Regulating S100a8, S100a9 Col1a1, and Col1a2. Neuropsychiatr Dis Treat. 2021;17:3301-3314. doi:10.2147/NDT.S331688

Lee GA, Chang YW, Lai JH, Chang TH, Huang SW, Yang CH, Shen TA, Lin WL, Wu YC, Tseng LW, et al. CCN1 Is a Therapeutic Target for Reperfused Ischemic Brain Injury. Transl Stroke Res. 2025;16(4):1044-1061. doi:10.1007/s12975-024-01279-0

Lv W, Lin Y, Song W, Sun K, Yu H, Zhang Y, Zhang C, Li L, Suo M, Hui R, et al. Variants of COL3A1 are associated with the risk of stroke recurrence and prognosis in the Chinese population: a prospective study. J Mol Neurosci. 2014;53(2):196-203. doi:10.1007/s12031-014-0283-x

Li Y, Chen W, Feng J. Astrocyte-derived Exosomal GJA1-20 k Targets Pink1-mediated Mitophagy to Attenuate Traumatic Brain Injury. Transl Stroke Res. 2025;16(6):2119-2129. doi:10.1007/s12975-025-01374-w

Wang PR, Masuda Y, Kitamura H, Yamanaka N. Tubulointerstitial injury of Thy-1 nephritis in uninephrectomized stroke-prone spontaneously hypertensive rats. J Nippon Med Sch. 2001;68(4):301-309. doi:10.1272/jnms.68.301

Chelluboina B, Chokkalla AK, Mehta SL, Morris-Blanco KC, Bathula S, Sankar S, Park JS, Vemuganti R. Tenascin-C induction exacerbates post-stroke brain damage. J Cereb Blood Flow Metab. 2022;42(2):253-263. doi:10.1177/0271678X211056392

Hou Y, Zhang L, Ma W, Jiang Y. NGR1 reduces neuronal apoptosis through regulation of ITGA11 following subarachnoid hemorrhage. Mol Med Rep. 2025;31(3):67. doi:10.3892/mmr.2025.13432

Mai N, Miller-Rhodes K, Prifti V, Kim M, O'Reilly MA, Halterman MW. Lung-Derived SOD3 Attenuates Neurovascular Injury After Transient Global Cerebral Ischemia. J Am Heart Assoc. 2019;8(9):e011801. doi:10.1161/JAHA.118.011801

Nakano F, Kanamaru H, Kawakita F, Liu L, Nakatsuka Y, Nishikawa H, Okada T, Suzuki H. Epidermal Growth Factor Receptor Mediates Neuronal Apoptosis After Subarachnoid Hemorrhage in Mice. Stroke. 2023;54(6):1616-1626. doi:10.1161/STROKEAHA.122.041977

Arac A, Brownell SE, Rothbard JB, Chen C, Ko RM, Pereira MP, Albers GW, Steinman L, Steinberg GK. Systemic augmentation of alphaB-crystallin provides therapeutic benefit twelve hours post-stroke onset via immune modulation. Proc Natl Acad Sci U S A. 2011;108(32):13287-13292. doi:10.1073/pnas.1107368108

Le Pichon CE, Dominguez SL, Solanoy H, Ngu H, Lewin-Koh N, Chen M, Eastham-Anderson J, Watts R, Scearce-Levie K. EGFR inhibitor erlotinib delays disease progression but does not extend survival in the SOD1 mouse model of ALS. PLoS One. 2013;8(4):e62342. doi:10.1371/journal.pone.0062342

Lin J, Huang P, Chen W, Ye C, Su H, Yao X. Key Molecules and Pathways Underlying Sporadic Amyotrophic Lateral Sclerosis: Integrated Analysis on Gene Expression Profiles of Motor Neurons. Front Genet. 2020;11:578143. doi:10.3389/fgene.2020.578143

Adey BN, Cooper-Knock J, Al Khleifat A, Fogh I, van Damme P, Corcia P, Couratier P, Hardiman O, McLaughlin R, Gotkine M, et al. Large-scale analyses of CAV1 and CAV2 suggest their expression is higher in post-mortem ALS brain tissue and affects survival. Front Cell Neurosci. 2023;17:1112405. doi:10.3389/fncel.2023.1112405

Camacho Leal Mdel P, Sciortino M, Tornillo G, Colombo S, Defilippi P, Cabodi S. p130Cas/BCAR1 scaffold protein in tissue homeostasis and pathogenesis. Gene. 2015;562(1):1-7. doi:10.1016/j.gene.2015.02.027

Zhang J, Hu J, Liu R, Zhou T, Luo X, Liang P, Xie Z, Zhao Q, Chen Y, Du D, et al. YAP maintains the dynamics of TDP-43 condensates and antagonizes TDP-43 pathological aggregates. Nat Cell Biol. 2025;27(7):1148-1160. doi:10.1038/s41556-025-01685-y

Bonfanti E, Bonifacino T, Raffaele S, Milanese M, Morgante E, Bonanno G, Abbracchio MP, Fumagalli M. Abnormal Upregulation of GPR17 Receptor Contributes to Oligodendrocyte Dysfunction in SOD1 G93A Mice. Int J Mol Sci. 2020;21(7):2395. doi:10.3390/ijms21072395

Mizuno Y, Amari M, Takatama M, Aizawa H, Mihara B, Okamoto K. Transferrin localizes in Bunina bodies in amyotrophic lateral sclerosis. Acta Neuropathol. 2006;112(5):597-603. doi:10.1007/s00401-006-0122-4

Mullick S, Chakraborty A, Porel P, Nath R, Chaudhary P, Islam A, Das J, Pramanik S, Panigrahy UP, Sridhar SB, et al. Decoding Neuroinflammatory Pathways: The Role of the CXCL12-CXCR4/CXCR7 Axis in ALS-Related Cognitive Impairment. Mol Neurobiol. 2026;63(1):513doi:10.1007/s12035-026-05807-xv

Sakowski SA, Schuyler AD, Feldman EL. Insulin-like growth factor-I for the treatment of amyotrophic lateral sclerosis. Amyotroph Lateral Scler. 2009;10(2):63-73. doi:10.1080/17482960802160370

Łukaszewicz-Zając M, Mroczko B, Słowik A. Matrix metalloproteinases (MMPs) and their tissue inhibitors (TIMPs) in amyotrophic lateral sclerosis (ALS). J Neural Transm (Vienna). 2014;121(11):1387-1397. doi:10.1007/s00702-014-1205-3

Rasà DM, Stoppa I, Bérenger-Currias N, Pasho E, Ciura S, Kabashi E, Martinat C, Boido M. Stress exposure affects amyotrophic lateral sclerosis pathogenesis via PI3K/Akt and focal adhesion pathways: evidence from three experimental models. Sci Rep. 2025;15(1):17583. doi:10.1038/s41598-025-02167-9

Sánchez-Torres JL, Yescas-Gómez P, Torres-Romero J, Espinosa OR, Canovas LL, Tecalco-Cruz ÁC, Ponce-Regalado MD, Alvarez-Sánchez ME. Matrix metalloproteinases deregulation in amyotrophic lateral sclerosis. J Neurol Sci. 2020;419:117175. doi:10.1016/j.jns.2020.117175

Guo W, Vandoorne T, Steyaert J, Staats KA, Van Den Bosch L. The multifaceted role of kinases in amyotrophic lateral sclerosis: genetic, pathological and therapeutic implications. Brain. 2020;143(6):1651-1673. doi:10.1093/brain/awaa022

Shtilbans A, Choi SG, Fowkes ME, Khitrov G, Shahbazi M, Ting J, Zhang W, Sun Y, Sealfon SC, Lange DJ. Differential gene expression in patients with amyotrophic lateral sclerosis. Amyotroph Lateral Scler. 2011;12(4):250-256. doi:10.3109/17482968.2011.560946

Liu Y, Ding M, Pan S, Zhou R, Yao J, Fu R, Yu H, Lu Z. MicroRNA-23a-3p Is Upregulated in Plasma Exosomes of Bulbar-onset ALS Patients and Targets ERBB4. Neuroscience. 2023;524:65-78. doi:10.1016/j.neuroscience.2023.05.030

Zhu Y, Li M, He Z, Pang X, Du R, Yu W, Zhang J, Bai J, Wang J, Huang X. Evaluating the causal association between microRNAs and amyotrophic lateral sclerosis. Neurol Sci. 2023;44(10):3567-3575. doi:10.1007/s10072-023-06860-3

Yuan X, Cao B, Wu Y, Chen Y, Wei Q, Ou R, Yang J, Chen X, Zhao B, et al. Association analysis of SNP rs11868035 in SREBF1 with sporadic Parkinson's disease, sporadic amyotrophic lateral sclerosis and multiple system atrophy in a Chinese population. Neurosci Lett. 2018;664:128-132. doi:10.1016/j.neulet.2017.11.015

Schiaffino L, Bonafede R, Scambi I, Parrella E, Pizzi M, Mariotti R. Acetylation state of RelA modulated by epigenetic drugs prolongs survival and induces a neuroprotective effect on ALS murine model. Sci Rep. 2018;8(1):12875. doi:10.1038/s41598-018-30659-4

Song J, Dikwella N, Sinske D, Roselli F, Knöll B. SRF deletion results in earlier disease onset in a mouse model of amyotrophic lateral sclerosis. JCI Insight. 2023;8(15):e167694. doi:10.1172/jci.insight.167694

Chen ZS, Ou M, Taylor S, Dafinca R, Peng SI, Talbot K, Chan HYE. Mutant GGGGCC RNA prevents YY1 from binding to Fuzzy promoter which stimulates Wnt/β-catenin pathway in C9ALS/FTD. Nat Commun. 2023;14(1):8420. doi:10.1038/s41467-023-44215-w

Turalde CWR, Moalong KMC, Espiritu AI, Prado MB Jr. Perampanel for amyotrophic lateral sclerosis: A systematic review and meta-analysis. Neurol Sci. 2022;43(2):889-897. doi:10.1007/s10072-022-05867-6

Nakazato T, Kanai K, Kataura T, Nojiri S, Hattori N, Saiki S. Plasma taurine is an axonal excitability-translatable biomarker for amyotrophic lateral sclerosis. Sci Rep. 2022;12(1):9155. Published 2022 Jun 1. doi:10.1038/s41598-022-13397-6

Norris FH, Tan Y, Fallat RJ, Elias L. Trial of oral physostigmine in amyotrophic lateral sclerosis. Clin Pharmacol Ther. 1993;54(6):680-682. doi:10.1038/clpt.1993.206

Figures

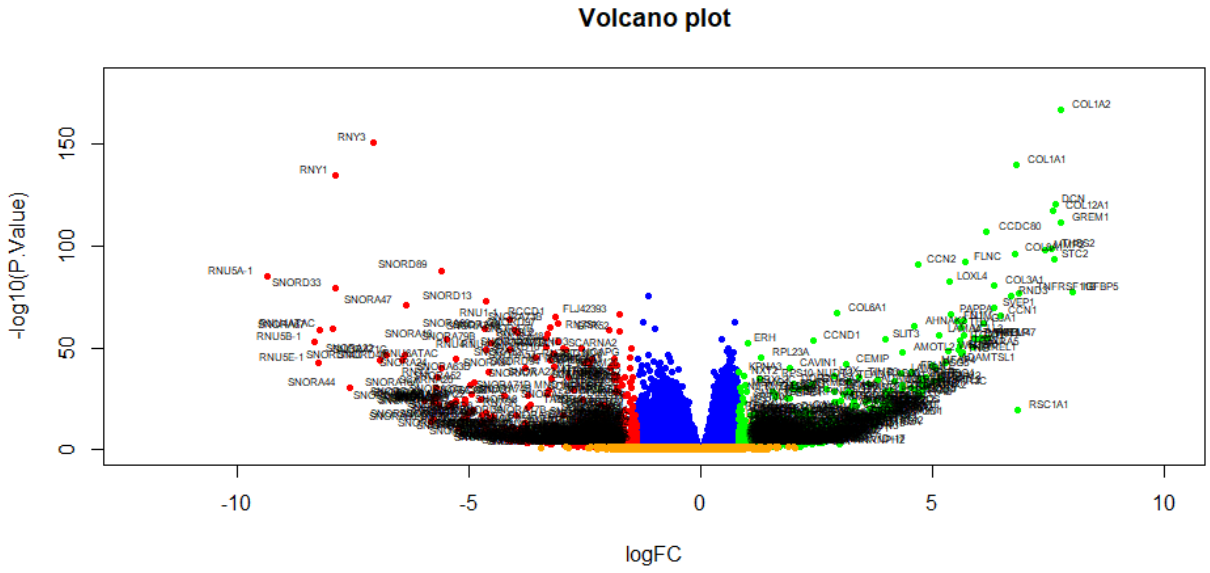


Fig. 1. Volcano plot of differentially expressed genes. Genes with a significant change of more than two-fold were selected. Green dot represented up regulated significant genes and red dot represented down regulated significant genes.

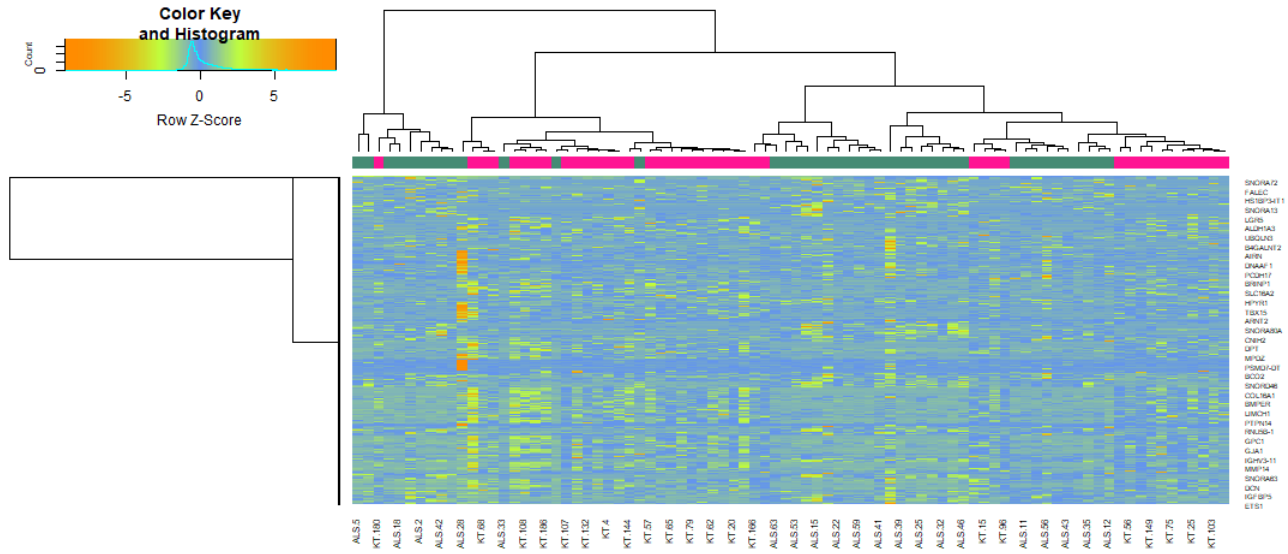
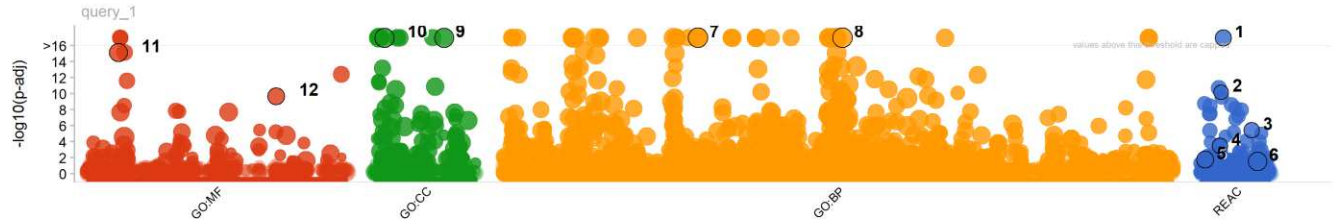


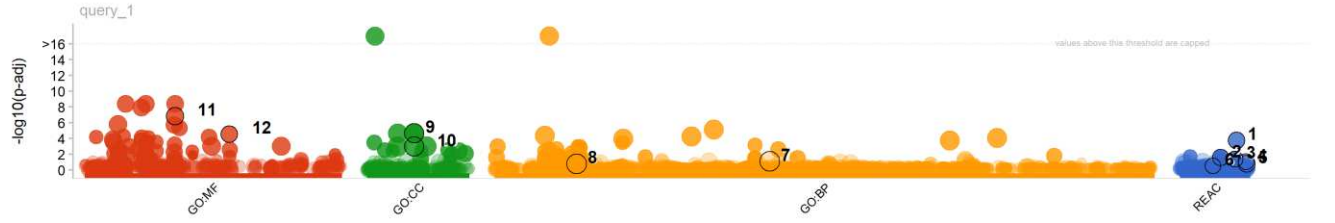
Fig. 2. Heat map of differentially expressed genes. Legend on the top left indicate log fold change of genes. (A1 – A 42 = ALS; B1 – B 42 = Normal control)



id	source	term_id	term_name	term_size	p_value
1	REAC	REAC:R-HSA-1474244	Extracellular matrix organization	298	2.9e-21
2	REAC	REAC:R-HSA-3000178	ECM proteoglycans	76	6.4e-11
3	REAC	REAC:R-HSA-381426	Regulation of Insulin-like Growth Factor (IGF) transport and uptake by Insulin-like Growth Factor Binding Proteins (IGFBPs)	124	3.7e-06
4	REAC	REAC:R-HSA-3781865	Diseases of glycosylation	140	3.3e-04
5	REAC	REAC:R-HSA-422475	Axon guidance	543	1.8e-02
6	REAC	REAC:R-HSA-162582	Signal Transduction	2558	2.8e-02
7	GO:BP	GO:0032501	multicellular organismal process	7322	1.1e-26
8	GO:BP	GO:0050896	response to stimulus	8999	6.6e-23
9	GO:CC	GO:0071944	cell periphery	6347	1.2e-45
10	GO:CC	GO:0005886	plasma membrane	5866	1.6e-19
11	GO:MF	GO:0005102	signaling receptor binding	1521	7.2e-16
12	GO:MF	GO:0050839	cell adhesion molecule binding	564	2.0e-10

g:Profiler (biit.cs.ut.ee/gprofiler)

Fig. 3. GO and REACTOME pathway enrichment analysis for up regulated genes. $p < 0.05$. Abbreviations: BP, biological process; CC, cell component; MF, molecular function. GO, Gene Ontology; REAC, REACTOME. The size of the circle represents the number of genes involved, and the abscissa represents the frequency of the genes involved in the term total genes.



id	source	term_id	term_name	term_size	p_value
1	REAC	REAC:R-HSA-9709957	Sensory Perception	576	1.7e-04
2	REAC	REAC:R-HSA-112316	Neuronal System	399	2.7e-02
3	REAC	REAC:R-HSA-425407	SLC-mediated transmembrane transport	248	4.0e-02
4	REAC	REAC:R-HSA-112315	Transmission across Chemical Synapses	258	8.7e-02
5	REAC	REAC:R-HSA-382551	Transport of small molecules	729	1.6e-01
6	REAC	REAC:R-HSA-6805567	Keratinization	216	2.9e-01
7	GO:BP	GO:0044238	primary metabolic process	12342	7.9e-02
8	GO:BP	GO:0009058	biosynthetic process	10664	1.6e-01
9	GO:CC	GO:0043232	intracellular membraneless organelle	6669	2.2e-05
10	GO:CC	GO:0043233	organelle lumen	6695	1.1e-03
11	GO:MF	GO:0022857	transmembrane transporter activity	1235	1.4e-07
12	GO:MF	GO:0046873	metal ion transmembrane transporter activity	540	2.8e-05

g:Profiler (biit.cs.ut.ee/gprofiler)

Fig. 4. GO and REACTOME pathway enrichment analysis for down regulated genes. $p < 0.05$. Abbreviations: BP, biological process; CC, cell component; MF, molecular function. GO, Gene

Ontology; REAC, REACTOME. The size of the circle represents the number of genes involved, and the abscissa represents the frequency of the genes involved in the term total genes.

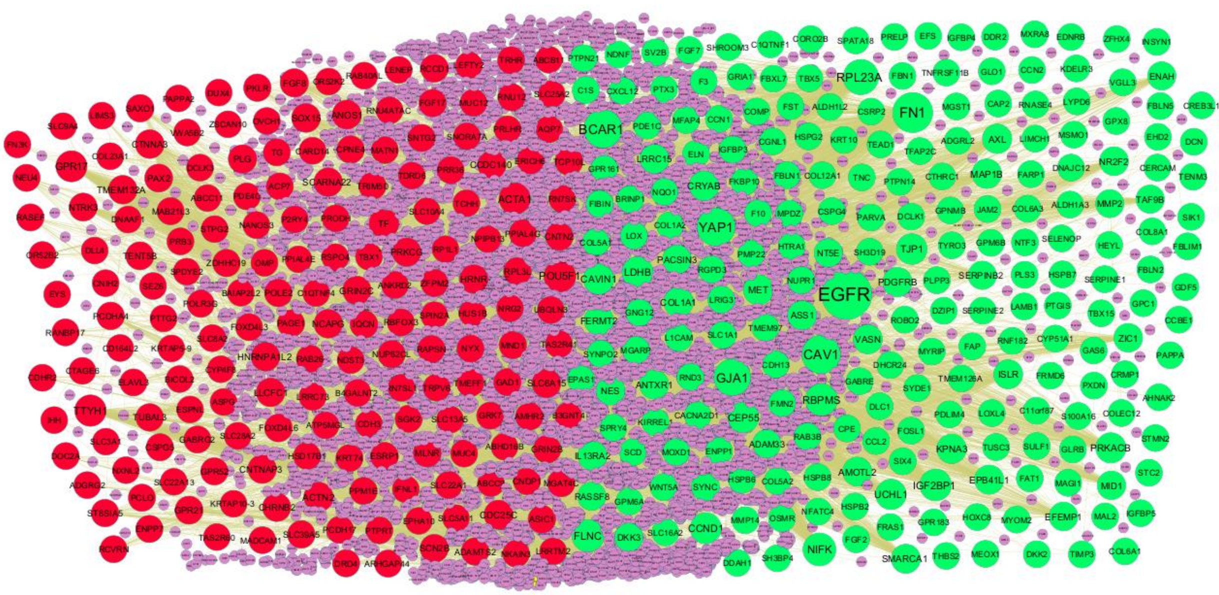


Fig. 5. PPI network of DEGs. Up regulated genes are marked in parrot green; down regulated genes are marked in orange.

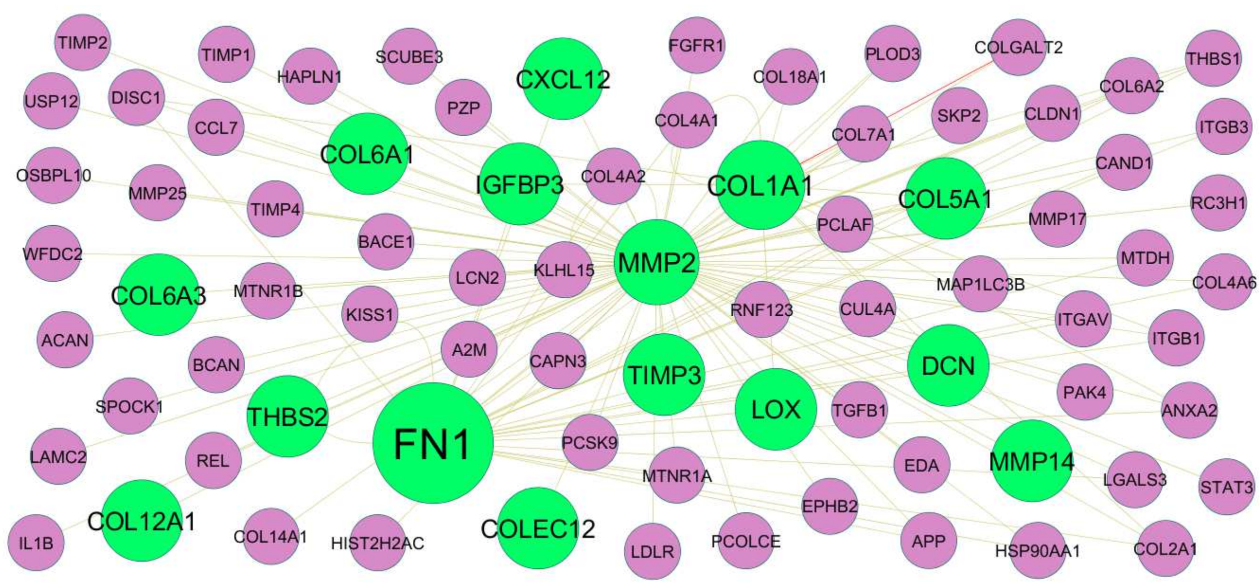


Fig. 6. Modules 1 was isolated form PPI of up regulated genes. Module 1 has 79 nodes and 119 edges for up regulated genes. Up regulated genes are marked in green



id	source	term_id	term_name	term_size	p_value
1	REAC	REAC:R-HSA-1474244	Extracellular matrix organization	298	1.1e-11
2	REAC	REAC:R-HSA-3000178	ECM proteoglycans	76	6.5e-09
3	REAC	REAC:R-HSA-381426	Regulation of Insulin-like Growth Factor (IGF) transport and uptake by Insulin-like Growth Factor Binding Proteins (IGFBPs)	124	2.8e-03
4	REAC	REAC:R-HSA-3781865	Diseases of glycosylation	140	4.0e-02
5	REAC	REAC:R-HSA-422475	Axon guidance	543	2.5e-03
6	REAC	REAC:R-HSA-162582	Signal Transduction	2558	2.7e-02
7	GO:BP	GO:0032501	multicellular organismal process	7322	2.7e-04
8	GO:BP	GO:0050896	response to stimulus	8999	8.5e-03
9	GO:CC	GO:0071944	cell periphery	6347	8.1e-06
10	GO:CC	GO:0005886	plasma membrane	5866	2.0e-01
11	GO:MF	GO:0005102	signaling receptor binding	1521	3.3e-02
12	GO:MF	GO:0050839	cell adhesion molecule binding	564	2.5e-03

g:Profiler (biit.cs.ut.ee/gprofiler)

Fig. 7. Enrichment analysis for module 1. The size of the circle represents the number of genes involved, and the abscissa represents the frequency of the genes involved in the term total genes.

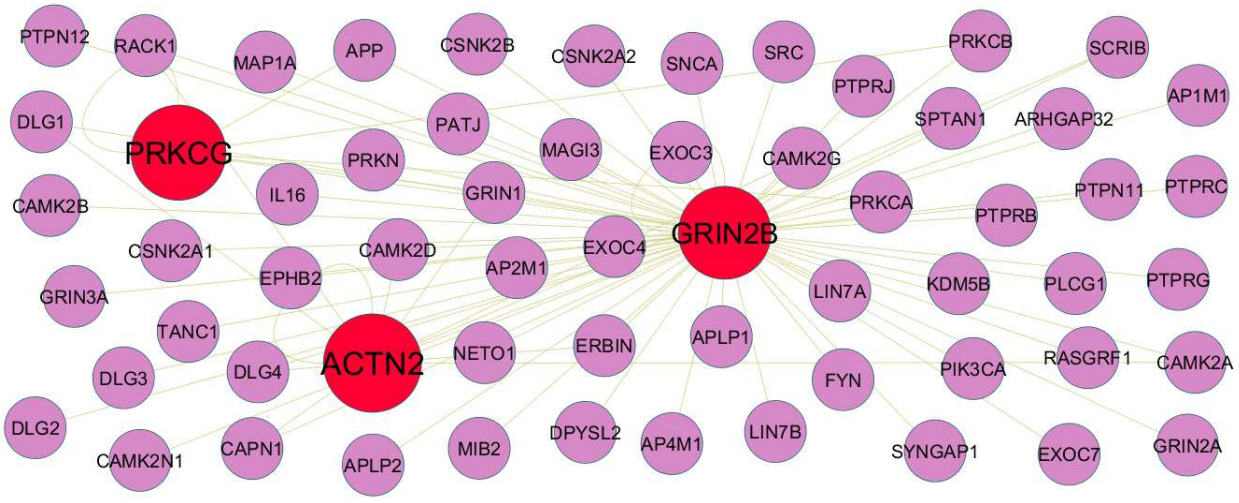
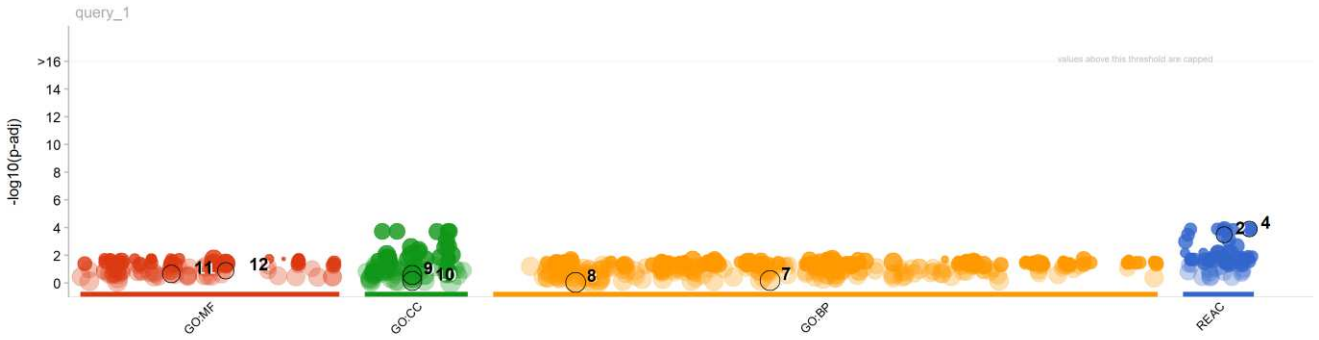


Fig. 8. Module 2 was isolated form PPI of up regulated genes. Module 2 has 61 nodes and 77 edges for down regulated genes. Down regulated genes are marked in red



id	source	term_id	term_name	term_size	p_value
2	REAC	REAC:R-HSA-112316	Neuronal System	399	3.2e-04
4	REAC	REAC:R-HSA-112315	Transmission across Chemical Synapses	258	1.3e-04
7	GO:BP	GO:0044238	primary metabolic process	12342	6.5e-01
8	GO:BP	GO:0009058	biosynthetic process	10664	8.8e-01
9	GO:CC	GO:0043232	intracellular membraneless organelle	6669	2.6e-01
10	GO:CC	GO:0043233	organelle lumen	6695	6.8e-01
11	GO:MF	GO:0022857	transmembrane transporter activity	1235	2.2e-01
12	GO:MF	GO:0046873	metal ion transmembrane transporter activity	540	1.3e-01

g:Profiler (biit.cs.ut.ee/gprofiler)

Fig. 9. Enrichment analysis for module 2. The size of the circle represents the number of genes involved, and the abscissa represents the frequency of the genes involved in the term total genes.

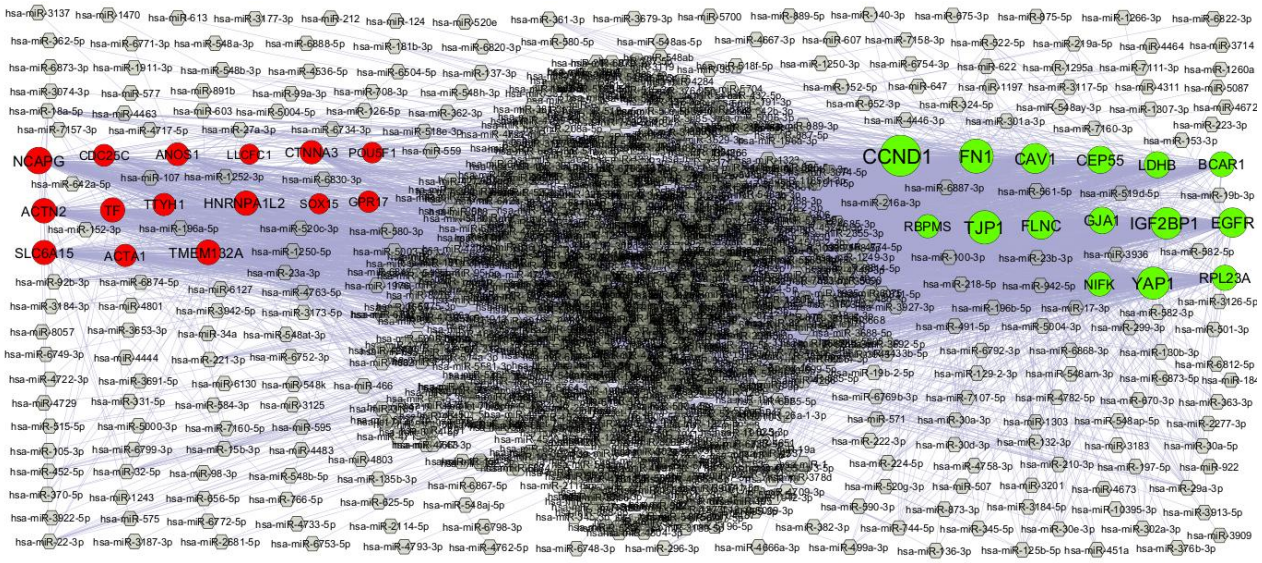


Fig. 10. Hub gene - miRNA regulatory network. The ash color diamond nodes represent the key miRNAs; up regulated genes are marked in green; down regulated genes are marked in red.

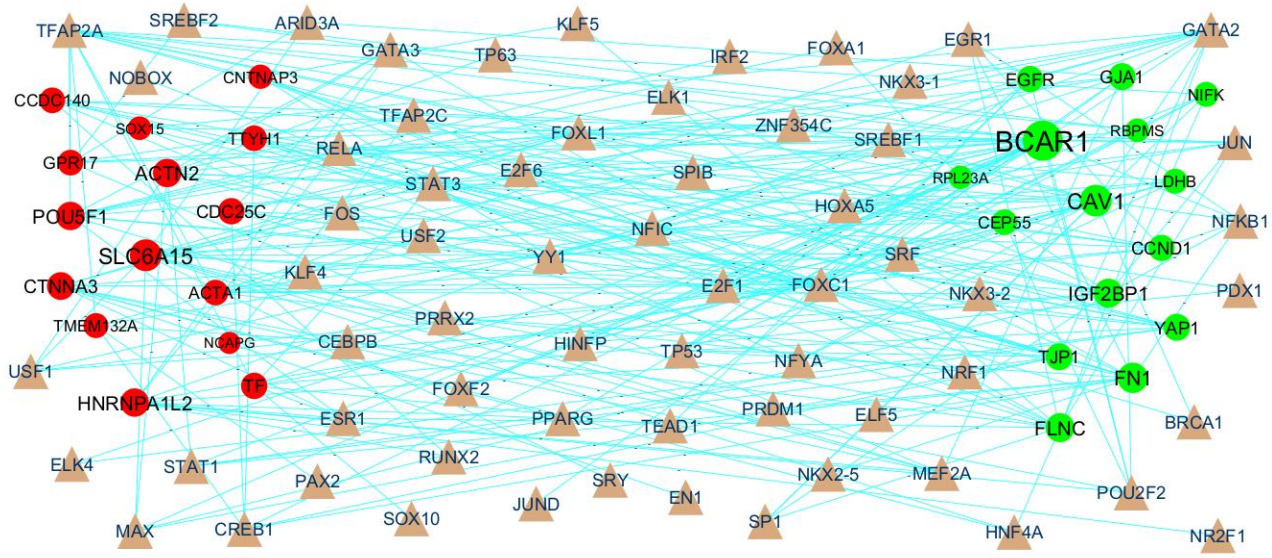
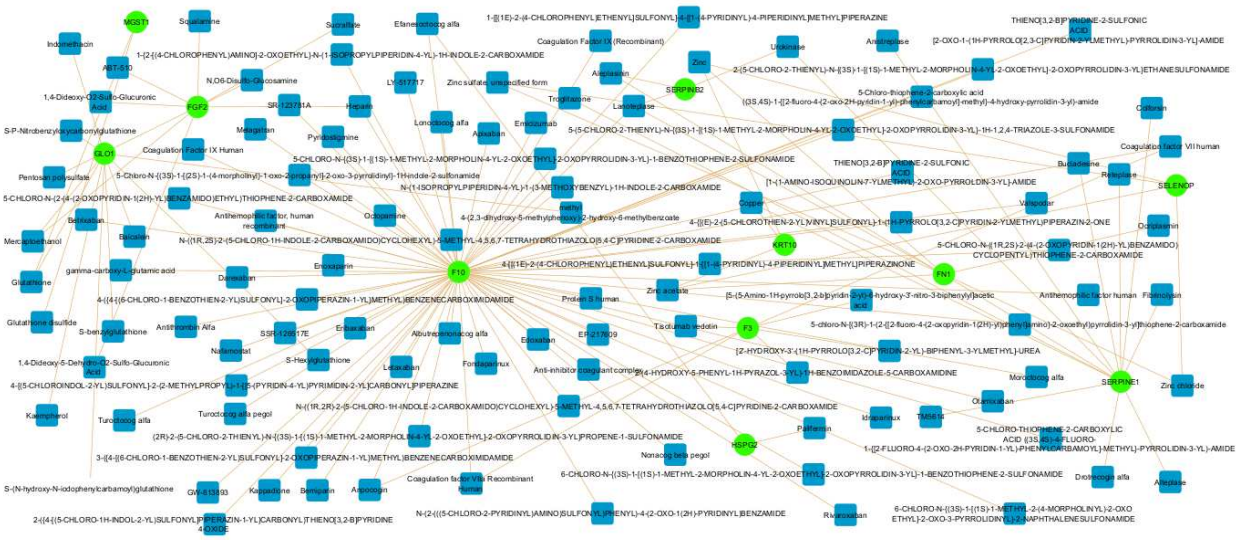
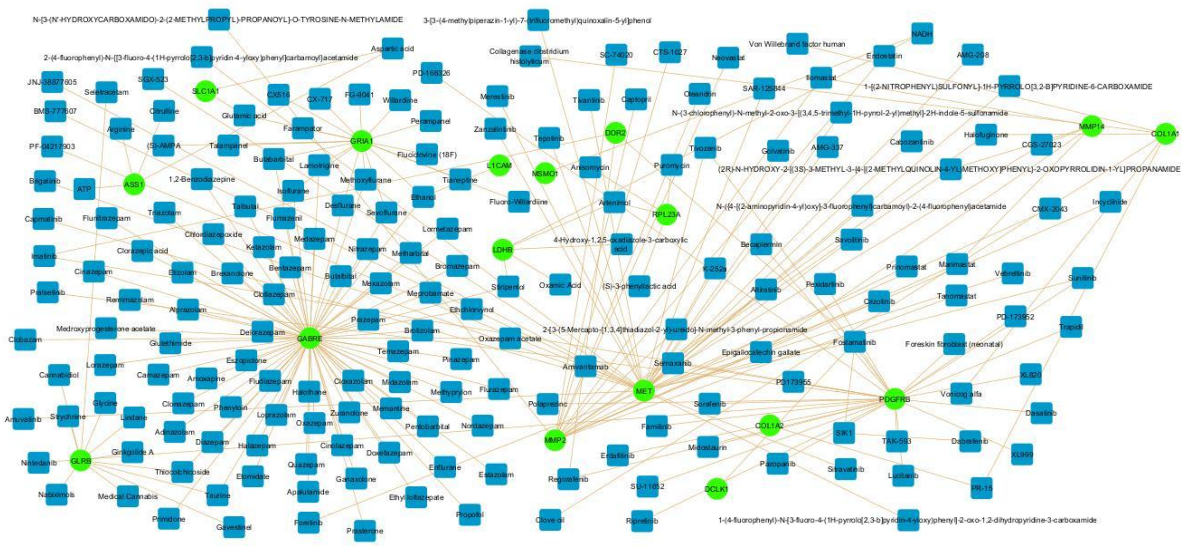


Fig. 11. Hub gene - TF regulatory network. The orange color triangle nodes represent the key TFs; up regulated genes are marked in green; down regulated genes are marked in red.

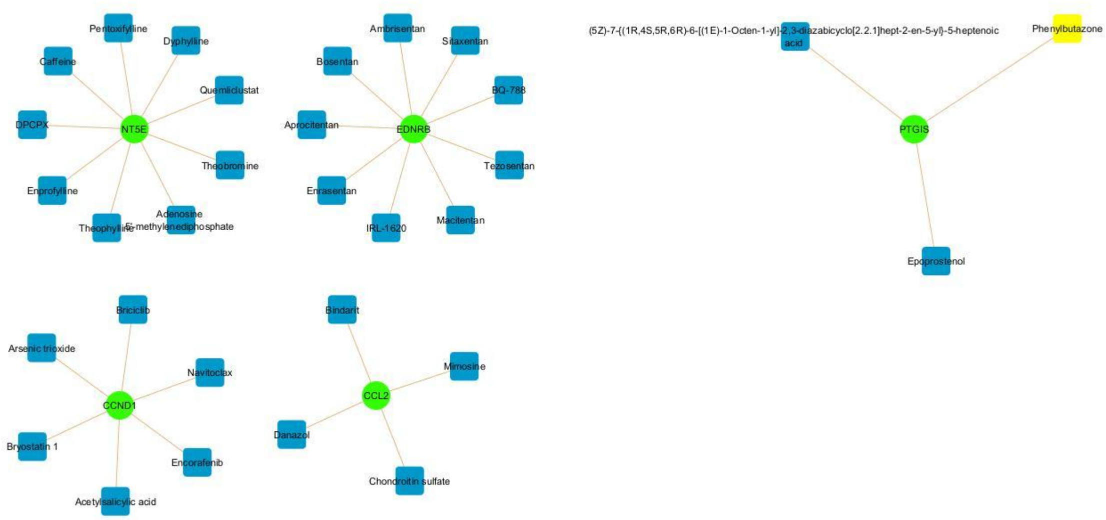
A



B



C


NT5E
Pentoxifylline
Dyphylline
Caffeine
Quemliclustat
DPCPX
Theobromine
Enprofylline
Theophylline
Adenosine 5'-methylenediphosphate
EDNRB
Ambrisentan
Sitaxentan
Bosentan
BQ-788
Aprocitentan
Tezosentan
Enrasentan
IRL-1620
Macitentan
(5Z)-7-{(1R,4S,5R,6R)-6-[(1E)-1-Octen-1-yl]-2,3-diazabicyclo[2.2.1]hept-2-en-5-yl}-5-heptenoic acid
Phenylbutazone
PTGIS
Epoprostenol
CCND1
Briciclib
Arsenic trioxide
Navitoclax
Bryostatin 1
Encorafenib
Acetylsalicylic acid
CCL2
Bindarit
Mimosine
Danazol
Chondroitin sulfate

D

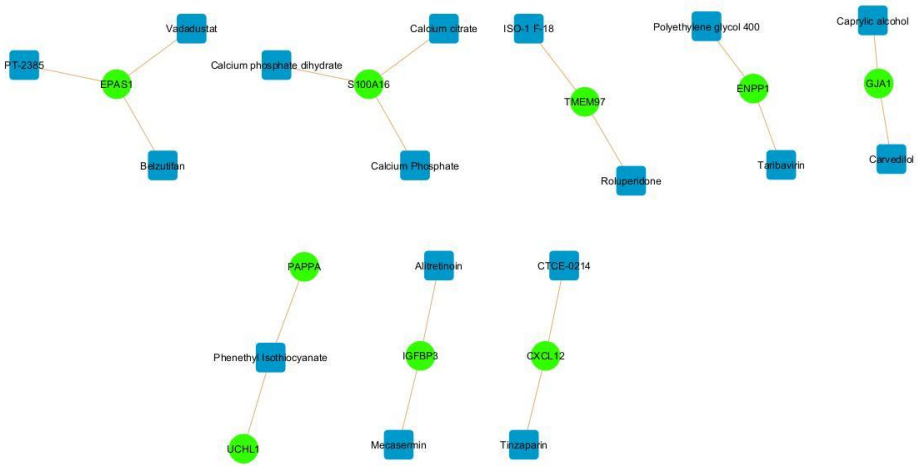
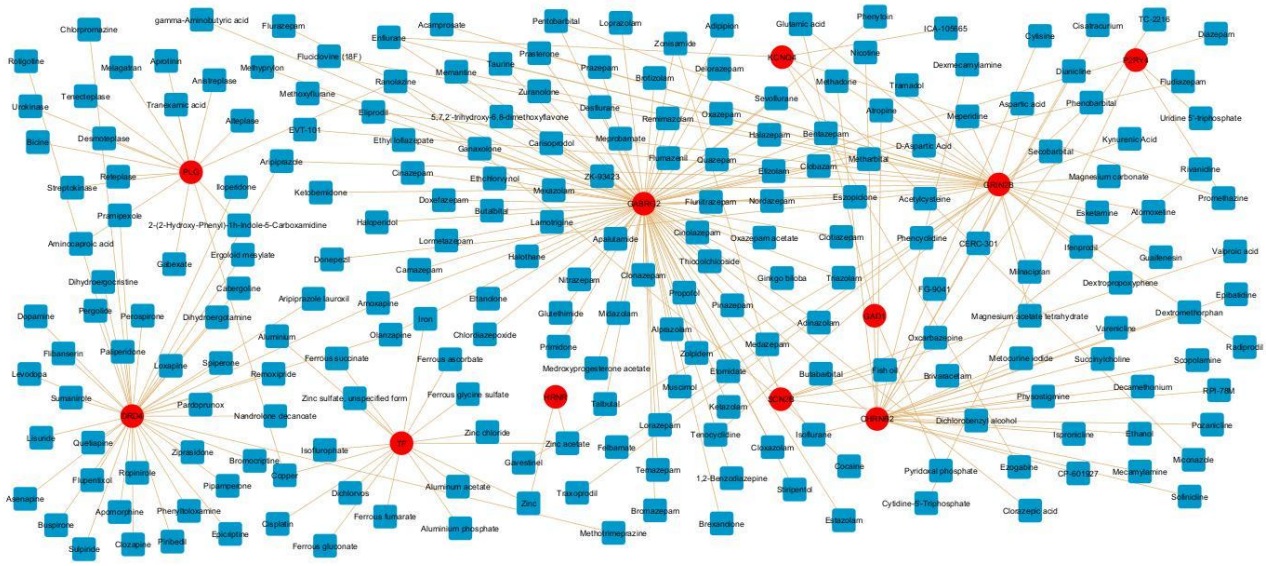


Fig. 12. Four drug-hub gene interaction networks include 1) Network A 2) Network B 3) Network C 4) Network D. The blue color rectangle nodes represent the drug molecule; up regulated genes are marked in green.

A



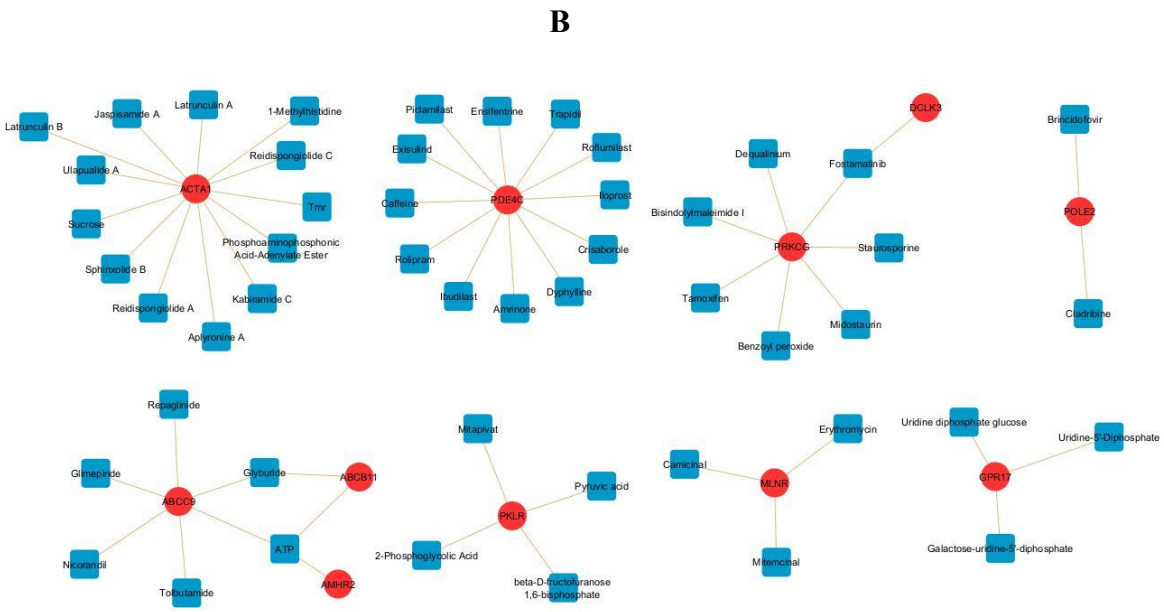


Fig. 13. Two drug-hub gene interaction networks include 1) Network A 2) Network B. The blue rectangle nodes represent the drug molecule; down regulated genes are marked in red

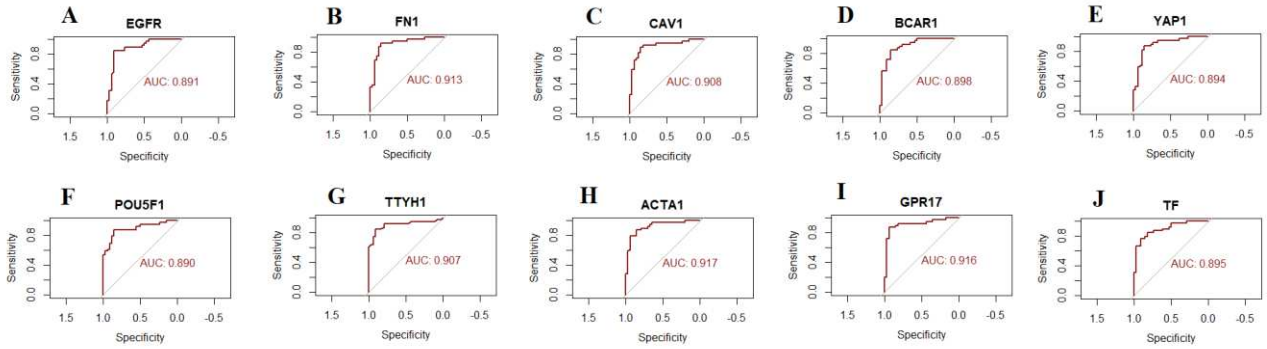


Fig. 14. ROC curve analyses of hub genes. A) EGFR B) FN1 C) CAV1 D) BCAR1 E) YAP1 F) POU5F1 G) TTYH1 H) ACTA1 I) GPR17 J) TF

Tables

Table 1 The statistical metrics for key differentially expressed genes (DEGs)

Gene Symbol	logFC	pValue	adj.P.Val	tvalue	Regulations	Gene Name

IGFBP5	8.023452	7.94E-78	1.01E-74	18.67479	Up	insulin like growth factor binding protein 5
COL1A2	7.776929	1.65E-167	4.64E-163	27.58573	Up	collagen type I alpha 2 chain
GREM1	7.772907	5.98E-112	2.10E-108	22.48381	Up	gremlin 1, DAN family BMP antagonist
DCN	7.651124	2.29E-121	1.29E-117	23.42667	Up	decorin
STC2	7.637326	6.84E-94	1.48E-90	20.55571	Up	stanniocalcin 2
COL12A1	7.589143	5.27E-118	2.11E-114	23.09444	Up	collagen type XII alpha 1 chain
THBS2	7.570886	2.96E-99	8.33E-96	21.14665	Up	thrombospondin 2
MMP2	7.426168	6.76E-99	1.73E-95	21.10767	Up	matrix metallopeptidase 2
TNFRSF11B	6.873739	8.50E-78	1.04E-74	18.67112	Up	TNF receptor superfamily member 11b
RSC1A1	6.841547	2.52E-20	5.35E-19	9.237637	Up	regulator of solute carriers 1
COL1A1	6.818553	1.26E-140	1.19E-136	25.24563	Up	collagen type I alpha 1 chain
COL8A1	6.766847	4.96E-97	1.16E-93	20.90367	Up	collagen type VIII alpha 1 chain
RND3	6.680955	6.20E-76	6.97E-73	18.44066	Up	Rho family GTPase 3
CCN1	6.459457	2.30E-66	1.84E-63	17.20841	Up	cellular communication network factor 1
COL3A1	6.336162	2.21E-81	3.11E-78	19.1069	Up	collagen type III alpha 1 chain
SVEP1	6.318088	1.61E-70	1.56E-67	17.75374	Up	sushi, von Willebrand factor type A, EGF and pentraxin domain containing 1
PRELP	6.17553	1.04E-55	4.35E-53	15.724	Up	proline and arginine rich end leucine rich repeat protein
CCDC80	6.15819	6.62E-108	2.07E-104	22.0666	Up	coiled-coil domain containing 80
GJA1	6.109932	1.69E-62	1.05E-59	16.68489	Up	gap junction protein alpha 1
TMEM47	6.049119	7.71E-56	3.43E-53	15.74266	Up	transmembrane protein 47
CDH11	5.917265	7.47E-55	2.92E-52	15.59835	Up	cadherin 11
PAMR1	5.898973	8.15E-56	3.52E-53	15.73921	Up	peptidase domain containing associated with muscle regeneration 1
MXRA5	5.866388	3.28E-51	1.11E-48	15.05335	Up	matrix remodeling associated 5
FLNC	5.711878	1.09E-92	2.19E-89	20.42099	Up	filamin C
LUM	5.686868	3.10E-64	2.29E-61	16.92203	Up	lumican
VGLL3	5.673528	3.35E-57	1.52E-54	15.93981	Up	vestigial like family member 3
KIRREL1	5.6417	2.26E-48	6.16E-46	14.61485	Up	kirre like nephrin family adhesion molecule 1
THY1	5.614875	1.02E-60	5.95E-58	16.43838	Up	Thy-1 cell surface antigen
TNC	5.606918	9.04E-48	2.35E-45	14.52008	Up	tenascin C
ITGBL1	5.585676	1.06E-51	3.62E-49	15.12817	Up	integrin subunit beta like 1
ITGA11	5.58373	3.24E-54	1.23E-51	15.50435	Up	integrin subunit alpha 11
SULF1	5.569652	6.79E-50	2.01E-47	14.85164	Up	sulfatase 1
FN1	5.548482	3.23E-64	2.32E-61	16.91962	Up	fibronectin 1
PAPPA	5.383399	6.37E-67	5.43E-64	17.2825	Up	pappalysin 1
LOXL4	5.353651	4.32E-83	6.39E-80	19.31126	Up	lysyl oxidase like 4
WNT5A	5.330339	6.08E-49	1.72E-46	14.70391	Up	Wnt family member 5A
ADAMTSL1	5.277336	3.25E-43	6.16E-41	13.78257	Up	ADAMTS like 1
PSG4	5.177092	1.06E-35	1.13E-33	12.47197	Up	pregnancy specific beta-1-glycoprotein 4
LAMA4	5.136619	3.19E-57	1.47E-54	15.94289	Up	laminin subunit alpha 4
PSG5	5.046699	1.23E-40	1.94E-38	13.3474	Up	pregnancy specific beta-1-glycoprotein 5
TENM2	5.038692	2.74E-34	2.61E-32	12.21038	Up	teneurin transmembrane protein 2
MFAP4	4.985237	4.55E-42	7.84E-40	13.59072	Up	microfibril associated protein 4

PPP1R3C	4.89683	1.48E-31	1.05E-29	11.68749	Up	protein phosphatase 1 regulatory subunit 3C
ISLR	4.869537	3.89E-36	4.26E-34	12.55169	Up	immunoglobulin superfamily containing leucine rich repeat
OSMR	4.792362	2.00E-34	1.93E-32	12.23577	Up	oncostatin M receptor
KCNK2	4.77579	9.89E-30	5.69E-28	11.3248	Up	potassium two pore domain channel subfamily K member 2
ANGPTL2	4.764506	1.55E-32	1.23E-30	11.87765	Up	angiopoietin like 2
SOD3	4.74832	1.31E-27	6.17E-26	10.88839	Up	superoxide dismutase 3
EGFR	4.741752	9.97E-36	1.07E-33	12.47695	Up	epidermal growth factor receptor
CCN2	4.692551	7.09E-92	1.33E-88	20.32926	Up	cellular communication network factor 2
CCN5	4.690872	1.66E-28	8.40E-27	11.07518	Up	cellular communication network factor 5
AHNAK2	4.603814	2.22E-61	1.36E-58	16.53034	Up	AHNAK nucleoprotein 2
STMN2	4.592815	1.26E-30	8.03E-29	11.50376	Up	stathmin 2
FBLN1	4.548287	3.21E-39	4.58E-37	13.102	Up	fibulin 1
EFEMP1	4.54628	2.99E-31	2.03E-29	11.62736	Up	EGF-like fibulin extracellular matrix protein 1
CRYAB	4.44135	1.45E-26	6.08E-25	10.66693	Up	crystallin alpha B
FST	4.358077	1.37E-32	1.10E-30	11.88772	Up	follistatin
AMOTL2	4.34983	2.50E-48	6.76E-46	14.60792	Up	angiomotin like 2
NNMT	4.334553	1.71E-30	1.07E-28	11.4777	Up	nicotinamide N-methyltransferase
LAMB1	4.320476	2.06E-38	2.71E-36	12.96005	Up	laminin subunit beta 1
DPT	4.302727	3.52E-22	9.24E-21	9.684081	Up	dermatopontin
ANTXR1	4.177145	1.32E-34	1.31E-32	12.26956	Up	ANTXR cell adhesion molecule 1
FGF1	4.163554	8.61E-20	1.72E-18	9.105159	Up	fibroblast growth factor 1
GNG12	4.107179	1.28E-22	3.56E-21	9.786772	Up	G protein subunit gamma 12
COL16A1	4.101581	9.89E-30	5.69E-28	11.32482	Up	collagen type XVI alpha 1 chain
LRRN4CL	4.050716	5.42E-27	2.42E-25	10.75815	Up	LRRN4 C-terminal like
ITIH5	4.047916	4.92E-24	1.58E-22	10.11141	Up	inter-alpha-trypsin inhibitor heavy chain 5
HAS2	4.030361	6.19E-21	1.41E-19	9.386761	Up	hyaluronan synthase 2
SNAI2	4.018202	4.99E-19	9.16E-18	8.912427	Up	snail family transcriptional repressor 2
SLIT3	3.989395	3.60E-55	1.44E-52	15.64496	Up	slit guidance ligand 3
EMX2OS	3.980563	1.12E-22	3.13E-21	9.800557	Up	EMX2 opposite strand/antisense RNA
GPX8	3.973343	5.16E-19	9.43E-18	8.908819	Up	glutathione peroxidase 8 (putative)
FLRT2	3.97186	4.08E-29	2.23E-27	11.2	Up	fibronectin leucine rich transmembrane protein 2
ABI3BP	3.961264	1.97E-18	3.36E-17	8.759133	Up	ABI family member 3 binding protein
STC1	3.958853	5.17E-22	1.32E-20	9.644785	Up	stanniocalcin 1
COL11A1	3.953214	1.97E-17	2.99E-16	8.49577	Up	collagen type XI alpha 1 chain
PRRX1	3.950963	8.71E-20	1.74E-18	9.103923	Up	paired related homeobox 1
SRPX2	3.94696	3.77E-22	9.86E-21	9.677109	Up	sushi repeat containing protein X-linked 2
PSG1	3.944223	4.71E-22	1.22E-20	9.654412	Up	pregnancy specific beta-1-glycoprotein 1
DKK1	3.937374	6.98E-23	2.00E-21	9.848144	Up	dickkopf Wnt signaling pathway inhibitor 1
IL13RA2	3.919118	4.14E-19	7.66E-18	8.933226	Up	interleukin 13 receptor subunit alpha 2
MKX	3.898719	2.41E-17	3.63E-16	8.472211	Up	mohawk homeobox
MRGPRF	3.871194	3.47E-20	7.25E-19	9.203315	Up	MAS related GPR family member F
RAB3B	3.821579	2.61E-35	2.71E-33	12.40014	Up	RAB3B, member RAS oncogene family
GRIA1	3.816914	3.03E-20	6.38E-19	9.217943	Up	glutamate ionotropic receptor AMPA type subunit 1

FGF5	3.774413	5.92E-16	7.56E-15	8.090925	Up	fibroblast growth factor 5
ATP8B1	3.770948	1.31E-24	4.47E-23	10.23986	Up	ATPase phospholipid transporting 8B1
PRSS12	3.736226	2.40E-12	2.01E-11	7.009281	Up	serine protease 12
CDH13	3.691547	1.02E-21	2.52E-20	9.574507	Up	cadherin 13
CACNA2D1	3.675247	2.74E-17	4.09E-16	8.457031	Up	calcium voltage-gated channel auxiliary subunit alpha2delta 1
HSPB7	3.661438	6.15E-15	6.97E-14	7.800828	Up	heat shock protein family B (small) member 7
GFRA1	3.650065	1.13E-20	2.48E-19	9.323478	Up	GDNF family receptor alpha 1
CREB3L1	3.624022	1.54E-24	5.22E-23	10.22424	Up	cAMP responsive element binding protein 3 like 1
ADAM33	3.62008	5.40E-33	4.55E-31	11.96529	Up	ADAM metallopeptidase domain 33
MASP1	3.562023	7.40E-24	2.34E-22	10.07123	Up	MBL associated serine protease 1
FMN2	3.520773	8.50E-17	1.20E-15	8.324106	Up	formin 2
FAM180A	3.496396	4.91E-12	3.98E-11	6.908034	Up	family with sequence similarity 180 member A
TIMP3	3.42866	2.90E-36	3.20E-34	12.57481	Up	TIMP metallopeptidase inhibitor 3
THSD4	3.410453	7.97E-18	1.27E-16	8.600091	Up	thrombospondin type 1 domain containing 4
STEAP2	3.382285	1.05E-16	1.46E-15	8.298977	Up	STEAP2 metalloreductase
PTGIS	3.368352	2.03E-22	5.48E-21	9.740268	Up	prostaglandin I2 synthase
GABBR2	3.365242	2.67E-15	3.15E-14	7.905556	Up	gamma-aminobutyric acid type B receptor subunit 2
OSR2	3.321309	5.98E-17	8.62E-16	8.365608	Up	odd-skipped related transciption factor 2
LRRC15	3.310242	2.16E-11	1.62E-10	6.694659	Up	leucine rich repeat containing 15
CLDN11	3.295959	7.94E-25	2.74E-23	10.28847	Up	claudin 11
BMPER	3.275075	1.04E-22	2.92E-21	9.808212	Up	BMP binding endothelial regulator
CNTN3	3.270466	3.89E-10	2.50E-09	6.258242	Up	contactin 3
AOX1	3.254153	8.99E-21	2.01E-19	9.347308	Up	aldehyde oxidase 1
TWIST2	3.236185	1.56E-28	7.91E-27	11.08069	Up	twist family bHLH transcription factor 2
CPXM2	3.202417	3.16E-29	1.75E-27	11.22267	Up	carboxypeptidase X, M14 family member 2
MARCHF4	3.18785	1.16E-15	1.43E-14	8.00867	Up	membrane associated ring-CH-type finger 4
TEAD1	3.179169	1.01E-34	1.01E-32	12.29148	Up	TEA domain transcription factor 1
ADAMTS12	3.145657	6.15E-14	6.28E-13	7.504868	Up	ADAM metallopeptidase with thrombospondin type 1 motif 12
ASS1	3.139226	1.05E-13	1.04E-12	7.434114	Up	argininosuccinate synthase 1
CEMIP	3.133663	1.40E-42	2.58E-40	13.67657	Up	cell migration inducing hyaluronidase 1
FBXL7	3.084245	4.95E-12	4.01E-11	6.906877	Up	F-box and leucine rich repeat protein 7
TWIST1	3.083776	2.00E-12	1.69E-11	7.034454	Up	twist family bHLH transcription factor 1
S100A16	3.07626	1.63E-11	1.24E-10	6.735863	Up	S100 calcium binding protein A16
SLIT2	3.068132	5.72E-28	2.78E-26	10.96363	Up	slit guidance ligand 2
EMX2	3.063827	9.59E-11	6.71E-10	6.473198	Up	empty spiracles homeobox 2
BRINP1	3.050493	1.59E-08	8.41E-08	5.65176	Up	BMP/retinoic acid inducible neural specific 1
CSPG4	3.023945	1.38E-24	4.67E-23	10.23514	Up	chondroitin sulfate proteoglycan 4
IGKV1D-17	2.984355	0.000911	0.002347	3.316651	Up	immunoglobulin kappa variable 1D-17
ELN	2.974008	8.88E-11	6.23E-10	6.484825	Up	elastin
POSTN	2.962093	1.80E-11	1.37E-10	6.721172	Up	periostin
PNPLA3	2.960349	1.15E-11	8.89E-11	6.78676	Up	patatin like domain 3, 1-acylglycerol-3-phosphate O-acyltransferase
COL6A1	2.948133	5.82E-68	5.28E-65	17.41997	Up	collagen type VI alpha 1 chain
MMP1	2.946797	3.01E-24	9.83E-23	10.15946	Up	matrix metallopeptidase 1

ZFHX4	2.943053	1.86E-11	1.41E-10	6.716584	Up	zinc finger homeobox 4
PTPN21	2.939888	1.11E-13	1.10E-12	7.426813	Up	protein tyrosine phosphatase non-receptor type 21
GPR176	2.889282	2.02E-14	2.16E-13	7.649321	Up	G protein-coupled receptor 176
NUPR1	2.888462	1.79E-13	1.72E-12	7.363572	Up	nuclear protein 1, transcriptional regulator
NFASC	2.885754	3.35E-29	1.86E-27	11.2173	Up	neurofascin
YAP1	2.885226	2.12E-24	7.04E-23	10.19362	Up	Yes1 associated transcriptional regulator
FHOD3	2.882614	2.54E-14	2.69E-13	7.619778	Up	formin homology 2 domain containing 3
LRIG3	2.878117	4.91E-09	2.77E-08	5.850173	Up	leucine rich repeats and immunoglobulin like domains 3
C11orf87	2.873595	5.27E-14	5.42E-13	7.525022	Up	chromosome 11 open reading frame 87
SRPX	2.872246	1.82E-15	2.18E-14	7.95313	Up	sushi repeat containing protein X-linked
SSTR1	2.86988	3.07E-10	2.00E-09	6.29537	Up	somatostatin receptor 1
GALNT15	2.867912	5.97E-14	6.10E-13	7.508727	Up	polypeptide N-acetylgalactosaminyltransferase 15
LOX	2.865695	3.85E-37	4.60E-35	12.73359	Up	lysyl oxidase
DKK2	2.857982	2.92E-13	2.73E-12	7.297957	Up	dickkopf Wnt signaling pathway inhibitor 2
PDE1C	2.853469	4.67E-15	5.36E-14	7.835362	Up	phosphodiesterase 1C
ROBO2	2.834851	4.02E-08	2.01E-07	5.489848	Up	roundabout guidance receptor 2
GLRB	2.794328	8.41E-08	4.03E-07	5.358012	Up	glycine receptor beta
F3	2.783137	2.94E-16	3.88E-15	8.175822	Up	coagulation factor III, tissue factor
FGF7	2.77734	9.37E-13	8.21E-12	7.139464	Up	fibroblast growth factor 7
KCNJ6	2.765989	6.72E-13	6.00E-12	7.184954	Up	potassium inwardly rectifying channel subfamily J member 6
OSR1	2.747721	8.01E-08	3.85E-07	5.366848	Up	odd-skipped related transcription factor 1
PTPN14	2.723243	1.18E-30	7.49E-29	11.50995	Up	protein tyrosine phosphatase non-receptor type 14
TFAP2C	2.721544	1.13E-07	5.30E-07	5.305178	Up	transcription factor AP-2 gamma
JPH2	2.704144	1.59E-10	1.08E-09	6.396447	Up	junctophilin 2
F10	2.683358	4.20E-05	0.000135	4.096239	Up	coagulation factor X
BHMT2	2.677223	3.12E-07	1.38E-06	5.115848	Up	betaine--homocysteine S-methyltransferase 2
HOXC6	2.668937	5.37E-08	2.64E-07	5.438636	Up	homeobox C6
LARP6	2.65656	3.98E-08	1.99E-07	5.49175	Up	La ribonucleoprotein 6, translational regulator
COX7A1	2.656168	9.30E-08	4.43E-07	5.339947	Up	cytochrome c oxidase subunit 7A1
NR2F2	2.640323	8.15E-08	3.91E-07	5.363808	Up	nuclear receptor subfamily 2 group F member 2
SYNC	2.638116	4.77E-15	5.47E-14	7.832798	Up	syncoilin, intermediate filament protein
CHST3	2.618173	1.39E-09	8.31E-09	6.057122	Up	carbohydrate sulfotransferase 3
COMP	2.612044	0.000276	0.000779	3.637042	Up	cartilage oligomeric matrix protein
TENM3	2.588397	6.36E-05	0.000199	3.99886	Up	teneurin transmembrane protein 3
PDLIM4	2.585277	3.41E-06	1.30E-05	4.644422	Up	PDZ and LIM domain 4
CPE	2.583375	4.77E-11	3.45E-10	6.578002	Up	carboxypeptidase E
KIAA1549L	2.573477	5.98E-12	4.80E-11	6.880007	Up	KIAA1549 like
FABP3	2.566738	1.34E-06	5.42E-06	4.833424	Up	fatty acid binding protein 3
HSPB8	2.544619	0.000242	0.000692	3.670101	Up	heat shock protein family B (small) member 8
TBX3	2.526021	1.91E-09	1.12E-08	6.005567	Up	T-box transcription factor 3
RARRES2	2.52336	2.62E-07	1.17E-06	5.14921	Up	retinoic acid receptor responder 2
MFAP2	2.518087	3.91E-07	1.70E-06	5.07318	Up	microfibril associated protein 2
LSAMP	2.509287	1.28E-07	5.98E-07	5.281564	Up	limbic system associated membrane protein

GRIA3	2.486905	4.70E-13	4.29E-12	7.233593	Up	glutamate ionotropic receptor AMPA type subunit 3
ADGRL2	2.484931	5.42E-08	2.66E-07	5.437065	Up	adhesion G protein-coupled receptor L2
BCAR1	2.468184	2.66E-12	2.22E-11	6.994614	Up	BCAR1 scaffold protein, Cas family member
ZIC1	2.464254	1.66E-05	5.68E-05	4.306838	Up	Zic family zinc finger 1
FBLIM1	2.434034	1.82E-08	9.54E-08	5.628369	Up	filamin binding LIM protein 1
CCND1	2.424855	2.49E-54	9.61E-52	15.52117	Up	cyclin D1
PDPN	2.420526	5.30E-05	0.000168	4.042176	Up	podoplanin
CSRP2	2.401414	0.000216	0.000622	3.699534	Up	cysteine and glycine rich protein 2
INSYN1	2.388842	0.002195	0.00524	3.062439	Up	inhibitory synaptic factor 1
COL5A2	2.38674	7.11E-33	5.88E-31	11.94249	Up	collagen type V alpha 2 chain
C1QTNF5	2.383048	1.52E-05	5.25E-05	4.325414	Up	C1q and TNF related 5
NFATC4	2.376564	4.24E-16	5.49E-15	8.131469	Up	nuclear factor of activated T cells 4
CCBE1	2.372374	4.19E-17	6.13E-16	8.407585	Up	collagen and calcium binding EGF domains 1
GPNMB	2.363924	6.06E-19	1.10E-17	8.890909	Up	glycoprotein nmb
DZIP1	2.356381	1.23E-07	5.76E-07	5.289013	Up	DAZ interacting zinc finger protein 1
PCDH18	2.352994	3.40E-13	3.15E-12	7.277502	Up	protocadherin 18
HAND2	2.341148	0.000397	0.001092	3.542154	Up	heart and neural crest derivatives expressed 2
FAP	2.336007	4.04E-15	4.67E-14	7.853542	Up	fibroblast activation protein alpha
ALDH1A3	2.316871	0.000233	0.000668	3.680081	Up	aldehyde dehydrogenase 1 family member A3
TAFA5	2.313188	1.41E-05	4.91E-05	4.341766	Up	TAFA chemokine like family member 5
KDELR3	2.312401	6.95E-06	2.54E-05	4.495094	Up	KDEL endoplasmic reticulum protein retention receptor 3
CAV1	2.2703	3.31E-20	6.93E-19	9.208373	Up	caveolin 1
SHISAL1	2.268373	2.55E-06	9.91E-06	4.703782	Up	shisa like 1
RSPO3	2.268279	2.78E-05	9.22E-05	4.190728	Up	R-spondin 3
FRMD6	2.259193	3.76E-31	2.51E-29	11.60775	Up	FERM domain containing 6
ACKR4	2.251527	1.94E-17	2.96E-16	8.497269	Up	atypical chemokine receptor 4
DCLK1	2.248156	0.000941	0.002418	3.307502	Up	doublecortin like kinase 1
SIX2	2.244379	0.000833	0.002161	3.34161	Up	SIX homeobox 2
SEMA3D	2.240788	6.26E-12	5.00E-11	6.873588	Up	semaphorin 3D
KCNIP3	2.201847	7.15E-05	0.000222	3.971313	Up	potassium voltage-gated channel interacting protein 3
CD276	2.199739	8.17E-12	6.43E-11	6.835473	Up	CD276 molecule
MFAP5	2.190281	1.66E-07	7.62E-07	5.233917	Up	microfibril associated protein 5
HOXC8	2.182192	0.000532	0.00143	3.46412	Up	homeobox C8
PIEZO2	2.180906	2.24E-06	8.77E-06	4.730348	Up	piezo type mechanosensitive ion channel component 2
MGARP	2.174392	9.92E-09	5.39E-08	5.73203	Up	mitochondria localized glutamic acid rich protein
LRP4	2.160948	0.000572	0.001527	3.444531	Up	LDL receptor related protein 4
RFPL4A	2.157409	0.01872	0.036255	2.35107	Up	ret finger protein like 4A
PDZRN3	2.154507	6.24E-07	2.65E-06	4.983486	Up	PDZ domain containing ring finger 3
GDNF	2.150184	0.001017	0.002594	3.285646	Up	glial cell derived neurotrophic factor
CPZ	2.149888	0.000556	0.00149	3.452092	Up	carboxypeptidase Z
MXRA8	2.133442	3.04E-17	4.51E-16	8.445142	Up	matrix remodeling associated 8
C1S	2.129238	1.07E-30	6.81E-29	11.51839	Up	complement C1s
FJX1	2.128962	0.000196	0.000567	3.724687	Up	four-jointed box kinase 1

CAP2	2.125212	0.000455	0.001236	3.505994	Up	cyclase associated actin cytoskeleton regulatory protein 2
AKR1C2	2.123216	0.000328	0.000916	3.592082	Up	aldo-keto reductase family 1 member C2
NES	2.113098	7.27E-12	5.76E-11	6.852197	Up	nestin
HSPB2	2.111668	0.007195	0.015408	2.687679	Up	heat shock protein family B (small) member 2
PLA2R1	2.102916	1.01E-05	3.58E-05	4.415964	Up	phospholipase A2 receptor 1
HOXA11	2.088095	0.008207	0.017329	2.643419	Up	homeobox A11
CLMP	2.080518	3.69E-18	6.11E-17	8.688022	Up	CXADR like cell adhesion molecule
STEAP1	2.037396	5.20E-05	0.000165	4.046665	Up	STEAP family member 1
TBX5	2.034345	0.008208	0.017329	2.643396	Up	T-box transcription factor 5
EFS	2.025836	0.000121	0.000361	3.845052	Up	embryonal Fyn-associated substrate
MYRIP	2.018701	1.66E-05	5.69E-05	4.306579	Up	myosin VIIA and Rab interacting protein
KCNK15	2.008387	0.008147	0.017214	2.645932	Up	potassium two pore domain channel subfamily K member 15
DDR2	1.994841	2.62E-33	2.25E-31	12.02533	Up	discoidin domain receptor tyrosine kinase 2
DKK3	1.994142	1.60E-19	3.12E-18	9.037563	Up	dickkopf Wnt signaling pathway inhibitor 3
NR2F1	1.981164	0.000428	0.001169	3.522332	Up	nuclear receptor subfamily 2 group F member 1
FBN1	1.976471	1.87E-30	1.16E-28	11.46976	Up	fibrillin 1
SIM1	1.95815	0.000842	0.002183	3.338724	Up	SIM bHLH transcription factor 1
RBPMS	1.957547	4.98E-08	2.46E-07	5.45208	Up	RNA binding protein, mRNA processing factor
TBX18	1.953417	8.65E-05	0.000265	3.925615	Up	T-box transcription factor 18
FIBIN	1.942527	0.002755	0.006439	2.993843	Up	fin bud initiation factor homolog
SERPINE2	1.930577	2.35E-26	9.57E-25	10.6222	Up	serpin family E member 2
NDNF	1.925565	0.002776	0.006483	2.991542	Up	neuron derived neurotrophic factor
SNX7	1.925541	4.20E-06	1.58E-05	4.601115	Up	sorting nexin 7
ECM2	1.9197	2.42E-05	8.11E-05	4.221677	Up	extracellular matrix protein 2
GREB1L	1.917813	0.00013	0.000389	3.826011	Up	GREB1 like retinoic acid receptor coactivator
SYDE1	1.915527	1.69E-07	7.74E-07	5.230735	Up	synapse defective Rho GTPase activating protein 1
MPDZ	1.915112	3.68E-10	2.38E-09	6.267142	Up	multiple PDZ domain crumbs cell polarity complex component
CAVIN1	1.907152	1.26E-40	1.98E-38	13.34528	Up	caveolae associated protein 1
NTF3	1.900952	0.012632	0.025464	2.493984	Up	neurotrophin 3
PDGFRL	1.888552	0.008165	0.017252	2.645165	Up	platelet derived growth factor receptor like
GPC1	1.861051	4.57E-26	1.80E-24	10.55993	Up	glypican 1
HECW1	1.850233	0.000247	0.000704	3.665386	Up	HECT, C2 and WW domain containing E3 ubiquitin protein ligase 1
FKBP10	1.843098	3.53E-15	4.10E-14	7.870722	Up	FKBP prolyl isomerase 10
RPL36A-HNRNPH2	1.832781	0.010581	0.021755	2.556233	Up	RPL36A-HNRNPH2 readthrough
IQCJ-SCHIP1	1.828948	0.001141	0.002883	3.253112	Up	IQCJ-SCHIP1 readthrough
CTHRC1	1.818791	4.19E-05	0.000135	4.096774	Up	collagen triple helix repeat containing 1
VSTM4	1.79116	0.000105	0.000318	3.878109	Up	V-set and transmembrane domain containing 4
PLPPR4	1.746366	9.67E-06	3.45E-05	4.42449	Up	phospholipid phosphatase related 4
ADGRL4	1.734783	0.007236	0.015487	2.685772	Up	adhesion G protein-coupled receptor L4
COL5A1	1.725114	1.88E-12	1.60E-11	7.042996	Up	collagen type V alpha 1 chain
FARP1	1.720709	1.54E-16	2.11E-15	8.253303	Up	FERM, ARH/RhoGEF and pleckstrin domain protein 1
DDAH1	1.712179	3.96E-11	2.88E-10	6.605693	Up	dimethylarginine dimethylaminohydrolase 1

HSPB6	1.705571	7.83E-06	2.83E-05	4.469815	Up	heat shock protein family B (small) member 6
EMP2	1.695582	0.000959	0.002459	3.302145	Up	epithelial membrane protein 2
TRBV11-3	1.694846	2.67E-05	8.89E-05	4.199753	Up	T cell receptor beta variable 11-3
GDF5	1.688016	0.015153	0.030021	2.428712	Up	growth differentiation factor 5
TBX15	1.687965	0.000743	0.001947	3.373167	Up	T-box transcription factor 15
BDKRB2	1.680785	0.00022	0.000632	3.695132	Up	bradykinin receptor B2
BICC1	1.673064	1.93E-12	1.64E-11	7.03929	Up	BicC family RNA binding protein 1
NALF2	1.664295	0.004262	0.009564	2.858095	Up	NALCN channel auxiliary factor 2
LYPD6	1.661277	0.008965	0.018751	2.613401	Up	LY6/PLAUR domain containing 6
SLC2A10	1.660694	1.53E-10	1.04E-09	6.401977	Up	solute carrier family 2 member 10
PLAC9	1.650749	0.020555	0.039394	2.316056	Up	placenta associated 9
HTR2B	1.649356	0.003191	0.007362	2.94872	Up	5-hydroxytryptamine receptor 2B
LGR5	1.630833	0.017782	0.034639	2.370135	Up	leucine rich repeat containing G protein-coupled receptor 5
IGFBP4	1.609416	7.99E-27	3.50E-25	10.72242	Up	insulin like growth factor binding protein 4
FBLN2	1.606973	5.96E-28	2.88E-26	10.95989	Up	fibulin 2
VASN	1.603142	1.06E-11	8.26E-11	6.797791	Up	vasorin
TUSC3	1.598146	0.00057	0.001523	3.445412	Up	tumor suppressor candidate 3
FGD1	1.597066	0.003475	0.007956	2.922284	Up	FYVE, RhoGEF and PH domain containing 1
CXCL12	1.590925	0.000355	0.000985	3.571614	Up	C-X-C motif chemokine ligand 12
IGKV2-29	1.584381	0.000395	0.001086	3.543641	Up	immunoglobulin kappa variable 2-29
SLC1A1	1.583591	1.86E-06	7.35E-06	4.768394	Up	solute carrier family 1 member 1
PPIC	1.583039	0.00559	0.012263	2.770912	Up	peptidylprolyl isomerase C
TJP1	1.577047	1.02E-08	5.55E-08	5.726857	Up	tight junction protein 1
IGF2BP1	1.577035	0.003016	0.00699	2.966148	Up	insulin like growth factor 2 mRNA binding protein 1
FRAS1	1.572012	1.57E-06	6.29E-06	4.801582	Up	Fraser extracellular matrix complex subunit 1
EVA1A	1.569301	0.000414	0.001134	3.531133	Up	eva-1 homolog A, regulator of programmed cell death
SHROOM3	1.565354	0.000285	0.000804	3.628315	Up	shroom family member 3
MAGI1	1.559677	2.92E-06	1.12E-05	4.676623	Up	membrane associated guanylate kinase, WW and PDZ domain containing 1
RASSF8	1.55934	1.66E-14	1.80E-13	7.674335	Up	Ras association domain family member 8
GAS6-DT	1.557909	0.017145	0.033537	2.383576	Up	GAS6 divergent transcript
MAP1B	1.553727	1.28E-12	1.11E-11	7.095926	Up	microtubule associated protein 1B
GAS6	1.539865	2.86E-29	1.59E-27	11.2315	Up	growth arrest specific 6
SIX4	1.536794	0.009437	0.019641	2.595788	Up	SIX homeobox 4
RHBDF1	1.515202	0.000453	0.001232	3.507026	Up	rhomboid 5 homolog 1
MET	1.50841	4.44E-06	1.66E-05	4.589422	Up	MET proto-oncogene, receptor tyrosine kinase
GABRE	1.505837	0.002018	0.004854	3.087572	Up	gamma-aminobutyric acid type A receptor subunit epsilon
ENOX1	1.504319	0.017762	0.034605	2.370551	Up	ecto-NOX disulfide-thiol exchanger 1
VIT	1.497646	3.33E-07	1.47E-06	5.103503	Up	vitrin
LAYN	1.483143	4.33E-10	2.77E-09	6.241492	Up	layilin
PARVA	1.456247	9.08E-11	6.37E-10	6.481557	Up	parvin alpha
IGKV1D-8	1.452371	5.79E-05	0.000183	4.021076	Up	immunoglobulin kappa variable 1D-8
SPRY4	1.439844	0.003397	0.0078	2.929318	Up	sprouty RTK signaling antagonist 4

ARSJ	1.436589	4.09E-09	2.33E-08	5.880338	Up	arylsulfatase family member J
FAT1	1.426917	2.03E-08	1.06E-07	5.609614	Up	FAT atypical cadherin 1
EML1	1.418848	0.007596	0.016169	2.669511	Up	EMAP like 1
UCHL1	1.406472	0.000255	0.000724	3.657591	Up	ubiquitin C-terminal hydrolase L1
PXDN	1.388129	5.10E-05	0.000162	4.051013	Up	peroxidasin
EMP1	1.384414	1.58E-16	2.16E-15	8.250566	Up	epithelial membrane protein 1
PLPP3	1.383493	1.70E-18	2.91E-17	8.775757	Up	phospholipid phosphatase 3
ADAMDEC1	1.382897	4.82E-08	2.39E-07	5.457742	Up	ADAM like decysin 1
TRDV3	1.375274	0.003406	0.007818	2.928523	Up	T cell receptor delta variable 3
SERINC4	1.374455	0.005025	0.011129	2.80544	Up	serine incorporator 4
ARNT2	1.369491	0.001302	0.003252	3.215469	Up	aryl hydrocarbon receptor nuclear translocator 2
DPYSL3	1.368573	0.000135	0.000401	3.817818	Up	dihydropyrimidinase like 3
MID1	1.353005	4.87E-07	2.09E-06	5.031352	Up	midline 1
POPDC1	1.340335	0.000982	0.002511	3.29568	Up	popeye domain cAMP effector 1
PACSIN3	1.330795	0.005719	0.012527	2.76345	Up	protein kinase C and casein kinase substrate in neurons 3
HMCN1	1.317502	2.12E-08	1.10E-07	5.602303	Up	hemicentin 1
GPR85	1.312989	0.003136	0.007243	2.954127	Up	G protein-coupled receptor 85
RPL23A	1.301562	6.47E-46	1.47E-43	14.22437	Up	ribosomal protein L23a
JAM2	1.291597	5.92E-05	0.000186	4.015995	Up	junctional adhesion molecule 2
RPS10-NUDT3	1.278148	1.03E-35	1.10E-33	12.47435	Up	RPS10-NUDT3 readthrough
TRDV2	1.276556	0.000235	0.000673	3.677796	Up	T cell receptor delta variable 2
PEDS1-UBE2V1	1.272695	0.003505	0.008018	2.919613	Up	PEDS1-UBE2V1 readthrough
TMEM98	1.253827	0.000212	0.000611	3.704466	Up	transmembrane protein 98
AXL	1.251554	2.87E-08	1.46E-07	5.549025	Up	AXL receptor tyrosine kinase
SH2D5	1.250444	0.023121	0.043737	2.271435	Up	SH2 domain containing 5
MAMDC2	1.24108	0.001196	0.003006	3.239892	Up	MAM domain containing 2
LIMCH1	1.238899	5.50E-09	3.09E-08	5.831361	Up	LIM and calponin homology domains 1
HLA-DQB2	1.236112	0.000802	0.002087	3.352233	Up	major histocompatibility complex, class II, DQ beta 2
CLSTN2	1.223283	0.009116	0.019027	2.607672	Up	calsyntenin 2
SERPINE1	1.21927	6.72E-17	9.63E-16	8.351867	Up	serpin family E member 1
MOXD1	1.214013	1.25E-05	4.37E-05	4.368887	Up	monooxygenase DBH like 1
TRBV13	1.211919	3.26E-05	0.000107	4.154831	Up	T cell receptor beta variable 13
IGKV1-37	1.20512	0.024178	0.045505	2.254282	Up	immunoglobulin kappa variable 1-37 (non-functional)
C1QTNF1	1.186785	0.014552	0.028937	2.443346	Up	C1q and TNF related 1
SYNPO2	1.183085	3.92E-19	7.28E-18	8.939145	Up	synaptopodin 2
EDNRB	1.178295	0.003977	0.008985	2.880015	Up	endothelin receptor type B
OGN	1.168848	0.016944	0.033177	2.387931	Up	osteoglycin
SIK1	1.164401	0.02252	0.042712	2.281478	Up	salt inducible kinase 1
CRMP1	1.163522	0.021264	0.04059	2.303266	Up	collapsin response mediator protein 1
PTX3	1.160889	3.35E-18	5.58E-17	8.698852	Up	pentraxin 3
DNAJC12	1.15976	0.006166	0.013398	2.738838	Up	DnaJ heat shock protein family (Hsp40) member C12
RNF182	1.156006	0.00129	0.003223	3.218278	Up	ring finger protein 182
EHD2	1.154076	1.93E-12	1.63E-11	7.039776	Up	EH domain containing 2

FGF2	1.143663	2.80E-07	1.24E-06	5.136669	Up	fibroblast growth factor 2
SV2B	1.138617	0.001042	0.002654	3.278846	Up	synaptic vesicle glycoprotein 2B
TRBV7-7	1.138263	0.019367	0.037363	2.338385	Up	T cell receptor beta variable 7-7
SH3D19	1.136111	0.000148	0.000438	3.79441	Up	SH3 domain containing 19
NQO1	1.136075	8.99E-14	8.96E-13	7.454951	Up	NAD(P)H quinone dehydrogenase 1
IGHV4-28	1.131615	0.000637	0.001685	3.415523	Up	immunoglobulin heavy variable 4-28
HTRA1	1.129946	7.05E-08	3.40E-07	5.389997	Up	HtrA serine peptidase 1
RCAN2	1.1074	1.16E-07	5.44E-07	5.300055	Up	regulator of calcineurin 2
UPK3A	1.10605	2.23E-09	1.30E-08	5.980285	Up	uroplakin 3A
CHODL	1.100431	0.001719	0.004196	3.134941	Up	chondrolectin
TRAV12-2	1.098364	5.28E-09	2.97E-08	5.838219	Up	T cell receptor alpha variable 12-2
ENAH	1.097956	2.18E-11	1.64E-10	6.693597	Up	ENAH actin regulator
CNN3	1.095255	1.88E-17	2.87E-16	8.500898	Up	calponin 3
PODN	1.092406	1.19E-09	7.18E-09	6.081879	Up	podocan
FKBP1C	1.078199	0.011677	0.023735	2.521771	Up	FKBP prolyl isomerase family member 1C
MMP14	1.068159	1.66E-17	2.56E-16	8.515099	Up	matrix metallopeptidase 14
TM4SF1	1.067094	0.001443	0.003573	3.185828	Up	transmembrane 4 L six family member 1
GPM6B	1.063659	0.001168	0.002945	3.246519	Up	glycoprotein M6B
LMCD1	1.061614	6.51E-07	2.75E-06	4.975314	Up	LIM and cysteine rich domains 1
CD248	1.048095	9.22E-07	3.82E-06	4.907507	Up	CD248 molecule
FERMT2	1.047165	3.07E-05	0.000101	4.168569	Up	FERM domain containing kindlin 2
ADAMTS5	1.045722	8.56E-12	6.72E-11	6.828875	Up	ADAM metallopeptidase with thrombospondin type 1 motif 5
LHFPL6	1.038606	2.52E-07	1.13E-06	5.156176	Up	LHFPL tetraspan subfamily member 6
COLEC12	1.037056	5.05E-05	0.00016	4.05352	Up	collectin subfamily member 12
PMP22	1.036524	9.82E-10	6.00E-09	6.112318	Up	peripheral myelin protein 22
HEYL	1.031584	0.002138	0.005115	3.070424	Up	hes related family bHLH transcription factor with YRPW motif like
NCS1	1.028242	1.35E-07	6.31E-07	5.271417	Up	neuronal calcium sensor 1
EPB41L1	1.024122	0.000104	0.000314	3.882166	Up	erythrocyte membrane protein band 4.1 like 1
BMP3	1.022824	0.007552	0.016087	2.671469	Up	bone morphogenetic protein 3
LRRN3	1.010948	0.000536	0.001441	3.461884	Up	leucine rich repeat neuronal 3
NT5E	1.0109	6.42E-12	5.12E-11	6.869923	Up	5'-nucleotidase ecto
SPATA18	1.010038	0.001879	0.00454	3.108728	Up	spermatogenesis associated 18
ERH	1.004586	9.53E-53	3.35E-50	15.28569	Up	ERH mRNA splicing and mitosis factor
TMEM126A	0.997029	4.26E-29	2.32E-27	11.19609	Up	transmembrane protein 126A
ENPP1	0.994519	1.96E-07	8.89E-07	5.203164	Up	ectonucleotide pyrophosphatase/phosphodiesterase 1
CXCL10	0.992529	0.000291	0.000821	3.622748	Up	C-X-C motif chemokine ligand 10
IGLV8-61	0.991418	0.007427	0.015854	2.677049	Up	immunoglobulin lambda variable 8-61
SERPINB2	0.990545	8.79E-10	5.40E-09	6.130007	Up	serpin family B member 2
GPR15	0.984331	0.000278	0.000786	3.634657	Up	G protein-coupled receptor 15
TRBV14	0.974117	0.000184	0.000537	3.739382	Up	T cell receptor beta variable 14
PRXL2C	0.970515	3.64E-32	2.78E-30	11.80593	Up	peroxiredoxin like 2C
KLRB1	0.97039	6.66E-11	4.73E-10	6.528174	Up	killer cell lectin like receptor B1
PDGFRB	0.970386	5.00E-09	2.82E-08	5.847334	Up	platelet derived growth factor receptor beta

TRAV25	0.969073	9.51E-08	4.52E-07	5.335856	Up	T cell receptor alpha variable 25
IGFBP3	0.965482	2.46E-10	1.62E-09	6.329739	Up	insulin like growth factor binding protein 3
SLC16A2	0.96295	0.002594	0.006102	3.012121	Up	solute carrier family 16 member 2
CEP55	0.957223	9.60E-07	3.96E-06	4.89976	Up	centrosomal protein 55
PHLDA3	0.956912	5.04E-08	2.49E-07	5.449939	Up	pleckstrin homology like domain family A member 3
TYRO3	0.956641	0.006677	0.014388	2.712544	Up	TYRO3 protein tyrosine kinase
BCAT1	0.956086	1.86E-07	8.47E-07	5.213061	Up	branched chain amino acid transaminase 1
HSPG2	0.955707	2.31E-12	1.94E-11	7.014544	Up	heparan sulfate proteoglycan 2
IGKV1-9	0.954284	0.000397	0.001092	3.542132	Up	immunoglobulin kappa variable 1-9
SMARCA1	0.954175	2.96E-05	9.78E-05	4.176229	Up	SNF2 related chromatin remodeling ATPase 1
HSD17B14	0.952926	0.001748	0.00426	3.13007	Up	hydroxysteroid 17-beta dehydrogenase 14
MGST1	0.948266	7.26E-15	8.16E-14	7.779858	Up	microsomal glutathione S-transferase 1
PIERCE2	0.946847	0.005046	0.01117	2.804087	Up	piercer of microtubule wall 2
IGHV3-11	0.942696	2.80E-05	9.27E-05	4.189276	Up	immunoglobulin heavy variable 3-11
MYOM2	0.941964	0.017407	0.033988	2.377988	Up	myomesin 2
FBLN5	0.939529	3.68E-10	2.38E-09	6.267054	Up	fibulin 5
DACT1	0.939403	7.13E-05	0.000221	3.971837	Up	dishevelled binding antagonist of beta catenin 1
ALDH1L2	0.93916	9.43E-08	4.49E-07	5.337425	Up	aldehyde dehydrogenase 1 family member L2
CERCAM	0.938312	1.72E-10	1.16E-09	6.384424	Up	cerebral endothelial cell adhesion molecule
GAS1	0.937421	7.71E-09	4.26E-08	5.774639	Up	growth arrest specific 1
STAC	0.936118	0.00284	0.006623	2.984527	Up	SH3 and cysteine rich domain
COL6A3	0.93372	4.06E-07	1.76E-06	5.065996	Up	collagen type VI alpha 3 chain
MAL2	0.932912	0.023021	0.043563	2.273084	Up	mal, T cell differentiation protein 2
GPR183	0.932248	6.06E-14	6.19E-13	7.506834	Up	G protein-coupled receptor 183
TRAV24	0.931877	7.44E-06	2.70E-05	4.480705	Up	T cell receptor alpha variable 24
NXT2	0.930003	8.69E-37	1.01E-34	12.66984	Up	nuclear transport factor 2 like export factor 2
FILIP1L	0.929717	5.09E-09	2.87E-08	5.844168	Up	filamin A interacting protein 1 like
NME1-NME2	0.927652	0.018482	0.035854	2.355825	Up	NME1-NME2 readthrough
KRT10	0.924331	3.36E-24	1.09E-22	10.14861	Up	keratin 10
TRBV7-9	0.922633	2.35E-08	1.21E-07	5.584298	Up	T cell receptor beta variable 7-9
CELA1	0.91885	0.002393	0.005665	3.036549	Up	chymotrypsin like elastase 1
SEMA5A	0.918204	4.57E-09	2.59E-08	5.862142	Up	semaphorin 5A
C6orf132	0.915398	0.005011	0.011101	2.806296	Up	chromosome 6 open reading frame 132
CGNL1	0.913007	0.011692	0.023762	2.521313	Up	cingulin like 1
POGLUT3	0.91287	2.90E-14	3.05E-13	7.602886	Up	protein O-glucosyltransferase 3
RNASE4	0.905781	1.52E-07	7.00E-07	5.250659	Up	ribonuclease A family member 4
L1CAM	0.902947	1.44E-15	1.75E-14	7.981998	Up	L1 cell adhesion molecule
SMIM30	0.901602	3.20E-26	1.29E-24	10.59323	Up	small integral membrane protein 30
RGS1	0.900677	2.81E-09	1.63E-08	5.942339	Up	regulator of G protein signaling 1
FAM111B	0.898742	1.07E-08	5.78E-08	5.719551	Up	FAM111 trypsin like peptidase B
CCR6	0.898308	5.62E-08	2.75E-07	5.430508	Up	C-C motif chemokine receptor 6
IGKV5-2	0.898283	0.003009	0.006977	2.966838	Up	immunoglobulin kappa variable 5-2
TKTL1	0.895181	1.61E-06	6.43E-06	4.797026	Up	transketolase like 1

KDM4D	0.894692	0.000292	0.000821	3.622677	Up	lysine demethylase 4D
SELENOP	0.892395	1.21E-07	5.65E-07	5.292371	Up	selenoprotein P
CD3G	0.89168	7.10E-12	5.63E-11	6.855611	Up	CD3 gamma subunit of T-cell receptor complex
SCD	0.888544	6.88E-11	4.88E-10	6.52335	Up	stearoyl-CoA desaturase
CYP51A1	0.883173	5.24E-18	8.55E-17	8.647957	Up	cytochrome P450 family 51 subfamily A member 1
GPM6A	0.881035	0.002152	0.005147	3.06848	Up	glycoprotein M6A
TRAV29DV5	0.878934	4.05E-07	1.76E-06	5.06668	Up	T cell receptor alpha variable 29/delta variable 5
DERPC	0.877909	9.80E-05	0.000298	3.895516	Up	DERPC proline and glycine rich nuclear protein
LDHB	0.876855	3.02E-12	2.50E-11	6.976766	Up	lactate dehydrogenase B
TSPAN13	0.873188	2.01E-13	1.91E-12	7.34844	Up	tetraspanin 13
FPR3	0.873071	1.07E-07	5.07E-07	5.313783	Up	formyl peptide receptor 3
AKR1C3	0.867961	9.27E-09	5.06E-08	5.743532	Up	aldo-keto reductase family 1 member C3
NIFK	0.865365	5.13E-29	2.77E-27	11.17956	Up	nucleolar protein interacting with the FHA domain of MKI67
IGHV3-21	0.864568	0.000155	0.000457	3.783419	Up	immunoglobulin heavy variable 3-21
TRBV12-5	0.862691	0.012237	0.02475	2.505236	Up	T cell receptor beta variable 12-5
TRBV7-2	0.861395	5.02E-06	1.87E-05	4.563945	Up	T cell receptor beta variable 7-2
PLA2G7	0.861162	2.24E-07	1.01E-06	5.178081	Up	phospholipase A2 group VII
GLO1	0.861014	5.32E-20	1.08E-18	9.1574	Up	glyoxalase I
EPAS1	0.86017	3.05E-15	3.58E-14	7.888812	Up	endothelial PAS domain protein 1
LOXL1	0.858811	9.22E-06	3.30E-05	4.434787	Up	lysyl oxidase like 1
TMEM97	0.854196	8.49E-10	5.23E-09	6.135499	Up	transmembrane protein 97
CORO2B	0.854166	3.65E-05	0.000119	4.128698	Up	coronin 2B
PRKACB	0.853831	1.70E-18	2.91E-17	8.775852	Up	protein kinase cAMP-activated catalytic subunit beta
GPR161	0.853683	2.53E-05	8.43E-05	4.21228	Up	G protein-coupled receptor 161
MSMO1	0.852607	2.85E-31	1.94E-29	11.63147	Up	methylsterol monooxygenase 1
ALPK2	0.850371	0.000169	0.000497	3.760652	Up	alpha kinase 2
DLC1	0.84498	2.08E-09	1.22E-08	5.991261	Up	DLC1 Rho GTPase activating protein
DYNLT5	0.84381	0.010648	0.021864	2.554032	Up	dynein light chain Tctex-type family member 5
IGHV4-30-2	0.843112	0.002308	0.005481	3.047391	Up	immunoglobulin heavy variable 4-30-2
MACROD2	0.841834	0.000607	0.001611	3.428576	Up	mono-ADP ribosylhydrolase 2
JCHAIN	0.841764	0.000964	0.002469	3.300873	Up	joining chain of multimeric IgA and IgM
LAMC1	0.841695	5.39E-12	4.34E-11	6.894831	Up	laminin subunit gamma 1
PLS3	0.839247	3.15E-06	1.20E-05	4.661089	Up	plastin 3
MEOX1	0.838624	6.65E-07	2.80E-06	4.971417	Up	mesenchyme homeobox 1
FOSL1	0.838453	0.004761	0.010595	2.82277	Up	FOS like 1, AP-1 transcription factor subunit
HSPA13	0.83809	3.80E-22	9.92E-21	9.676394	Up	heat shock protein family A (Hsp70) member 13
TAF9B	0.837697	1.88E-16	2.56E-15	8.22921	Up	TATA-box binding protein associated factor 9b
CCL2	0.837137	0.005242	0.011565	2.79179	Up	C-C motif chemokine ligand 2
TRAV1-2	0.834935	1.26E-05	4.41E-05	4.367059	Up	T cell receptor alpha variable 1-2
COL15A1	0.834229	0.001811	0.004398	3.119517	Up	collagen type XV alpha 1 chain
PDK4	0.831934	1.54E-07	7.09E-07	5.248074	Up	pyruvate dehydrogenase kinase 4
SH3BP4	0.831046	9.37E-13	8.21E-12	7.139419	Up	SH3 domain binding protein 4
TRAV10	0.830482	8.43E-05	0.000259	3.931729	Up	T cell receptor alpha variable 10

RGPD3	0.829212	4.65E-08	2.31E-07	5.464331	Up	RANBP2 like and GRIP domain containing 3
ETS1	0.827664	1.48E-15	1.80E-14	7.978971	Up	ETS proto-oncogene 1, transcription factor
GZMK	0.82699	6.18E-06	2.27E-05	4.520254	Up	granzyme K
KPNA3	0.826609	8.53E-39	1.14E-36	13.02759	Up	karyopherin subunit alpha 3
WNT5B	0.826401	5.58E-06	2.06E-05	4.541567	Up	Wnt family member 5B
DHCR24	0.825934	6.65E-10	4.16E-09	6.174164	Up	24-dehydrocholesterol reductase
RFK	0.825117	1.63E-19	3.18E-18	9.035347	Up	riboflavin kinase
IGHV1-2	0.82301	0.002738	0.006402	2.995769	Up	immunoglobulin heavy variable 1-2
NPR3	0.822681	0.000143	0.000426	3.802217	Up	natriuretic peptide receptor 3
RNU5A-1	-9.36757	9.35E-86	0.042712	-19.6256	Down	RNA, U5A small nuclear 1
RNU5B-1	-8.32978	1.01E-53	9.24E-21	-15.431	Down	RNA, U5B small nuclear 1
RNU5E-1	-8.2645	3.75E-43	2.92E-52	-13.7722	Down	RNA, U5E small nuclear 1
SNORA67	-8.23002	1.19E-59	4.91E-05	-16.2887	Down	small nucleolar RNA, H/ACA box 67
RNU4ATAC	-7.93251	6.23E-60	3.15E-12	-16.3281	Down	RNA, U4atac small nuclear
SNORD33	-7.88055	2.77E-80	1.94E-11	-18.9744	Down	small nucleolar RNA, C/D box 33
RNY1	-7.87757	4.59E-135	0.043563	-24.7342	Down	RNA, Ro60-associated Y1
SNORA44	-7.56853	4.18E-31	0.004398	-11.5987	Down	small nucleolar RNA, H/ACA box 44
RNY3	-7.06451	1.97E-151	0.021864	-26.2113	Down	RNA, Ro60-associated Y3
SNORD14C	-6.92929	9.52E-45	1.05E-59	-14.035	Down	small nucleolar RNA, C/D box 14C
SNORA22	-6.77358	1.58E-47	2.77E-27	-14.4816	Down	small nucleolar RNA, H/ACA box 22
SNORD46	-6.45843	1.51E-44	1.62E-09	-14.0022	Down	small nucleolar RNA, C/D box 46
SNORA71C	-6.40011	2.20E-47	1.08E-09	-14.459	Down	small nucleolar RNA, H/ACA box 71C
SNORA47	-6.37221	1.85E-71	0.006439	-17.8749	Down	small nucleolar RNA, H/ACA box 47
SNORD32A	-5.95652	9.36E-25	6.28E-13	-10.2726	Down	small nucleolar RNA, C/D box 32A
SNORA60	-5.82607	1.15E-14	2.38E-09	-7.72173	Down	small nucleolar RNA, H/ACA box 60
RNA5S1	-5.777	3.34E-24	2.52E-20	-10.1493	Down	RNA, 5S ribosomal 1
SNORD22	-5.76022	2.23E-26	0.000457	-10.6271	Down	small nucleolar RNA, C/D box 22
SNORA3A	-5.75667	5.20E-16	0.006102	-8.10679	Down	small nucleolar RNA, H/ACA box 3A
SNORA16A	-5.72058	5.54E-31	5.65E-07	-11.5747	Down	small nucleolar RNA, H/ACA box 16A
SNORD67	-5.70868	9.71E-26	4.64E-163	-10.4889	Down	small nucleolar RNA, C/D box 67
RNY4	-5.67699	2.92E-36	3.91E-07	-12.5745	Down	RNA, Ro60-associated Y4
SNORA64	-5.66503	6.72E-23	1.76E-06	-9.852	Down	small nucleolar RNA, H/ACA box 64
SNORA24	-5.59567	5.60E-41	2.70E-05	-13.4057	Down	small nucleolar RNA, H/ACA box 24
SNORD89	-5.59058	1.14E-88	1.22E-08	-19.9638	Down	small nucleolar RNA, C/D box 89
SNORA10	-5.49459	3.35E-55	1.46E-15	-15.6496	Down	small nucleolar RNA, H/ACA box 10
SNORD118	-5.43878	2.67E-22	1.16E-93	-9.71251	Down	small nucleolar RNA, C/D box 118
SNORA70	-5.37735	1.07E-23	0.00699	-10.035	Down	small nucleolar RNA, H/ACA box 70
SNORA20	-5.28886	2.34E-24	0.00454	-10.1839	Down	small nucleolar RNA, H/ACA box 20
RNU6ATAC	-5.27715	1.83E-45	1.16E-09	-14.1515	Down	RNA, U6atac small nuclear
SNORA26	-5.27463	7.66E-25	0.000135	-10.2919	Down	small nucleolar RNA, H/ACA box 26
SNORA61	-5.22076	4.86E-11	3.13E-21	-6.57513	Down	small nucleolar RNA, H/ACA box 61
SNORD55	-5.14442	6.57E-16	3.98E-11	-8.07823	Down	small nucleolar RNA, C/D box 55
SNORD104	-5.09121	6.18E-24	1.84E-63	-10.0891	Down	small nucleolar RNA, C/D box 104

SNORA14B	-5.09081	2.19E-25	2.91E-17	-10.4118	Down	small nucleolar RNA, H/ACA box 14B
SNORA22C	-5.07415	3.29E-23	2.25E-31	-9.92349	Down	small nucleolar RNA, H/ACA box 22C
RNU12	-5.06201	1.15E-16	1.76E-06	-8.28862	Down	RNA, U12 small nuclear
SNORA78	-4.99605	3.60E-19	2.77E-09	-8.9486	Down	small nucleolar RNA, H/ACA box 78
SCARNA20	-4.9847	1.05E-32	5.98E-07	-11.9102	Down	small Cajal body-specific RNA 20
SNORA37	-4.95264	3.26E-28	5.47E-14	-11.0143	Down	small nucleolar RNA, H/ACA box 37
SNORD99	-4.9225	3.53E-20	2.10E-108	-9.20135	Down	small nucleolar RNA, C/D box 99
SNORA52	-4.87838	4.56E-34	2.91E-17	-12.1687	Down	small nucleolar RNA, H/ACA box 52
SCARNA22	-4.74141	1.38E-25	0.000668	-10.4559	Down	small Cajal body-specific RNA 22
SNORD57	-4.7408	1.50E-13	1.31E-32	-7.38705	Down	small nucleolar RNA, C/D box 57
SNORA77B	-4.71956	1.18E-17	0.043737	-8.55533	Down	small nucleolar RNA, H/ACA box 77B
SNORD21	-4.7007	2.46E-14	2.46E-07	-7.62419	Down	small nucleolar RNA, C/D box 21
SNORA63	-4.65718	7.93E-60	3.85E-07	-16.3134	Down	small nucleolar RNA, H/ACA box 63
RNU4-1	-4.64048	1.35E-49	9.22E-05	-14.8055	Down	RNA, U4 small nuclear 1
SNORD8	-4.63627	3.10E-19	2.61E-32	-8.9652	Down	small nucleolar RNA, C/D box 8
RNU2-1	-4.63486	2.74E-11	0.006977	-6.65982	Down	RNA, U2 small nuclear 1
SNORD13	-4.63058	7.64E-74	1.98E-38	-18.1785	Down	small nucleolar RNA, C/D box 13
SNORA63D	-4.59027	8.00E-39	3.52E-53	-13.0325	Down	small nucleolar RNA, H/ACA box 63D
SNORA68	-4.55743	1.61E-16	5.63E-11	-8.24814	Down	small nucleolar RNA, H/ACA box 68
SNORD110	-4.53256	6.88E-16	1.99E-07	-8.07261	Down	small nucleolar RNA, C/D box 110
SNORA79B	-4.52221	2.43E-53	0.000632	-15.3744	Down	small nucleolar RNA, H/ACA box 79B
SNORA38	-4.49748	9.45E-17	1.07E-33	-8.31146	Down	small nucleolar RNA, H/ACA box 38
SNORD105B	-4.44552	4.22E-10	7.18E-09	-6.2456	Down	small nucleolar RNA, C/D box 105B
PPIAL4G	-4.30493	1.09E-07	4.67E-23	-5.31124	Down	peptidylprolyl isomerase A like 4G
SNORA38B	-4.25415	3.33E-27	0.006623	-10.803	Down	small nucleolar RNA, H/ACA box 38B
SNORD95	-4.24495	4.22E-11	5.06E-08	-6.59609	Down	small nucleolar RNA, C/D box 95
SNORA80D	-4.1763	2.48E-10	0.000168	-6.32842	Down	small nucleolar RNA, H/ACA box 80D
SNORA9	-4.16242	9.05E-06	9.27E-05	-4.43874	Down	small nucleolar RNA, H/ACA box 9
RNU1-1	-4.13309	6.80E-65	6.38E-19	-17.0111	Down	RNA, U1 small nuclear 1
RNU4-2	-4.11486	4.59E-50	0.016087	-14.8779	Down	RNA, U4 small nuclear 2
RNU6-7	-4.09926	7.51E-05	1.12E-05	-3.95962	Down	RNA, U6 small nuclear 7
SNORA50B	-4.07626	7.05E-12	0.000821	-6.85672	Down	small nucleolar RNA, H/ACA box 50B
RNVU1-7	-4.07017	4.04E-06	6.72E-11	-4.60943	Down	RNA, variant U1 small nuclear 7
SNORA49	-4.02264	1.46E-59	9.43E-18	-16.2762	Down	small nucleolar RNA, H/ACA box 49
SNORD100	-3.99131	6.91E-11	1.07E-28	-6.52262	Down	small nucleolar RNA, C/D box 100
SNORD116-15	-3.99118	1.32E-10	4.43E-07	-6.42429	Down	small nucleolar RNA, C/D box 116-15
SNORD9	-3.9813	7.91E-18	4.10E-14	-8.60085	Down	small nucleolar RNA, C/D box 9
SNORA65	-3.97267	1.43E-07	4.55E-31	-5.26114	Down	small nucleolar RNA, H/ACA box 65
SNORA71A	-3.96588	1.78E-58	2.71E-33	-16.1222	Down	small nucleolar RNA, H/ACA box 71A
SNORD56	-3.93113	7.32E-06	0.002161	-4.48429	Down	small nucleolar RNA, C/D box 56
SNORD116-17	-3.92921	2.37E-07	1.20E-15	-5.16784	Down	small nucleolar RNA, C/D box 116-17
SNORA62	-3.91674	0.000132	2.11E-15	-3.82207	Down	small nucleolar RNA, H/ACA box 62
SNORA66	-3.90697	3.84E-10	0.005115	-6.26045	Down	small nucleolar RNA, H/ACA box 66

SNORD27	-3.86244	0.000125	4.52E-07	-3.8355	Down	small nucleolar RNA, C/D box 27
SCARNA3	-3.78154	8.96E-14	0.025464	-7.45536	Down	small Cajal body-specific RNA 3
SNORA84	-3.78068	4.78E-41	3.05E-13	-13.4175	Down	small nucleolar RNA, H/ACA box 84
RNVU1-28	-3.77669	2.83E-11	0.000199	-6.65498	Down	RNA, variant U1 small nuclear 28
DUX4	-3.77062	0.00024	5.78E-08	-3.67279	Down	double homeobox 4
SNORD14D	-3.74194	0.00021	1.32E-20	-3.7067	Down	small nucleolar RNA, C/D box 14D
SNORA40B	-3.73025	3.01E-10	2.01E-11	-6.2985	Down	small nucleolar RNA, H/ACA box 40B
RN7SK	-3.72978	9.26E-22	0.000692	-9.58486	Down	RNA component of 7SK nuclear ribonucleoprotein
SCARNA21	-3.72905	2.71E-27	1.36E-58	-10.822	Down	small Cajal body-specific RNA 21
SNORA80E	-3.70586	7.39E-07	2.88E-26	-4.95074	Down	small nucleolar RNA, H/ACA box 80E
SNORD35A	-3.69128	0.000129	1.10E-07	-3.82777	Down	small nucleolar RNA, C/D box 35A
SNORA8	-3.67442	6.44E-23	1.58E-05	-9.8563	Down	small nucleolar RNA, H/ACA box 8
SNORD14A	-3.66348	2.15E-08	0.000497	-5.5996	Down	small nucleolar RNA, C/D box 14A
SCARNA18	-3.56481	2.50E-06	0.001169	-4.70797	Down	small Cajal body-specific RNA 18
SNORA12	-3.55763	4.34E-46	8.62E-16	-14.2522	Down	small nucleolar RNA, H/ACA box 12
SNORD117	-3.43189	4.08E-05	2.48E-19	-4.10274	Down	small nucleolar RNA, C/D box 117
SNORA33	-3.35549	7.78E-05	2.78E-26	-3.95112	Down	small nucleolar RNA, H/ACA box 33
RN7SL2	-3.34696	7.82E-56	1.94E-38	-15.7418	Down	RNA component of signal recognition particle 7SL2
SNORA2C	-3.34194	7.15E-51	7.84E-40	-15.0018	Down	small nucleolar RNA, H/ACA box 2C
SNORA71E	-3.32485	0.000554	1.52E-54	-3.4531	Down	small nucleolar RNA, H/ACA box 71E
SNORA7B	-3.31763	1.35E-57	0.00016	-15.9966	Down	small nucleolar RNA, H/ACA box 7B
SNORA74B	-3.29452	5.13E-28	1.04E-74	-10.9734	Down	small nucleolar RNA, H/ACA box 74B
SNORA71D	-3.28122	7.16E-30	1.43E-14	-11.353	Down	small nucleolar RNA, H/ACA box 71D
TMEFF1	-3.27628	8.81E-08	4.26E-08	-5.34975	Down	transmembrane protein with EGF like and two follistatin like domains 1
HRNR	-3.26028	7.50E-05	3.96E-06	-3.95997	Down	hornerin
SNORD97	-3.25899	7.67E-61	3.82E-06	-16.4554	Down	small nucleolar RNA, C/D box 97
SNORA57	-3.25188	9.30E-45	8.77E-06	-14.0366	Down	small nucleolar RNA, H/ACA box 57
SNORA13	-3.24552	0.001768	2.49E-07	-3.12664	Down	small nucleolar RNA, H/ACA box 13
SNORA2A	-3.22786	7.68E-07	2.73E-12	-4.94337	Down	small nucleolar RNA, H/ACA box 2A
SNORA7A	-3.22346	1.67E-35	5.58E-17	-12.4359	Down	small nucleolar RNA, H/ACA box 7A
SNORA21	-3.22121	0.001005	8.21E-12	-3.28913	Down	small nucleolar RNA, H/ACA box 21
SNORD116-16	-3.18251	8.37E-05	4.51E-16	-3.93357	Down	small nucleolar RNA, C/D box 116-16
SNORD94	-3.17594	1.13E-41	0.001092	-13.5241	Down	small nucleolar RNA, C/D box 94
SNORD10	-3.15686	3.16E-48	1.72E-12	-14.5919	Down	small nucleolar RNA, C/D box 10
SNORA59B	-3.15648	4.34E-13	6.16E-41	-7.2445	Down	small nucleolar RNA, H/ACA box 59B
RCCD1	-3.12511	1.08E-65	1.72E-46	-17.1185	Down	RCC1 domain containing 1
SNORA80B	-3.09856	1.36E-08	9.92E-21	-5.67888	Down	small nucleolar RNA, H/ACA box 80B
SNORA48	-3.08529	2.02E-53	0.007243	-15.3864	Down	small nucleolar RNA, H/ACA box 48
SNORA73B	-3.07945	5.82E-63	8.43E-05	-16.7484	Down	small nucleolar RNA, H/ACA box 73B
SLC9A4	-3.06161	4.04E-07	0.030021	-5.0669	Down	solute carrier family 9 member A4
SNORA17B	-2.98204	2.11E-17	1.13E-33	-8.48744	Down	small nucleolar RNA, H/ACA box 17B
SNORA73A	-2.96603	1.57E-50	0.00524	-14.9495	Down	small nucleolar RNA, H/ACA box 73A

SNORD116-2	-2.94609	0.005669	6.00E-12	-2.76636	Down	small nucleolar RNA, C/D box 116-2
NYX	-2.918	1.47E-09	1.10E-17	-6.04726	Down	nyctalopin
RN7SL1	-2.9053	4.19E-50	0.000673	-14.884	Down	RNA component of signal recognition particle 7SL1
RNVU1-31	-2.90229	2.74E-10	2.64E-07	-6.31299	Down	RNA, variant U1 small nuclear 31
SCARNA1	-2.87082	2.03E-06	5.42E-13	-4.75007	Down	small Cajal body-specific RNA 1
PLG	-2.86544	1.30E-10	2.07E-104	-6.42723	Down	plasminogen
SNORD116-3	-2.85802	0.019091	2.78E-30	-2.34374	Down	small nucleolar RNA, C/D box 116-3
RASEF	-2.84887	1.44E-09	4.60E-35	-6.05109	Down	RAS and EF-hand domain containing
SNORA23	-2.84589	2.64E-36	7.49E-29	-12.5825	Down	small nucleolar RNA, H/ACA box 23
OR52H1	-2.79971	4.73E-10	2.19E-89	-6.22786	Down	olfactory receptor family 52 subfamily H member 1
SNORA11B	-2.79172	1.32E-05	1.16E-28	-4.35608	Down	small nucleolar RNA, H/ACA box 11B
SNORA46	-2.7768	0.00849	1.86E-27	-2.63195	Down	small nucleolar RNA, H/ACA box 46
MND1	-2.75074	7.23E-30	2.71E-36	-11.3523	Down	meiotic nuclear divisions 1
RMRP	-2.67298	1.63E-08	0.006402	-5.64683	Down	RNA component of mitochondrial RNA processing endoribonuclease
SNORD88C	-2.66723	0.001855	2.16E-13	-3.11252	Down	small nucleolar RNA, C/D box 88C
SNORA80A	-2.65507	6.30E-15	1.01E-06	-7.79778	Down	small nucleolar RNA, H/ACA box 80A
SYNAGE	-2.64972	0.002247	0.002087	-3.05554	Down	synapse stability regulating cerebellar lncRNA
SNORD116-22	-2.64547	0.018004	0.000259	-2.36553	Down	small nucleolar RNA, C/D box 116-22
SNORD41	-2.6446	0.000145	2.92E-21	-3.79975	Down	small nucleolar RNA, C/D box 41
SNORA63E	-2.62674	0.000196	0.000389	-3.72378	Down	small nucleolar RNA, H/ACA box 63E
STX18-IT1	-2.59442	6.08E-08	1.13E-06	-5.41631	Down	STX18 intronic transcript 1
SNORA72	-2.59258	0.003602	0.019027	-2.91106	Down	small nucleolar RNA, H/ACA box 72
RP1L1	-2.59241	8.85E-07	6.10E-13	-4.91564	Down	RP1 like 1
SNORA14A	-2.59203	0.001034	0.005147	-3.28104	Down	small nucleolar RNA, H/ACA box 14A
MT-ND3	-2.58412	9.60E-51	2.29E-61	-14.9822	Down	NADH dehydrogenase subunit 3
GABRG2	-2.58145	0.000426	4.37E-05	-3.52335	Down	gamma-aminobutyric acid type A receptor subunit gamma2
SNORD71	-2.57142	0.005265	3.11E-78	-2.79037	Down	small nucleolar RNA, C/D box 71
SNORA54	-2.54382	1.74E-25	5.22E-23	-10.4335	Down	small nucleolar RNA, H/ACA box 54
SNORA5A	-2.53761	1.05E-07	2.56E-16	-5.31756	Down	small nucleolar RNA, H/ACA box 5A
HNRNPA1L2	-2.50624	0.020881	9.78E-05	-2.31012	Down	heterogeneous nuclear ribonucleoprotein A1 like 2
RNF225	-2.49538	1.03E-05	7.62E-07	-4.4115	Down	ring finger protein 225
RNVU1-4	-2.48192	1.01E-11	0.002459	-6.80553	Down	RNA, variant U1 small nuclear 4
DBET	-2.47929	0.023714	0.007818	-2.26173	Down	D4Z4 binding element transcript
MT-ATP8	-2.47749	4.06E-43	0.015408	-13.7663	Down	ATP synthase F0 subunit 8
TMEM132A	-2.4756	1.23E-07	8.55E-17	-5.28867	Down	transmembrane protein 132A
SHISA9	-2.43331	4.07E-09	0.028937	-5.8813	Down	shisa family member 9
KRT74	-2.42871	0.001314	1.74E-18	-3.21298	Down	keratin 74
RPPH1	-2.41171	1.55E-42	0.001685	-13.669	Down	ribonuclease P RNA component H1
RNU5F-1	-2.41023	0.017235	3.50E-25	-2.38166	Down	RNA, U5F small nuclear 1
ADGRG2	-2.35585	0.013049	1.33E-88	-2.48242	Down	adhesion G protein-coupled receptor G2
B4GALNT2	-2.35235	1.80E-06	0.000222	-4.77502	Down	beta-1,4-N-acetyl-galactosaminyltransferase 2 (SID blood group)
RN7SL3	-2.34991	2.75E-45	0.005481	-14.1229	Down	RNA component of signal recognition particle 7SL3

SNORA11F	-2.34587	6.28E-06	6.11E-17	-4.51681	Down	small nucleolar RNA, H/ACA box 11F
SNORA70I	-2.32603	0.001276	0.015487	-3.22123	Down	small nucleolar RNA, H/ACA box 70I
H1-7	-2.32255	3.95E-05	2.69E-13	-4.11035	Down	H1.7 linker histone
SNORA3B	-2.32192	0.018139	0.003006	-2.36278	Down	small nucleolar RNA, H/ACA box 3B
ZFPM2	-2.31662	1.31E-12	3.58E-14	-7.09308	Down	zinc finger protein, FOG family member 2
ACTN2	-2.3098	0.00628	0.033988	-2.73282	Down	actinin alpha 2
RNVU1-26	-2.30657	0.009916	2.97E-08	-2.57873	Down	RNA, variant U1 small nuclear 26
RNVU1-15	-2.28558	1.18E-09	9.54E-08	-6.08229	Down	RNA, variant U1 small nuclear 15
SNORA31	-2.28259	0.003493	5.28E-65	-2.92068	Down	small nucleolar RNA, H/ACA box 31
IHO1	-2.27789	7.27E-05	3.45E-05	-3.96711	Down	interactor of HORMAD1 1
FAM138F	-2.25699	0.004844	7.00E-07	-2.81725	Down	family with sequence similarity 138 member F
OR56A1	-2.22158	5.98E-08	0.000135	-5.41929	Down	olfactory receptor family 56 subfamily A member 1
OR2L3	-2.21336	6.46E-07	1.24E-06	-4.97704	Down	olfactory receptor family 2 subfamily L member 3
RNVU1-2A	-2.21203	0.025971	0.036255	-2.22664	Down	RNA, variant U1 small nuclear 2A
PCLO	-2.20727	3.90E-05	2.39E-07	-4.11359	Down	piccolo presynaptic cytomatrix protein
PART1	-2.19677	0.002515	8.11E-05	-3.02156	Down	prostate androgen-regulated transcript 1
PTPRT	-2.19591	0.001145	3.15E-14	-3.25218	Down	protein tyrosine phosphatase receptor type T
CSPG5	-2.19272	7.80E-06	1.06E-07	-4.47073	Down	chondroitin sulfate proteoglycan 5
EPHA10	-2.17778	4.59E-06	1.60E-11	-4.58292	Down	EPH receptor A10
TCHH	-2.17537	0.000153	0.000438	-3.78592	Down	trichohyalin
TAS2R41	-2.17301	7.92E-23	1.46E-07	-9.83548	Down	taste 2 receptor member 41
SPINK9	-2.17198	7.65E-06	0.000724	-4.47484	Down	serine peptidase inhibitor Kazal type 9
CT70	-2.16622	3.95E-05	1.41E-19	-4.11019	Down	cancer/testis associated transcript 70
NRG2	-2.15402	8.95E-06	3.45E-10	-4.441	Down	neuregulin 2
CDH3	-2.14882	0.000136	2.80E-06	-3.8157	Down	cadherin 3
SNORA74D	-2.14222	0.01044	0.002654	-2.56091	Down	small nucleolar RNA, H/ACA box 74D
RSPH10B	-2.13603	2.41E-05	2.00E-21	-4.22341	Down	radial spoke head 10 homolog B
RAB40AL	-2.13503	5.63E-08	1.80E-24	-5.43032	Down	RAB40A like
IHH	-2.1297	0.000309	0.002183	-3.60723	Down	Indian hedgehog signaling molecule
RNVU1-2	-2.12755	0.001458	0.010595	-3.18301	Down	RNA, variant U1 small nuclear 2
PSMD7-DT	-2.11841	1.25E-08	0.039394	-5.69245	Down	PSMD7 divergent transcript
FOXD4L3	-2.11409	3.46E-05	3.18E-18	-4.14087	Down	forkhead box D4 like 3
PCDHA4	-2.11373	0.000611	1.64E-10	-3.42651	Down	protocadherin alpha 4
SNHG25	-2.11169	3.09E-17	9.83E-23	-8.44326	Down	small nucleolar RNA host gene 25
POTEM	-2.11168	0.000722	8.26E-11	-3.38114	Down	POTE ankyrin domain family member M
CD164L2	-2.10636	0.007033	1.75E-27	-2.69529	Down	CD164 molecule like 2
PDE4C	-2.10352	6.75E-05	1.10E-12	-3.985	Down	phosphodiesterase 4C
OR52B2	-2.0987	2.23E-07	0.0078	-5.17894	Down	olfactory receptor family 52 subfamily B member 2
E2F3-IT1	-2.09763	7.93E-16	0.012263	-8.05527	Down	E2F3 intronic transcript 1
RNU2-2	-2.09272	5.01E-23	2.87E-08	-9.88136	Down	RNA, U2 small nuclear 2
RNVU1-27	-2.08881	1.97E-13	1.47E-06	-7.35064	Down	RNA, variant U1 small nuclear 27
FBXO39	-2.07755	4.24E-09	0.008018	-5.87446	Down	F-box protein 39
FGF8	-2.06484	0.007077	2.75E-06	-2.69318	Down	fibroblast growth factor 8

PRODH	-2.06171	8.03E-05	6.23E-10	-3.94347	Down	proline dehydrogenase 1
TTTY2B	-2.05255	0.016322	0.000221	-2.40162	Down	testis expressed transcript, Y-linked 2B
DNAJB5-DT	-2.0524	0.001833	4.41E-05	-3.11608	Down	DNAJB5 divergent transcript
SLC13A5	-2.04419	0.011619	1.14E-36	-2.52352	Down	solute carrier family 13 member 5
ZSCAN10	-2.04335	0.00083	0.000361	-3.34273	Down	zinc finger and SCAN domain containing 10
AMHR2	-2.04246	0.001503	2.09E-06	-3.17401	Down	anti-Mullerian hormone receptor type 2
A3GALT2	-2.02664	3.43E-07	5.76E-11	-5.09807	Down	alpha 1,3-galactosyltransferase 2
CTNNA3	-2.02426	1.30E-05	0.009564	-4.36075	Down	catenin alpha 3
TCP10L	-2.02186	1.89E-21	0.003223	-9.51102	Down	t-complex 10 like
MGAT4C	-2.01397	0.000174	4.26E-34	-3.75463	Down	MGAT4 family member C
SLC6A15	-2.01329	0.008421	1.29E-117	-2.63471	Down	solute carrier family 6 member 15
VWA5B2	-2.00515	0.019575	0.000779	-2.33439	Down	von Willebrand factor A domain containing 5B2
AQP7	-1.99814	6.99E-05	1.72E-18	-3.97656	Down	aquaporin 7
SNORA50C	-1.99747	0.018726	5.35E-19	-2.35095	Down	small nucleolar RNA, H/ACA box 50C
LGI4	-1.99366	1.02E-05	6.31E-07	-4.41187	Down	leucine rich repeat LGI family member 4
ACTA1	-1.99149	0.00286	5.55E-08	-2.98237	Down	actin alpha 1, skeletal muscle
DLL4	-1.98658	5.24E-06	1.30E-08	-4.555	Down	delta like canonical Notch ligand 4
PAPPA2	-1.98657	2.67E-07	5.69E-28	-5.14553	Down	pappalysin 2
FALEC	-1.97454	5.23E-05	5.69E-05	-4.04519	Down	focally amplified lncRNA regulator of ECM1
RN7SK	-1.97166	1.40E-59	0.02475	-16.2787	Down	RNA component of 7SK nuclear ribonucleoprotein
SLC39A5	-1.9693	5.48E-05	1.20E-05	-4.03401	Down	solute carrier family 39 member 5
GPR17	-1.9673	1.97E-05	8.03E-29	-4.26842	Down	G protein-coupled receptor 17
KBTBD12	-1.96592	5.16E-06	5.12E-11	-4.55826	Down	kelch repeat and BTB domain containing 12
TDRD6	-1.96357	0.000684	4.29E-12	-3.39573	Down	tudor domain containing 6
MT-ND1	-1.96145	8.82E-41	2.00E-09	-13.3719	Down	NADH dehydrogenase subunit 1
OR4F17	-1.95822	1.28E-12	7.66E-18	-7.0969	Down	olfactory receptor family 4 subfamily F member 17
SLC3A1	-1.93947	8.06E-08	2.18E-14	-5.36586	Down	solute carrier family 3 member 1
PRB3	-1.93531	0.000254	6.39E-80	-3.65831	Down	proline rich protein BstNI subfamily 3
HCP5B	-1.93356	4.65E-05	0.021755	-4.07265	Down	HLA complex P5B
GRIN2C	-1.9274	0.000896	9.61E-52	-3.32127	Down	glutamate ionotropic receptor NMDA type subunit 2C
KRTAP10-3	-1.90206	0.003214	0.012527	-2.94648	Down	keratin associated protein 10-3
CEP295NL	-1.89273	3.49E-42	5.48E-21	-13.61	Down	CEP295 N-terminal like
ASTILCS	-1.87962	0.00925	6.13E-16	-2.60268	Down	antisense transcript of PTP4A3, liver carcinoma survival associated
SPDYE2	-1.87702	0.005632	0.004196	-2.76846	Down	speedy/RINGO cell cycle regulator family member E2
MT-ATP6	-1.87517	1.33E-37	2.51E-29	-12.8165	Down	ATP synthase F0 subunit 6
MT-ND6	-1.86374	4.94E-45	0.000804	-14.0814	Down	NADH dehydrogenase subunit 6
SCARNA7	-1.86323	3.28E-35	0.000622	-12.3819	Down	small Cajal body-specific RNA 7
LRRTM2	-1.85903	0.000369	1.66E-05	-3.56126	Down	leucine rich repeat transmembrane neuronal 2
MT-ND4	-1.85404	2.58E-36	0.005665	-12.5842	Down	NADH dehydrogenase subunit 4
BICDL2	-1.84141	3.80E-11	2.06E-05	-6.61174	Down	BICD family like cargo adaptor 2
NPIPB11	-1.84119	1.89E-29	1.01E-32	-11.2681	Down	nuclear pore complex interacting protein family member B11
KCNIP4-IT1	-1.83814	0.002462	0.037363	-3.02803	Down	KCNIP4 intronic transcript 1
NPIPB13	-1.82338	2.61E-31	2.01E-19	-11.6391	Down	nuclear pore complex interacting protein family, member B13

MT-ND2	-1.82168	5.37E-37	2.77E-08	-12.7075	Down	NADH dehydrogenase subunit 2
P2RY4	-1.81717	3.98E-11	0.001527	-6.60495	Down	pyrimidinergic receptor P2Y4
CCAT2	-1.81577	2.08E-08	0.001086	-5.60483	Down	colon cancer associated transcript 2
MT-ND4L	-1.81549	3.85E-35	0.000318	-12.3689	Down	NADH dehydrogenase subunit 4L
CYP4F8	-1.8115	0.008497	1.10E-30	-2.63164	Down	cytochrome P450 family 4 subfamily F member 8
CNTN2	-1.80813	0.015714	0.002469	-2.41548	Down	contactin 2
SCARNA5	-1.80542	1.97E-42	2.23E-27	-13.6517	Down	small Cajal body-specific RNA 5
SLC28A1	-1.80478	0.01234	0.011565	-2.50227	Down	solute carrier family 28 member 1
GOLGA8J	-1.80236	0.016361	1.08E-18	-2.40076	Down	golgin A8 family member J
KRTAP16-1	-1.79824	0.004839	1.56E-67	-2.81755	Down	keratin associated protein 16-1
NPHP3-ACAD11	-1.79676	0.00055	0.015854	-3.45511	Down	NPHP3-ACAD11 readthrough (NMD candidate)
AKT3-IT1	-1.79346	1.55E-15	6.71E-10	-7.97295	Down	AKT3 intronic transcript 1
PRKCG	-1.79345	0.005731	4.88E-10	-2.76279	Down	protein kinase C gamma
OR5B21	-1.79336	9.48E-12	6.29E-06	-6.81426	Down	olfactory receptor family 5 subfamily B member 21
RNVU1-6	-1.79272	0.002844	3.63E-16	-2.98411	Down	RNA, variant U1 small nuclear 6
CFAP157	-1.78163	0.009788	4.03E-07	-2.58324	Down	cilia and flagella associated protein 157
TTYH1	-1.77801	0.002593	2.32E-61	-3.0123	Down	tweety family member 1
OR2L8	-1.77584	1.72E-06	7.91E-27	-4.7837	Down	olfactory receptor family 2 subfamily L member 8
SCARNA17	-1.77462	2.26E-29	1.04E-09	-11.252	Down	small Cajal body-specific RNA 17
HS1BP3-IT1	-1.77317	4.19E-08	0.001611	-5.48266	Down	HS1BP3 intronic transcript 1
SLC28A2	-1.7729	0.019661	1.01E-34	-2.33276	Down	solute carrier family 28 member 2
GPR52	-1.76784	1.08E-58	3.58E-05	-16.1529	Down	G protein-coupled receptor 52
FLJ42393	-1.75635	3.12E-67	0.001092	-17.3237	Down	uncharacterized LOC401105
LRRC73	-1.75389	2.01E-05	2.88E-10	-4.26327	Down	leucine rich repeat containing 73
MT-CO2	-1.75269	4.30E-35	9.91E-06	-12.36	Down	cytochrome c oxidase subunit II
KRTAP10-2	-1.74995	0.003227	0.000186	-2.94522	Down	keratin associated protein 10-2
EZHIP	-1.74859	4.68E-08	1.12E-08	-5.46293	Down	EZH inhibitory protein
AFF4-DT	-1.74542	0.024828	3.62E-49	-2.24407	Down	AFF4 divergent transcript
ASPG	-1.74476	0.004182	2.50E-09	-2.86406	Down	asparaginase
UBQLN3	-1.74241	3.76E-06	1.64E-11	-4.62427	Down	ubiquilin 3
ANKRD18B	-1.73792	5.87E-05	1.62E-10	-4.01794	Down	ankyrin repeat domain 18B
MYH9-DT	-1.73746	0.000727	0.002594	-3.37905	Down	MYH9 divergent transcript
MACC1-OT1	-1.73587	0.000494	8.96E-13	-3.48375	Down	MACC1 3' UTR overlapping transcript 1
DNAAF1	-1.7279	0.022925	2.38E-09	-2.27468	Down	dynein axonemal assembly factor 1
ST7-OT4	-1.72782	6.40E-18	3.40E-07	-8.6252	Down	ST7 overlapping transcript 4
RPL3L	-1.72546	0.000759	9.86E-21	-3.36749	Down	ribosomal protein L3 like
C1QTNF4	-1.72101	5.07E-08	4.16E-09	-5.44867	Down	C1q and TNF related 4
CNDP1	-1.72012	0.003841	0.033177	-2.89097	Down	carnosine dipeptidase 1
SGK2	-1.71923	3.27E-10	1.94E-29	-6.28545	Down	serum/glucocorticoid regulated kinase 2
NDST3	-1.71534	2.83E-06	0.000265	-4.68283	Down	N-deacetylase and N-sulfotransferase 3
DCLK3	-1.71434	0.008452	2.75E-07	-2.63345	Down	doublecortin like kinase 3
SMIM34	-1.71026	0.000547	5.43E-64	-3.45638	Down	small integral membrane protein 34
DANT2	-1.70705	0.015093	7.25E-19	-2.43014	Down	DXZ4 associated non-coding transcript 2, distal

DOCK7-DT	-1.70549	0.003556	0.006483	-2.91511	Down	DOCK7 divergent transcript
FGF22	-1.70153	4.74E-05	0.035854	-4.06797	Down	fibroblast growth factor 22
CARD14	-1.70032	4.66E-05	0.000119	-4.07212	Down	caspase recruitment domain family member 14
NTRK3	-1.70022	2.89E-05	0.004854	-4.18166	Down	neurotrophic receptor tyrosine kinase 3
MT-ND5	-1.69645	2.48E-32	0.034639	-11.8381	Down	NADH dehydrogenase subunit 5
FLJ20712	-1.69587	6.50E-10	1.05E-29	-6.17772	Down	uncharacterized FLJ20712
AMANZI	-1.69259	0.000168	0.002347	-3.76322	Down	a master non-coding RNA antagonizing inflammation
SLC10A4	-1.68801	2.76E-05	6.93E-19	-4.19214	Down	solute carrier family 10 member 4
PAX2	-1.67879	0.0044	1.63E-11	-2.84795	Down	paired box 2
ESPNL	-1.67697	4.97E-05	0.001523	-4.05715	Down	espin like
STPG2	-1.67636	2.60E-11	2.11E-114	-6.66774	Down	sperm tail PG-rich repeat containing 2
H2AB2	-1.67194	7.48E-05	1.29E-24	-3.96051	Down	H2A.B variant histone 2
PKLR	-1.66975	8.21E-05	2.58E-40	-3.93816	Down	pyruvate kinase L/R
HSD17B1	-1.66908	3.13E-07	0.04059	-5.11548	Down	hydroxysteroid 17-beta dehydrogenase 1
KBTBD11-OT1	-1.66817	0.003394	0.033537	-2.9296	Down	KBTBD11 overlapping transcript 1
RSPO4	-1.66037	4.57E-05	2.99E-16	-4.07683	Down	R-spondin 4
PTCSC1	-1.6585	9.83E-15	0.000298	-7.74138	Down	papillary thyroid carcinoma susceptibility candidate 1
RCVRN	-1.65567	7.35E-06	0.000101	-4.4833	Down	recoverin
SCMH1-DT	-1.6537	0.010394	0.001441	-2.56245	Down	SCMH1 divergent transcript
CBY3	-1.65321	0.008071	0.000786	-2.64909	Down	chibby family member 3
RAPSN	-1.6499	3.24E-16	1.48E-90	-8.16391	Down	receptor associated protein of the synapse
TAF11L5	-1.64619	1.18E-07	0.000107	-5.29593	Down	TATA-box binding protein associated factor 11 like 5
OVCH1	-1.64614	0.021144	4.34E-11	-2.3054	Down	ovochymase 1
BAIAP2L2	-1.64145	2.52E-20	3.20E-34	-9.23747	Down	BAR/IMD domain containing adaptor protein 2 like 2
PRNCR1	-1.6398	1.65E-27	0.01117	-10.8673	Down	prostate cancer associated non-coding RNA 1
KCNS1	-1.6378	8.30E-05	0.014388	-3.93554	Down	potassium voltage-gated channel modifier subfamily S member 1
MUC4	-1.63337	0.001768	7.74E-07	-3.12659	Down	mucin 4, cell surface associated
OR52K2	-1.6307	1.75E-36	0.023762	-12.6149	Down	olfactory receptor family 52 subfamily K member 2
CLEC18B	-1.62896	1.82E-07	0.007956	-5.2168	Down	C-type lectin domain family 18 member B
ADAMTS2	-1.62865	3.38E-05	0.00143	-4.1459	Down	ADAM metallopeptidase with thrombospondin type 1 motif 2
SEZ6	-1.62766	0.021502	0.000611	-2.29906	Down	seizure related 6 homolog
OOSP1	-1.62669	0.01217	1.21E-07	-2.50716	Down	oocyte secreted protein 1
OR2L2	-1.62567	8.90E-09	5.68E-05	-5.75043	Down	olfactory receptor family 2 subfamily L member 2
GRIN2B	-1.62371	0.025321	1.75E-14	-2.23646	Down	glutamate ionotropic receptor NMDA type subunit 2B
ELAVL3	-1.62092	0.022493	7.04E-23	-2.28194	Down	ELAV like RNA binding protein 3
SOX15	-1.6205	5.47E-05	0.019641	-4.03458	Down	SRY-box transcription factor 15
NXNL2	-1.61822	0.001795	3.35E-50	-3.12226	Down	nucleoredoxin like 2
PAGE1	-1.61621	0.009145	6.43E-06	-2.60657	Down	PAGE family member 1
CCDC200	-1.6115	0.005885	6.97E-14	-2.75413	Down	coiled-coil domain containing 200
LEFTY2	-1.60951	0.002084	0.017252	-3.07798	Down	left-right determination factor 2
ARHGAP19-SLIT1	-1.60648	3.93E-08	5.40E-09	-5.49413	Down	ARHGAP19-SLIT1 readthrough (NMD candidate)
AIRN	-1.60446	0.002864	8.89E-07	-2.98199	Down	antisense of IGF2R non-protein coding RNA

C21orf91-OT1	-1.60413	4.97E-05	0.000567	-4.0572	Down	C21orf91 overlapping transcript 1
MMP21	-1.60323	3.59E-05	0.000985	-4.13254	Down	matrix metallopeptidase 21
GRK7	-1.6012	4.50E-14	5.69E-28	-7.5458	Down	G protein-coupled receptor kinase 7
SNORA74A	-1.59932	0.009038	3.43E-53	-2.6106	Down	small nucleolar RNA, H/ACA box 74A
COL23A1	-1.59916	2.39E-05	0.017329	-4.22477	Down	collagen type XXIII alpha 1 chain
GAD1	-1.59751	0.000349	8.89E-11	-3.57611	Down	glutamate decarboxylase 1
CHRNB2	-1.59708	0.015851	6.08E-25	-2.41233	Down	cholinergic receptor nicotinic beta 2 subunit
POLE2	-1.59549	9.56E-28	2.22E-11	-10.917	Down	DNA polymerase epsilon 2, accessory subunit
HBA2	-1.59441	2.57E-19	0.008985	-8.98579	Down	hemoglobin subunit alpha 2
H1-6	-1.5938	1.55E-14	5.76E-07	-7.68314	Down	H1.6 linker histone, cluster member
SCARNA6	-1.59322	1.85E-27	2.01E-07	-10.8569	Down	small Cajal body-specific RNA 6
HPYR1	-1.59269	1.51E-08	8.33E-96	-5.66085	Down	Helicobacter pylori responsive 1
IGLV1-50	-1.58873	0.003614	0.000165	-2.90999	Down	immunoglobulin lambda variable 1-50 (non-functional)
C12orf50	-1.5808	1.00E-06	0.000401	-4.89117	Down	chromosome 12 open reading frame 50
BLTP3B-DT	-1.57777	0.000921	1.24E-10	-3.31373	Down	BLTP3B divergent transcript
MATN1	-1.57232	0.000179	2.50E-11	-3.7472	Down	matrilin 1
IBA57-DT	-1.57186	8.90E-05	2.31E-07	-3.91868	Down	IBA57 divergent transcript
NPIPA2	-1.57044	0.016258	2.56E-15	-2.40308	Down	nuclear pore complex interacting protein family member A2
SLC4A9	-1.56894	0.000152	8.41E-08	-3.78846	Down	solute carrier family 4 member 9
CCDC73	-1.56853	3.45E-05	2.16E-15	-4.14152	Down	coiled-coil domain containing 73
CTAGE6	-1.56712	1.42E-09	0.023735	-6.05304	Down	CTAGE family member 6
TBX1	-1.56415	6.43E-06	1.11E-11	-4.5119	Down	T-box transcription factor 1
SLC5A11	-1.56399	5.16E-05	0.00149	-4.0483	Down	solute carrier family 5 member 11
IFNL1	-1.56286	0.004132	2.96E-16	-2.86788	Down	interferon lambda 1
KRTAP5-9	-1.55561	0.011808	5.07E-07	-2.51784	Down	keratin associated protein 5-9
ASIC1	-1.55136	6.59E-05	4.67E-14	-3.99051	Down	acid sensing ion channel subunit 1
OR2T11	-1.55067	3.03E-05	0.000183	-4.17132	Down	olfactory receptor family 2 subfamily T member 11
SNTG2	-1.54994	3.70E-05	1.70E-06	-4.12552	Down	syntrophin gamma 2
ABCC11	-1.54981	0.008167	1.41E-10	-2.64509	Down	ATP binding cassette subfamily C member 11
LLCFC1	-1.54929	1.88E-07	0.000426	-5.21126	Down	LLLL and CFNLAS motif containing 1
TUBAL3	-1.54839	0.020401	0.017214	-2.31889	Down	tubulin alpha like 3
POU5F1	-1.5475	2.57E-06	5.95E-58	-4.7021	Down	POU class 5 homeobox 1
ZDHHC19	-1.54736	2.92E-06	1.47E-54	-4.67636	Down	zDHHC palmitoyltransferase 19
BACH1-IT3	-1.54372	3.36E-06	3.56E-21	-4.64741	Down	BACH1 intronic transcript 3
MAB21L3	-1.54352	1.42E-13	3.88E-15	-7.39475	Down	mab-21 like 3
B3GNT4	-1.54185	1.84E-06	1.80E-13	-4.77021	Down	UDP-GlcNAc:betaGal beta-1,3-N-acetylglucosaminyltransferase 4
PPM1E	-1.54157	0.004044	8.31E-09	-2.8747	Down	protein phosphatase, Mg2+/Mn2+ dependent 1E
SLC8A2	-1.5359	0.020667	1.73E-95	-2.31401	Down	solute carrier family 8 member A2
OR5AN1	-1.53561	8.11E-06	1.58E-22	-4.46216	Down	olfactory receptor family 5 subfamily AN member 1
TF	-1.53524	1.95E-24	2.35E-45	-10.2017	Down	transferrin
ADAM20	-1.53384	6.90E-41	1.11E-48	-13.3902	Down	ADAM metallopeptidase domain 20
RNVU1-33	-1.53161	0.024554	1.93E-32	-2.24834	Down	RNA, variant U1 small nuclear 33
MLNR	-1.52876	0.004299	3.09E-08	-2.85532	Down	motilin receptor

OR2B6	-1.52803	7.83E-06	0.001947	-4.46975	Down	olfactory receptor family 2 subfamily B member 6
TAS2R3	-1.52345	1.28E-33	2.54E-05	-12.0845	Down	taste 2 receptor member 3
OR56A4	-1.52228	0.001164	1.04E-12	-3.24752	Down	olfactory receptor family 56 subfamily A member 4
ESRP1	-1.52158	0.024647	8.40E-27	-2.24688	Down	epithelial splicing regulatory protein 1
NCAPG	-1.51825	3.97E-46	4.58E-37	-14.2585	Down	non-SMC condensin I complex subunit G
NKAIN3	-1.51812	0.014668	1.37E-10	-2.44048	Down	sodium/potassium transporting ATPase interacting 3
CDC25C	-1.51398	1.27E-10	6.00E-09	-6.43046	Down	cell division cycle 25C
RENO1	-1.51312	1.07E-13	0.002883	-7.43179	Down	regulator of early neurogenesis 1
CDHR2	-1.51269	2.28E-13	9.16E-18	-7.33126	Down	cadherin related family member 2
KCNQ4	-1.51091	2.09E-07	0.00426	-5.19112	Down	potassium voltage-gated channel subfamily Q member 4
PPIAL4H	-1.51088	4.88E-15	6.37E-10	-7.83002	Down	peptidylprolyl isomerase A like 4H
PCDH17	-1.50853	0.000173	0.000314	-3.75478	Down	protocadherin 17
MADCAM1	-1.50763	1.29E-14	0.002945	-7.70657	Down	mucosal vascular addressin cell adhesion molecule 1
ABHD16B	-1.50652	0.001107	0.000162	-3.26173	Down	abhydrolase domain containing 16B
ACP7	-1.50453	0.011688	1.30E-05	-2.52144	Down	acid phosphatase 7, tartrate resistant (putative)
SCN2B	-1.50448	0.000214	1.17E-06	-3.70179	Down	sodium voltage-gated channel beta subunit 2
TAS2R30	-1.50411	3.53E-31	1.27E-16	-11.6132	Down	taste 2 receptor member 30
CNIH2	-1.50403	3.52E-12	5.42E-06	-6.95534	Down	cornichon family AMPA receptor auxiliary protein 2
IQCN	-1.50293	1.02E-25	5.49E-15	-10.4844	Down	IQ motif containing N
PVALB	-1.50289	3.01E-09	3.12E-18	-5.93118	Down	parvalbumin
H3-5	-1.50251	0.008629	9.57E-25	-2.62642	Down	H3.5 histone
GPR21	-1.50199	4.17E-34	4.49E-07	-12.1761	Down	G protein-coupled receptor 21
SCARNA10	-1.5019	5.42E-19	2.42E-25	-8.90335	Down	small Cajal body-specific RNA 10
DNAI7	-1.49975	3.94E-05	5.30E-07	-4.11084	Down	dynein axonemal intermediate chain 7
DISC1-IT1	-1.49674	9.88E-09	0.003573	-5.73273	Down	DISC1 intronic transcript 1
SLC22A13	-1.49654	2.58E-09	2.87E-16	-5.95654	Down	solute carrier family 22 member 13
FOXD4L4	-1.495	7.46E-16	1.38E-06	-8.0628	Down	forkhead box D4 like 4
ST8SIA5	-1.4941	0.001319	8.47E-07	-3.21184	Down	ST8 alpha-N-acetyl-neuraminide alpha-2,8-sialyltransferase 5
NKX6-3	-1.49391	0.003723	2.59E-08	-2.90074	Down	NK6 homeobox 3
SCARNA2	-1.49289	1.52E-50	5.25E-05	-14.9516	Down	small Cajal body-specific RNA 2
FOXD4L6	-1.49221	0.007311	5.88E-31	-2.68235	Down	forkhead box D4 like 6
HUS1B	-1.4903	3.55E-15	1.23E-30	-7.86992	Down	HUS1 checkpoint clamp component B
LIMS3	-1.48839	1.10E-05	0.011101	-4.39562	Down	LIM zinc finger domain containing 3
RAB26	-1.48455	0.005211	1.01E-74	-2.79371	Down	RAB26, member RAS oncogene family
FRG1-DT	-1.48157	7.04E-11	4.01E-11	-6.51988	Down	FRG1 divergent transcript
ANOS1	-1.48148	0.001762	2.83E-05	-3.12759	Down	anosmin 1
ARHGAP44	-1.47871	0.000758	0.000704	-3.36761	Down	Rho GTPase activating protein 44
CXorf65	-1.47847	5.90E-10	5.00E-11	-6.19302	Down	chromosome X open reading frame 65
LENEP	-1.47755	0.000183	0.001236	-3.74146	Down	lens epithelial protein
FNDC7	-1.47687	0.00505	6.43E-11	-2.80381	Down	fibronectin type III domain containing 7
C18orf15	-1.47618	1.42E-16	1.22E-20	-8.26307	Down	chromosome 18 putative open reading frame 15
NHERF4	-1.47573	1.00E-08	2.66E-07	-5.73058	Down	NHERF family PDZ scaffold protein 4
NUP62CL	-1.47475	1.56E-21	7.56E-15	-9.53112	Down	nucleoporin 62 C-terminal like

ABCC9	-1.47419	2.25E-17	0.001232	-8.48002	Down	ATP binding cassette subfamily C member 9
CZIB-DT	-1.4726	0.000525	4.35E-53	-3.46764	Down	CZIB divergent transcript
TLE1-DT	-1.47252	0.003099	0.003252	-2.95774	Down	TLE1 divergent transcript
NEU4	-1.47038	0.014625	4.09E-16	-2.44153	Down	neuraminidase 4
MUC12	-1.4702	0.001191	5.36E-14	-3.24097	Down	mucin 12, cell surface associated
NPIPB12	-1.46721	2.28E-36	6.97E-73	-12.594	Down	nuclear pore complex interacting protein family member B12
HYMAI	-1.46536	5.53E-22	1.10E-33	-9.63787	Down	hydatidiform mole associated and imprinted
PTTG2	-1.46381	9.07E-22	1.44E-52	-9.587	Down	pituitary tumor-transforming 2
TRHR	-1.46288	0.011454	0.034605	-2.52854	Down	thyrotropin releasing hormone receptor
PCAT2	-1.46216	0.004251	1.09E-22	-2.85894	Down	prostate cancer associated transcript 2
CNTNAP3	-1.45951	1.72E-05	0.000537	-4.29838	Down	contactin associated protein family member 3
TAS2R60	-1.45764	1.12E-10	0.002418	-6.44993	Down	taste 2 receptor member 60
RANBP17	-1.45727	2.43E-16	3.36E-17	-8.19877	Down	RAN binding protein 17
SAXO1	-1.45658	7.35E-05	0.013398	-3.96475	Down	stabilizer of axonemal microtubules 1
MAPT-IT1	-1.45603	0.011612	0.045505	-2.52371	Down	MAPT intronic transcript 1
TENT5B	-1.45402	0.000656	5.23E-09	-3.40724	Down	terminal nucleotidyltransferase 5B
POLR3G	-1.44955	3.15E-26	4.47E-23	-10.5949	Down	RNA polymerase III subunit G
ERICH6	-1.44851	0.000943	0.002511	-3.30706	Down	glutamate rich 6
ERI3-IT1	-1.44594	1.60E-11	5.44E-07	-6.73833	Down	ERI3 intronic transcript 1
CPNE4	-1.44505	3.28E-05	2.01E-47	-4.15296	Down	copine 4
GALNTL6	-1.44492	0.00027	2.65E-06	-3.64217	Down	polypeptide N-acetylgalactosaminyltransferase like 6
KASH5	-1.44305	0.012228	4.80E-11	-2.50549	Down	KASH domain containing 5
PPIAL4E	-1.44302	0.000134	1.47E-43	-3.81838	Down	peptidylprolyl isomerase A like 4E
VSIG8	-1.44189	0.012104	6.81E-29	-2.5091	Down	V-set and immunoglobulin domain containing 8
NANOS3	-1.44031	0.003547	1.80E-14	-2.91591	Down	nanos C2HC-type zinc finger 3
COLCA1	-1.44004	3.34E-06	5.39E-08	-4.64843	Down	colorectal cancer associated 1
SLC22A1	-1.43808	5.96E-18	1.69E-11	-8.63325	Down	solute carrier family 22 member 1
PRR36	-1.43634	8.84E-06	8.21E-12	-4.44367	Down	proline rich 36
PRLHR	-1.43598	0.012371	0.017329	-2.50138	Down	prolactin releasing hormone receptor
CCDC140	-1.4308	0.025875	4.73E-10	-2.22808	Down	CCDC140 long non-coding RNA
ENPP7	-1.43013	0.004321	3.30E-05	-2.85375	Down	ectonucleotide pyrophosphatase/phosphodiesterase 7
IFITM10	-1.42956	1.54E-11	1.59E-27	-6.74384	Down	interferon induced transmembrane protein 10
TG	-1.42945	1.67E-14	7.09E-07	-7.67396	Down	thyroglobulin
FGF17	-1.42783	0.001865	6.17E-26	-3.111	Down	fibroblast growth factor 17
ACAD9-DT	-1.42442	2.98E-07	1.87E-05	-5.12492	Down	ACAD9 divergent transcript
COXFA4L3	-1.42339	0.010796	6.76E-46	-2.54923	Down	cytochrome c oxidase associated subunit FA4L3
OR52I2	-1.42052	0.005423	6.19E-13	-2.78077	Down	olfactory receptor family 52 subfamily I member 2
CLEC18C	-1.41843	1.50E-05	1.19E-136	-4.3283	Down	C-type lectin domain family 18 member C
TRIM50	-1.41714	0.012578	9.63E-16	-2.4955	Down	tripartite motif containing 50
EYS	-1.41617	2.04E-05	0.007362	-4.26048	Down	EGF-like photoreceptor maintenance factor
NME9	-1.41474	0.002596	2.34E-22	-3.01191	Down	NME/NM23 family member 9
SNORA5C	-1.41472	0.001195	0.000916	-3.24002	Down	small nucleolar RNA, H/ACA box 5C
FN3K	-1.41461	7.07E-18	2.03E-29	-8.61372	Down	fructosamine 3 kinase

SPIN2A	-1.41071	9.32E-15	1.91E-12	-7.74824	Down	spindlin family member 2A
SLC25A2	-1.4097	1.27E-09	1.63E-08	-6.07147	Down	solute carrier family 25 member 2
TRPV6	-1.40861	0.000209	2.27E-05	-3.70759	Down	transient receptor potential cation channel subfamily V member 6
REELD1	-1.40572	1.47E-08	0.011129	-5.66451	Down	reeler domain containing 1
LILRB5	-1.40184	4.61E-07	0.016169	-5.04168	Down	leukocyte immunoglobulin like receptor B5
DOC2A	-1.40158	0.000316	7.35E-06	-3.60211	Down	double C2 domain alpha
ABCB11	-1.39556	5.98E-05	2.74E-23	-4.01361	Down	ATP binding cassette subfamily B member 11
RPL34-DT	-1.3922	1.31E-07	7.28E-18	-5.27718	Down	RPL34 divergent transcript
ANKRD2	-1.39139	0.005259	2.82E-08	-2.7907	Down	ankyrin repeat domain 2
TAF11L2	-1.39116	3.92E-07	8.89E-05	-5.07266	Down	TATA-box binding protein associated factor 11 like 2
RBFOX3	-1.38944	0.009705	0.001134	-2.58615	Down	RNA binding fox-1 homolog 3
DRD4	-1.38865	2.97E-06	8.16E-14	-4.67303	Down	dopamine receptor D4
MICALL2-DT	-1.38804	0.003262	0.000821	-2.94192	Down	MICALL2 divergent transcript
OMP	-1.38483	0.00665	0.018751	-2.71388	Down	olfactory marker protein
STRC	-1.38397	1.95E-07	2.33E-08	-5.20446	Down	stereocilin
ATP5MGL	-1.38256	2.19E-09	6.16E-46	-5.98295	Down	ATP synthase membrane subunit g like
BCO2	-1.38084	5.31E-12	1.23E-51	-6.89711	Down	beta-carotene oxygenase 2
FAM41C	-1.37988	2.74E-13	2.32E-27	-7.30679	Down	family with sequence similarity 41 member C

Table 2 The enriched GO terms of the up and down regulated differentially expressed genes

GO ID	CATEGORY	GO Name	adjusted_p_value	negative_log10_of_adjusted_p_value	Gene Count	Gene
			Up regulated genes			
GO:0032501	BP	multicellular organismal process	1.12E-26	25.94961275	275	IGFBP5,COL1A2,GREM1,DCN,STC2,COL12A1,THBS2,MMP2,TNFRSF11B,COL1A1,COL8A1,CCN1,COL3A1,SVEP1,PRELP,GJA1,CDH11,LUM,KIRREL1,THY1,TNC,ITGA11,SULF1,FN1,PAPPA,WNT5A,LAMA4,PSG5,TENM2,KCNK2,SOD3,EGFR,CCN2,STMN2,FBLN1,EFEMP1,CRYAB,FST,AMOTL2,LAMB1,ANTXR1,FGF1,COL16A1,HAS2,SNAI2,SLIT3,FLRT2,ABI3BP,STC1,COL11A1,PRRX1,SRPX2,DKK1,IL13RA2,GRIA1,FGF5,ATP8B1,CDH13,CACNA2D1,HSPB7,GFRA1,CREB3L1,TIMP3,PTGIS,OSR2,CLDN11,BMPER,TWIST2,TEAD1,ADAMTS12,ASS1,CEMIP,TWIST1,SLIT2,EMX2,BRINP1,CSPG4,ELN,POSTN,COL6A1,GPR176,NUPR1,NFASC,YAP1,FHOD3,LRIG3,SSTR1,LOX,DKK2,ROBO2,GLRB,F3,FGF7,OSR1,PTPN14,TFAP2C,JPH2,F10,HOXC6,NR2F2,CHST3,COMP,TENM3,PDLIM4,CPE,TBX3,RARRES2,MFAP2,LSAMP,ZIC1,CCND1,PDPN,INSYN1,COL5A2,NFATC4,CCBE1,GPNMB,DZIP1,PCDH18,HAND2,FAP,ALDH1A3,TAFA5,CAV1,RSPO3,DCLK1,SIX2,SEMA3D,CD276,MFAP5,HOXC8,PIEZO2,MGARP,LRP4,GDNF,MXRA8,FJX1,AKR1C2,NES,PLA2R1,HOXA11,CLMP,TBX5,DDR2,DKK3,NR2F1,FBN1,SIM1,TBX18,SERPINE2,NDNF,GREB1L,SYDE1,NTF3,GPC1,HECW1,FKBP10,CTHRC1,VSTM4,PLPPR4,COL5A1,FARP1,DDAH1,HSPB6,EMP2,GDF5,TBX15,BDKRB2,BICC1,SLC2A10,HTR2B,LGR5,VASN,TUSC3,CXCL12,SLC1A1,TJP1,IGF2BP1,FRAS1,SHROOM3,MAP1B,GAS6,SIX4,MET,GABRE,VIT,PARVA,SPRY4,FAT1,EML1,UCHL1,PXDN,PLPP3,ARNT2,DPYSL3,MID1,HMCN1,JAM2,TMEM98,AXL,MAMDC2,HLA-DQB2,CLSTN2,SERPINE1,C1QTNF1,EDNRB,OGN,SIK1,CRMP1,PTX3,FGF2,UPK3A,CHODL,ENAH,MMP14,TM4SF1,GPM6B,LMCD1,CD248,FERMT2,ADAMTS5,PMP22,HEYL,NCS1,BMP3,LRRN3,NT5E,TMEM126A,ENPP1,CXCL10,SERPINB2,GPR15,PDGFRB,IGFBP3,SLC16A2,TYRO3,HSPG2,SMARCA1,PIERCE2,MYOM2,DACT1,STAC,MAL2,GPR183,CELA1,SEMA5A,L1CA

						M,CCR6,SELENOP,CD3G,SCD,CYP51A1,GPM6A,AKR1C3,PLA2G7,EPAS1,LOXL1,CORO2B,PRKACB,GPR161,ALPK2,DLC1,MACROD2,JCHAIN,LAMC1,PLS3,MEOX1,FOSL1,CCL2,COL15A1,PDK4,ETS1,WNT5B,DHCR24,NPR3
GO:0050896	BP	response to stimulus	6.61E-23	22.18004597	304	IGFBP5,COL1A2,GREM1,DCN,STC2,MMP2,TNFRSF11B,COL1A1,RND3,CCN1,COL3A1,SVEP1,PRELP,CCDC80,GJA1,MXRA5,THY1,TNC,ITGBL1,ITGA11,SULF1,FN1,PAPPA,WNT5A,TENM2,MFAP4,OSMR,KCNK2,SOD3,EGFR,CCN2,CCN5,STMN2,FBLN1,EFEMP1,CRYAB,FST,AMOTL2,NNMT,LAMB1,FGF1,GNG12,COL16A1,HAS2,SNAI2,SLIT3,GPX8,FLRT2,ABI3BP,STC1,COL11A1,PRRX1,DKK1,IL13RA2,MRGPRF,GRIA1,FGF5,CDH13,CACNA2D1,HSPB7,GFRA1,CREB3L1,MASP1,FMN2,TIMP3,STEAP2,PTGIS,GABBR2,LRRC15,BMPER,AOX1,TWIST2,TEAD1,ADAMTS12,ASS1,TWIST1,S100A16,SLIT2,EMX2,BRINP1,CSPG4,IGKV1D-17,POSTN,PNPLA3,COL6A1,MMP1,GPR176,NUPR1,YAP1,SRPX,SSTR1,LOX,DKK2,PDE1C,ROBO2,GLRB,F3,FGF7,OSR1,F10,NR2F2,COMP,TENM3,CPE,HSPB8,TBX3,RARRES2,GRIA3,ADGRL2,BCAR1,ZIC1,CCND1,PDPN,INSYN1,COL5A2,NFATC4,CCBE1,GPNMB,DZIP1,HAND2,FAP,ALDH1A3,TAFA5,CAV1,RSPO3,FRMD6,ACKR4,DCLK1,SEMA3D,KCNIP3,CD276,PIEZO2,MGARP,LRP4,RFPL4A,GDNF,CPZ,C1S,CAP2,AKR1C2,HSPB2,PLA2R1,HOXA11,EFS,DDR2,DKK3,NR2F1,FBN1,RBPMS,TBX18,FIBIN,SERPINE2,NDNF,SYDE1,NTF3,PDGFRL,GPC1,HECW1,FKBP10,CTHRC1,PLPPR4,ADGRL4,COL5A1,FARP1,DDAH1,HSPB6,EMP2,TRBV11-3,GDF5,BDKRB2,BICC1,LYPD6,SLC2A10,HTR2B,LGR5,IGFBP4,VASN,FGD1,CXCL12,SLC1A1,TJP1,IGF2BP1,SHROOM3,MAGI1,RASSF8,MAP1B,GAS6,RHBDF1,MET,PARVA,IGKV1D-8,SPRY4,FAT1,UCHL1,PXDN,PLPP3,ADAMDEC1,TRDV3,ARNT2,DPYSL3,MID1,HMCN1,GPR85,TRDV2,TMEM98,AXL,HLA-DQB2,SERPINE1,TRBV13,IGKV1-37,C1QTNF1,EDNRB,OGN,SIK1,PTX3,FGF2,TRBV7-7,NQO1,IGHV4-28,HTRA1,RCAN2,TRAV12-2,MMP14,LMCD1,FERMT2,ADAM

						TS5,COLEC12,HEYL,BMP3,NT5E,SPATA18,TMEM126A,ENPP1,CXCL10,IGLV8-61,SERPINB2,GPR15,TRBV14,PRXL2C,KLRB1,PDGFRB,TRAV25,IGFBP3,CEP55,PHLDA3,TYRO3,HSPG2,IGKV1-9,MGST1,IGHV3-11,FBLN5,DACT1,GAS1,STAC,COL6A3,GPR183,TRAV24,TRBV7-9,CELA1,SEMA5A,CGNL1,RNASE4,L1CAM,SMIM30,RGS1,CCR6,IGKV5-2,KDM4D,SELENOP,CD3G,SCD,GPM6A,TRAV29DV5,FPR3,AKR1C3,IGHV3-21,TRBV12-5,TRBV7-2,PLA2G7,EPAS1,LOXL1,TMEM97,CORO2B,PRKACB,GPR161,ALPK2,DLC1,IGHV4-30-2,MACROD2,JCHAIN,LAMC1,FOSL1,TAF9B,CCL2,TRAV1-2,COL15A1,PDK4,SH3BP4,TRAV10,ETS1,WNT5B,DHCR24,IGHV1-2,NPR3
GO:0071944	CC	cell periphery	1.22E-45	44.91445103	284	COL1A2,GREM1,DCN,COL12A1,THBS2,MMP2,TNFRSF11B,RSC1A1,COL1A1,COL8A1,RND3,CCN1,COL3A1,PRELP,CCDC80,GJA1,TMEM47,CDH11,MXRA5,FLNC,LUM,KIRREL1,THY1,TNC,ITGBL1,ITGA11,SULF1,FN1,LOXL4,WNT5A,LAMA4,TENM2,MFAP4,OSMR,KCNK2,ANGPTL2,SOD3,EGFR,CCN2,CCN5,AHNAK2,FBLN1,EFEMP1,CRYAB,AMOTL2,LAMB1,DPT,ANTXR1,FGF1,GNG12,COL16A1,HAS2,FLRT2,ABI3BP,STC1,COL11A1,SRPX2,DKK1,IL13RA2,MRGPRF,RAB3B,GRIA1,ATP8B1,PRSS12,CDH13,CACNA2D1,GFRA1,FMN2,TIMP3,THSD4,STEAP2,PTGIS,GABBR2,LRRC15,CLDN11,BMPER,CNTN3,ADAMTS12,CEMIP,S100A16,CSPG4,IGKV1D-17,ELN,POSTN,COL6A1,MMP1,GPR176,NFASC,LRIG3,SRPX,SSTR1,LOX,ROBO2,GLRB,F3,KCNJ6,OSR1,JPH2,F10,SYNC,COMP,TENM3,PDLIM4,CPE,RARRES2,MFAP2,LSAMP,GRIA3,ADGRL2,BCAR1,FBLIM1,PDPN,COL5A2,C1QTNF5,CCBE1,GPNMB,PCDH18,FAP,CAV1,FRMD6,ACKR4,DCLK1,SEMA3D,KCNIP3,CD276,MFAP5,PIEZO2,LRP4,MXRA8,CAP2,PLA2R1,CLMP,STEAP1,EFS,MYRIP,KCNK15,DDR2,FBN1,SERPINE2,NDNF,ECM2,SYDE1,MPDZ,CAVIN1,GPC1,RPL36A-HNRNPH2,CTHRC1,VSTM4,PLPPR4,ADGRL4,COL5A1,FARP1,EMP2,TRBV11-

						3,GDF5,BDKRB2,NALF2,LYPD6,SLC2A10,HTR2B,LGR5,FBLN2,VASN,TUSC3,CXCL12,SLC1A1,TJP1,FRAS1,EVA1A,SHROOM3,MAGI1,MAP1B,MET,GABRE,ENOX1,VIT,PARVA,IGKV1D-8,SPRY4,FAT1,UCHL1,PXDN,EMP1,PLPP3,ADAMDEC1,TRDV3,PACSIN3,HMCN1,GPR85,JAM2,TRDV2,TMEM98,AXL,HLA-DQB2,CLSTN2,SERPINE1,TRBV13,IGKV1-37,C1QTNF1,EDNRB,OGN,PTX3,EHD2,SV2B,TRBV7-7,SH3D19,IGHV4-28,HTRA1,UPK3A,TRAV12-2,ENAH,PODN,MMP14,TM4SF1,GPM6B,CD248,FERMT2,ADAMTS5,COLEC12,PMP22,NCS1,EPB41L1,LRRN3,NT5E,TMEM126A,ENPP1,CXCL10,IGLV8-61,SERPINB2,GPR15,TRBV14,KLRB1,PDGFRB,TRAV25,SLC16A2,CEP55,PHLDA3,TYRO3,HSPG2,IGKV1-9,MGST1,IGHV3-11,FBLN5,CERCAM,GAS1,STAC,COL6A3,MAL2,GPR183,TRAV24,KRT10,TRBV7-9,SEMA5A,L1CAM,RGS1,CCR6,IGKV5-2,CD3G,GPM6A,TRAV29DV5,TSPAN13,FPR3,IGHV3-21,TRBV12-5,TRBV7-2,GLO1,LOXL1,TMEM97,PRKACB,GPR161,MSMO1,ALPK2,DLC1,IGHV4-30-2,LAMC1,PLS3,FOSL1,HSPA13,TRAV1-2,COL15A1,TRAV10,WNT5B,IGHV1-2,NPR3
GO:0005886	CC	plasma membrane	1.59E-19	18.79835383	219	MMP2,TNFRSF11B,RSC1A1,RND3,GJA1,TMEM47,CDH11,FLNC,KIRREL1,THY1,ITGBL1,ITGA11,SULF1,FN1,WNT5A,TENM2,OSMR,KCNK2,EGFR,CCN2,AHNAK2,CRYAB,AMOTL2,ANTXR1,GNG12,HAS2,FLRT2,STC1,SRPX2,DKK1,IL13RA2,MRGPRF,RAB3B,GRIA1,ATP8B1,PRSS12,CDH13,CACNA2D1,GFRA1,FMN2,STEAP2,PTGIS,GABBR2,LRRC15,CLDN11,CNTN3,CEMIP,S100A16,CSPG4,IGKV1D-17,COL6A1,GPR176,NFASC,LRIG3,SSTR1,ROBO2,GLRB,F3,KCNJ6,JPH2,F10,SYNC,TENM3,PDLIM4,CPE,LSAMP,GRIA3,ADGRL2,BCAR1,PDPN,C1QTNF5,GPNMB,PCDH18,FAP,CAV1,FRMD6,ACKR4,DCLK1,SEMA3D,KCNIP3,CD276,PIEZO2,LRP4,MXRA8,CAP2,PLA2R1,C

						LMP,STEAP1,EFS,KCNK15,DDR2,SYDE1,MPDZ,CAVIN1,GPC1,RPL36A-HNRNPH2,VSTM4,PLPPR4,ADGRL4,FARP1,EMP2,TRBV11-3,GDF5,BDKRB2,NALF2,LYPD6,SLC2A10,HTR2B,LGR5,VASN,TUSC3,CXCL12,SLC1A1,TJP1,FRAS1,EVA1A,SHROOM3,MAGI1,MAP1B,MET,GABRE,ENOX1,PARVA,IGKV1D-8,SPRY4,FAT1,UCHL1,EMP1,PLPP3,TRDV3,PACSIN3,HMCN1,GPR85,JAM2,TRDV2,TMEM98,AXL,HLA-DQB2,CLSTN2,SERPINE1,TRBV13,IGKV1-37,C1QTNF1,EDNRB,EHD2,SV2B,TRBV7-7,SH3D19,IGHV4-28,HTRA1,UPK3A,TRAV12-2,ENAH,MMP14,TM4SF1,GPM6B,CD248,FERMT2,COLEC12,PMP22,NCS1,EPB41L1,NT5E,TMEM126A,ENPP1,CXCL10,IGLV8-61,SERPINB2,GPR15,TRBV14,KLRB1,PDGFRB,TRAV25,SLC16A2,CEP55,PHLDA3,TYRO3,HSPG2,IGKV1-9,MGST1,IGHV3-11,CERCAM,GAS1,STAC,COL6A3,MAL2,GPR183,TRAV24,KRT10,TRBV7-9,SEMA5A,L1CAM,RGS1,CCR6,IGKV5-2,CD3G,GPM6A,TRAV29DV5,TSPAN13,FPR3,IGHV3-21,TRBV12-5,TRBV7-2,GLO1,TMEM97,PRKACB,GPR161,MSMO1,ALPK2,DLC1,IGHV4-30-2,PLS3,FOSL1,HSPA13,TRAV1-2,TRAV10,WNT5B,IGHV1-2,NPR3
GO:0005102	MF	signaling receptor binding	7.16E-16	15.14526434	90	IGFBP5,GREM1,STC2,TNFRSF11B,CCN1,COL3A1,SVEP1,GJA1,THY1,TNC,ITGBL1,ITGA11,FN1,WNT5A,LAMA4,OSMR,ANGPTL2,EGFR,CCN2,CCN5,FBLN1,EFEMP1,FST,FGF1,COL16A1,SLIT3,FLRT2,STC1,SRPX2,DKK1,GRIA1,FGF5,GFRA1,SLIT2,DKK2,FGF7,PTPN14,COMP,CPE,RARRES2,PDPN,NFATC4,GPNMB,FAP,TAFA5,CAV1,RSPO3,SEMA3D,CD276,LRP4,GDNF,NES,DKK3,FBN1,SERPINE2,ECM2,NTF3,CTHRC1,COL5A1,EMP2,GDF5,BDKRB2,IGFBP4,CXCL12,GAS6,UCHL1,PXDN,PLPP3,ARNT2,JAM2,SERPINE1,EDNRB,OGN,FGF2,MMP14,FERMT2,ADAMTS5,BMP3,ENPP1,CXCL10,PDGFRB,HSPG2,FBLN5,TRBV7-9,SEMA5A,CD3G,TRAV29DV5,JC

						HAIN,CCL2,WNT5B
GO:0050839	MF	cell adhesion molecule binding	2.00E-10	9.699174493	43	CCN1,COL3A1,SVEP1,CDH11,KIRREL1,THY1,TNC,ITGBL1,ITGA11,FN1,TENM2,EGFR,CCN2,CCN5,FBLN1,FGF1,COL16A1,CDH13,GFRA1,POSTN,NFASC,COMP,TENM3,CPE,GPNMB,FAP,FBN1,ECM2,COL5A1,EMP2,VASN,CXCL12,TJP1,PARVA,PLPP3,RPL23A,JAM2,FGF2,CNN3,MMP14,FERMT2,ADAMTS5,FBLN5
				Down regulated genes		
GO:0044238	BP	primary metabolic process	0.078505494	1.105099947	240	RNU5A-1,RNU5B-1,RNU5E-1,SNORA67,RNU4ATAC,SNORA44,SNORD14C,SNORA22,SNORD46,SNORA71C,SNORA47,SNORA60,SNORA3A,SNORD67,SNORA64,SNORA24,SNORD89,SNORA10,SNORD118,SNORA20,RNU6ATAC,SNORA26,SNORA61,SNORD55,SNORD104,SNORA14B,SNORA22C,RNU12,SNORA78,SCARNA20,SNORA37,SNORD99,SNORA52,SCARNA22,SNORD57,SNORA77B,SNORD21,RNU4-1,SNORD8,RNU2-1,SNORD13,SNORA68,SNORD110,SNORA79B,SNORA38,SNORD105B,PPIAL4G,SNORA38B,SNORD95,SNORA80D,SNORA9,RNU1-1,RNU4-2,RNU6-7,SNORA50B,RNVU1-7,SNORA49,SNORD100,SNORD116-15,SNORD9,SNORA65,SNORA71A,SNORD56,SNORD116-17,SNORA66,SCARNA3,SNORA84,RNVU1-28,SNORD14D,SNORA40B,SCARNA21,SNORA80E,SNORD35A,SNORA8,SNORD14A,SCARNA18,SNORA12,SNORD117,SNORA33,SNORA2C,SNORA71E,SNORA7B,SNORA74B,SNORA71D,SNORD97,SNORA57,SNORA13,SNORA2A,SNORA7A,SNORA21,SNORD116-16,SNORD94,SNORD10,SNORA80B,SNORA48,SNORA73B,SNORA73A,SNORD116-2,RNVU1-31,SCARNA1,PLG,SNORD116-3,SNORA23,SNORA11B,SNORA46,MND1,RMRP,SNORD88C,SNORA80A,SNORD116-22,SNORD41,SNORA14A,MT-ND3,SNORD71,SNORA54,SNORA5A,HNRNPA1L2,RNF225,RNVU1-4,MT-ATP8,TMEM132A,RPPH1,RNU5F-1,B4GALNT2,SNORA11F,H1-

						7,SNORA3B,ZFPM2,ACTN2,RNVU1-26,RNVU1-15,SNORA31,IHO1,RNVU1-2A,PTPRT,EPHA10,RAB40AL,IHH,RNVU1-2,FOXD4L3,RNVU1-27,FBXO39,FGF8,PRODH,ZSCAN10,AMHR2,A3GALT2,TCP10L,MGAT4C,SNORA50C,DLL4,PAPPA2,SLC39A5,TDRD6,MT-ND1,SLC3A1,GRIN2C,SPDYE2,MT-ATP6,MT-ND6,SCARNA7,MT-ND4,MT-ND2,MT-ND4L,CYP4F8,SCARNA5,PRKCG,RNVU1-6,SCARNA17,SLC28A2,ASPG,UBQLN3,RPL3L,CNDP1,SGK2,NDST3,DCLK3,FGF22,CARD14,NTRK3,MT-ND5,PAX2,PKLR,HSD17B1,TAF11L5,OVCH1,ADAMTS2,SOX15,MMP21,GRK7,SNORA74A,GAD1,CHRNB2,POLE2,H1-6,SCARNA6,TBX1,IFNL1,POU5F1,ZDHHC19,B3GNT4,PPM1E,SLC8A2,TF,ADAM20,RNVU1-33,ESRP1,CDC25C,PPIAL4H,ABHD16B,SCARNA10,SLC22A13,FOXD4L4,ST8SIA5,NKX6-3,SCARNA2,FOXD4L6,HUS1B,ABCC9,NEU4,TENT5B,POLR3G,GALNTL6,KASH5,PPIAL4E,NANOS3,ENPP7,TRIM50,NME9,SNORA5C,FN3K,SPIN2A,SLC25A2,ABCB11,ANKRD2,TAF11L2,RBFOX3,DRD4,ATP5MGL,BCO2
GO:0009058	BP	biosynthetic process	0.161798134	0.791026491	209	RNU5A-1,RNU5B-1,RNU5E-1,SNORA67,RNU4ATAC,SNORA44,SNORD14C,SNORA22,SNORD46,SNORA71C,SNORA47,SNORA60,SNORA3A,SNORD67,SNORA64,SNORA24,SNORD89,SNORA10,SNORD118,SNORA20,RNU6ATAC,SNORA26,SNORA61,SNORD55,SNORD104,SNORA14B,SNORA22C,RNU12,SNORA78,SCARNA20,SNORA37,SNORD99,SNORA52,SCARNA22,SNORD57,SNORA77B,SNORD21,RNU4-1,SNORD8,RNU2-1,SNORD13,SNORA68,SNORD110,SNORA79B,SNORA38,SNORD105B,PPIAL4G,SNORA38B,SNORD95,SNORA80D,SNORA9,RNU1-1,RNU4-2,RNU6-7,SNORA50B,RNVU1-7,SNORA49,SNORD100,SNORD116-15,SNORD9,SNORA65,SNORA71A,SNORD56,SNORD116-17,SNORA66,SCARNA3,SNORA84,RNVU1-

						28,SNORD14D,SNORA40B,SCARNA21,SNORA80E,SNORD35A,SNORA8,SNORD14A,SCARNA18,SNORA12,SNORD117,SNORA33,SNORA2C,SNORA71E,SNORA7B,SNORA74B,SNORA71D,SNORD97,SNORA57,SNORA13,SNORA2A,SNORA7A,SNORA21,SNORD116-16,SNORD94,SNORD10,SNORA80B,SNORA48,SNORA73B,SNORA73A,SNORD116-2,RNVU1-31,SCARNA1,SNORD116-3,SNORA23,SNORA11B,SNORA46,RMRP,SNORD88C,SNORA80A,SNORD116-22,SNORD41,SNORA14A,MT-ND3,SNORD71,SNORA54,SNORA5A,HNRNPA1L2,RNVU1-4,MT-ATP8,RPPH1,RNU5F-1,B4GALNT2,SNORA11F,SNORA3B,ZFPM2,ACTN2,RNVU1-26,RNVU1-15,SNORA31,RNVU1-2A,CDH3,IHH,RNVU1-2,FOXD4L3,RNVU1-27,FGF8,ZSCAN10,A3GALT2,TCP10L,MGAT4C,SNORA50C,ACTA1,DLL4,SLC39A5,TDRD6,MT-ND1,SLC3A1,MT-ATP6,MT-ND6,SCARNA7,MT-ND4,MT-ND2,MT-ND4L,SCARNA5,RNVU1-6,SCARNA17,EZHIP,RPL3L,C1QTNF4,NDST3,FGF22,CARD14,NTRK3,MT-ND5,PAX2,PKLR,HSD17B1,TAF11L5,ADAMTS2,SOX15,SNORA74A,GAD1,POLE2,SCARNA6,C12ORF50,TBX1,IFNL1,POU5F1,ZDHHC19,B3GNT4,SLC8A2,TF,RNVU1-33,ESRP1,PPIAL4H,SCN2B,PVALB,SCARNA10,FOXD4L4,ST8SIA5,NKX6-3,SCARNA2,FOXD4L6,ABCC9,TENT5B,POLR3G,GALNTL6,PPIAL4E,NANOS3,ENPP7,TG,FGF17,NME9,SNORA5C,SPIN2A,SLC25A2,ABCB11,ANKRD2,TAF11L2,RBFOX3,ATP5MGL
GO:0043232	CC	intracellular membraneless organelle	2.17239E-05	4.66306157	161	SNORA67,SNORA44,SNORD14C,SNORA22,SNORD46,SNORA71C,SNORA47,SNORA60,RNA5S1,SNORA3A,SNORD67,SNORA64,SNORA24,SNORD89,SNORA10,SNORD118,SNORA20,SNORA26,SNORA61,SNORD55,SNORD104,SNORA14B,SNORA22C,SNORA78,SCARNA20,SNORA37,SNORD99,SNORA52,SCARNA22,SNORD57,SNORA77B,SNORD21,SNORD8,SNORD13,SNORA68,SNORD110,SNORA79B,SNO

						RA38,SNORD105B,SNORA38B,SNORD95,SNORA80D,SNORA9,SNORA50B,SNORA49,SNORD100,SNORD116-15,SNORD9,SNORA65,SNORA71A,SNORD56,SNORD116-17,SNORA66,SCARNA3,SNORA84,SNORD14D,SNORA40B,SCARNA21,SNORA80E,SNORD35A,SNORA8,SNORD14A,SCARNA18,SNORA12,SNORD117,SNORA33,SNORA2C,SNORA71E,SNORA7B,SNORA74B,SNORA71D,SNORD97,SNORA57,SNORA13,SNORA2A,SNORA7A,SNORA21,SNORD116-16,SNORD94,SNORD10,RCCD1,SNORA80B,SNORA48,SNORA73B,SNORA73A,SNORD116-2,SCARNA1,SNORD116-3,SNORA23,SNORA11B,SNORA46,SNORD88C,SNORA80A,SNORD116-22,SNORD41,RP1L1,SNORA14A,SNORD71,SNORA54,SNORA5A,KRT74,SNORA11F,H1-7,SNORA3B,ZFPM2,ACTN2,SNORA31,IHO1,PCLO,TCHH,RSPH10B,FOXD4L3,CTNNA3,AQP7,SNORA50C,ACTA1,TDRD6,KRTAP10-3,CEP295NL,SCARNA7,SCARNA5,KRTAP16-1,NPHP3-ACAD11,CFAP157,SCARNA17,KRTAP10-2,DNAAF1,RPL3L,PAX2,RAPSN,GRIN2B,SOX15,SNORA74A,POLE2,H1-6,SCARNA6,TBX1,KRTAP5-9,SNTG2,TUBAL3,POU5F1,PPM1E,NCAPG,H3-5,SCARNA10,DNAI7,FOXD4L4,NKX6-3,SCARNA2,FOXD4L6,HUS1B,ABCC9,SAXO1,KASH5,NANOS3,EYS,NME9,SNORA5C,DOC2A,ANKRD2,DRD4
GO:0043233	CC	organelle lumen	0.001090993	2.962178092	152	SNORA67,SNORA44,SNORD14C,SNORA22,SNORD46,SNORA71C,SNORA47,SNORA60,SNORA3A,SNORD67,SNORA64,SNORA24,SNORD89,SNORA10,SNORD118,SNORA20,SNORA26,SNORA61,SNORD55,SNORD104,SNORA14B,SNORA22C,SNORA78,SCARNA20,SNORA37,SNORD99,SNORA52,SCARNA22,SNORD57,SNORA77B,SNORD21,SNORD8,SNORD13,SNORA68,SNORD110,SNORA79B,SNORA38,SNORD105B,SNORA38B,SNORD95,SNORA80D,SNORA9,SNORA50B,SNORA49,SNORD100,SNORD116-15,SNORD9,SNORA65,SNORA71A

						,SNORD56,SNORD116-17,SNORA66,SCARNA3,SNORA84,SNORD14D,SNORA40B,SCARNA21,SNORA80E,SNORD35A,SNORA8,SNORD14A,SCARNA18,SNORA12,SNORD117,SNORA33,SNORA2C,SNORA71E,SNORA7B,SNORA74B,SNORA71D,HRNR,SNORD97,SNORA57,SNORA13,SNORA2A,SNORA7A,SNORA21,SNORD116-16,SNORD94,SNORD10,SNORA80B,SNORA48,SNORA73B,SNORA73A,SNORD116-2,SCARNA1,PLG,SNORD116-3,SNORA23,SNORA11B,SNORA46,SNORD88C,SNORA80A,SNORD116-22,SNORD41,SNORA14A,SNORD71,SNORA54,SNORA5A,TMEM132A,SNORA11F,SNORA3B,ZFPM2,ACTN2,SNORA31,IHO1,CSPG5,PRODH,SLC13A5,ZSCAN10,SNORA50C,SCARNA7,SCARNA5,SLC28A1,SCARNA17,MT-CO2,EZHIP,DNAAF1,SGK2,PAX2,TAF11L5,BAIAP2L2,MUC4,LEFTY2,SNORA74A,COL23A1,POLE2,SCARNA6,SNTG2,POU5F1,ZDHHC19,PPM1E,TF,ESRP1,NCAPG,CDC25C,ABHD16B,H3-5,SCARNA10,SCARNA2,HUS1B,NEU4,MUC12,POLR3G,KASH5,NANOS3,SNORA5C,SPIN2A,DOC2A,ANKRD2,TAF11L2,BCO2
GO:0022857	MF	transmembrane transporter activity	1.38E-07	6.859457537	43	SLC9A4,MT-ND3,GABRG2,MT-ATP8,SLC13A5,SLC6A15,AQP7,SLC39A5,MT-ND1,SLC3A1,GRIN2C,MT-ATP6,MT-ND6,MT-ND4,MT-ND2,MT-ND4L,SLC28A1,TTYH1,SLC28A2,MT-CO2,ASPG,SGK2,MT-ND5,SLC10A4,KCNS1,GRIN2B,CHRNB2,SLC4A9,SLC5A11,ASIC1,ABCC11,SLC8A2,KCNQ4,SCN2B,SLC22A13,NHERF4,ABCC9,SLC22A1,SLC25A2,TRPV6,ABCB11,DRD4,ATP5MGL
GO:0046873	MF	metal ion transmembrane transporter activity	2.7593E-05	4.559201661	23	SLC9A4,SLC13A5,SLC6A15,SLC39A5,GRIN2C,SLC28A1,TTYH1,SLC28A2,ASPG,SGK2,SLC10A4,KCNS1,GRIN2B,SLC4A9,SLC5A11,ASIC1,SLC8A2,KCNQ4,SCN2B,ABCC9,SLC22A1,TRPV6,DRD4

Table 3 The enriched pathway terms of the up and down regulated differentially expressed genes

Pathway ID	Pathway Name	adjusted_p_value	negative_log10_of_adjusted_p_value	Gene Count	Gene
Up regulated genes					
REAC:R-HSA-1474244	Extracellular matrix organization	2.92E-21	20.53506045	46	COL1A2,DCN,COL12A1,MMP2,COL1A1,COL8A1,COL3A1,LUM,TNC,ITGA11,FN1,LOXL4,LAMA4,MFAP4,FBLN1,EFEMP1,LAMB1,COL16A1,COL11A1,ELN,COL6A1,MMP1,LOX,COMP,MFAP2,COL5A2,MFAP5,LRP4,DDR2,FBN1,COL5A1,GDF5,FBLN2,PXDN,JAM2,SERPINE1,FGF2,HTRA1,MMP14,ADAMTS5,HSPG2,FBLN5,COL6A3,LOXL1,LAMC1,COL15A1
REAC:R-HSA-3000178	ECM proteoglycans	2.80E-10	9.552322879	14	FN1,LOXL4,MFAP4,FBLN1,EFEMP1,ELN,LOX,MFAP2,MFAP5,FBN1,GDF5,FBLN2,FBLN5,LOXL1
REAC:R-HSA-381426	Regulation of Insulin-like Growth Factor (IGF) transport and uptake by Insulin-like Growth Factor Binding Proteins (IGFBPs)	3.68143E-06	5.433984042	16	IGFBP5,STC2,MMP2,CCN1,TNC,FN1,PAPPA,LAMB1,MMP1,MXRA8,FBN1,IGFBP4,EVA1A,GAS6,IGFBP3,LAMC1
REAC:R-HSA-3781865	Diseases of glycosylation	0.000333421	3.477006491	14	DCN,THBS2,PRELP,LUM,ADAMTSL1,THSD4,ADAMTS12,CSPG4,CHST3,GPC1,OGN,ADAMTS5,HSPG2,SEMA5A
REAC:R-HSA-422475	Axon guidance	0.017727964	1.751341142	26	MMP2,COL3A1,EGFR,LAMB1,SLIT3,GFRA1,SLIT2,COL6A1,NFASC,ROBO2,COL5A2,GDNF,CAP2,GPC1,COL5A1,CXCL12,MET,DPYSL3,RPL23A,CRMP1,ENAH,COL6A3,SEMA5A,L1CAM,PRKACB,LAMC1
REAC:R-HSA-162582	Signal Transduction	0.028401854	1.546653308	84	COL1A2,THBS2,MMP2,COL1A1,RND3,COL3A1,GJA1,FN1,WNT5A,LAMA4,EGFR,STMN2,FST,AMOTL2,LAMB1,FGF1,GNG12,SNAI2,FLRT2,COL11A1,DKK1,GFRA1,GABBR2,COL6A1,GPR176,YAP1,SSTR1,DKK2,PDE1C,F3,FGF7,BCAR1,CCND1,COL5A2,GPNMB,DZIP1,ALDH1A3,CAV1,RSPO3,ACKR4,GDNF,FBN1,SYDE1,CAVIN1,NTF3,HECW1,PLPPR4,COL5A1,FARP1,BDKRB2,HTR2B,LGR5,FGD1,CXCL12,TJP1,IGF2

					BP1,MET,AXL,SERPINE1,EDNRB,FGF2,FERMT2,HEYL,CXCL10,GPR15,PDGFRB,DACT1,GAS1,COL6A3,GPR183,RGS1,CCR6,SCD,FPR3,AKR1C3,EPAS1,PRKACB,GPR161,DLC1,LAMC1,FOSL1,CCL2,PDK4,WNT5B
Down regulated genes					
REAC:R-HSA-9709957	Sensory Perception	0.000170407	3.768513361	24	OR52H1,OR2L3,PCLO,TAS2R41,OR52B2,OR4F17,OR5B21,OR2L8,ESPNL,HSD17B1,RCVRN,OR52K2,OR2L2,GRK7,OR2T11,OR5AN1,OR2B6,TAS2R3,OR56A4,KCNQ4,SCN2B,TAS2R30,STRC,BCO2
REAC:R-HSA-112316	Neuronal System	0.026876387	1.570629117	15	GABRG2,ACTN2,GRIN2C,LRRTM2,PRKCG,NTRK3,KCNS1,GRIN2B,GAD1,CHRNB2,TUBAL3,PPM1E,KCNQ4,ABCC9,SLC22A1
REAC:R-HSA-425407	SLC-mediated transmembrane transport	0.040194178	1.395836853	11	SLC9A4,SLC13A5,SLC6A15,SLC39A5,SLC3A1,SLC28A1,SLC28A2,SLC4A9,SLC5A11,SLC8A2,SLC22A1
REAC:R-HSA-112315	Transmission across Chemical Synapses	0.086975837	1.060601385	10	GABRG2,ACTN2,GRIN2C,PRKCG,GRIN2B,GAD1,CHRNB2,TUBAL3,PPM1E,SLC22A1
REAC:R-HSA-382551	Transport of small molecules	0.155242664	0.808988915	18	SLC9A4,SLC13A5,SLC6A15,AQP7,SLC39A5,SLC3A1,SLC28A1,SLC28A2,SGK2,SLC4A9,SLC5A11,ASIC1,ABCC11,SLC8A2,TF,ABCC9,SLC22A1,TRPV6
REAC:R-HSA-6805567	Keratinization	0.290974441	0.536145157	7	KRT74,TCHH,SPINK9,KRTAP10-3,KRTAP16-1,KRTAP10-2,KRTAP5-9

Table 4 Topology table for up and down regulated genes

Regulation	Node	Degree	Betweenness	Stress	Closeness
Up	EGFR	1499	0.243711	5.81E+08	0.435788
Up	FN1	846	0.107965	2.88E+08	0.404672
Up	CAV1	735	0.07742	2.23E+08	0.38607
Up	BCAR1	726	0.09556	2.41E+08	0.386505
Up	YAP1	708	0.07834	2.58E+08	0.390839
Up	GJA1	627	0.075199	1.68E+08	0.395508
Up	RPL23A	544	0.052197	2.11E+08	0.367647
Up	NIFK	392	0.031161	1.54E+08	0.340616
Up	RBPMS	337	0.046697	1.03E+08	0.340264
Up	FLNC	335	0.037249	96639596	0.360673

Up	IGF2BP1	311	0.023787	89404560	0.350529
Up	CCND1	271	0.022599	1.23E+08	0.33323
Up	LDHB	255	0.018065	58139562	0.354134
Up	TJP1	246	0.023613	37396052	0.379946
Up	CEP55	238	0.025531	55070948	0.354222
Up	UCHL1	230	0.022176	43823502	0.356742
Up	CAVIN1	225	0.020759	36617030	0.369644
Up	PRKACB	222	0.018076	55656886	0.344074
Up	MET	194	0.01118	20856814	0.357634
Up	CRYAB	171	0.017223	35279634	0.335525
Up	MAP1B	171	0.011552	48550618	0.331901
Up	KPNA3	167	0.013426	55670528	0.327403
Up	AXL	164	0.011534	22211676	0.352446
Up	COL1A1	162	0.01472	15286974	0.35981
Up	PDGFRB	161	0.008975	14447712	0.358202
Up	FERMT2	154	0.009748	24166420	0.344724
Up	EPB41L1	153	0.011525	26620890	0.343357
Up	SMARCA1	149	0.013583	34740920	0.330214
Up	VASN	146	0.013521	29440280	0.338692
Up	AMOTL2	144	0.011759	22510326	0.335893
Up	ANTXR1	139	0.012891	24863950	0.343055
Up	ISLR	137	0.01388	44184174	0.320166
Up	LRRC15	135	0.01788	30187894	0.320142
Up	ASS1	134	0.011879	20034062	0.341076
Up	IL13RA2	132	0.015773	14267186	0.348847
Up	NR2F2	130	0.015708	19187606	0.339147
Up	NES	124	0.0102	28354058	0.326604
Up	ZIC1	122	0.013526	15159052	0.317193
Up	EFEMP1	121	0.010896	30788530	0.324233
Up	PACSIN3	117	0.007518	20144726	0.33393
Up	MID1	109	0.009471	31107228	0.322951
Up	SERPINB2	97	0.008551	16485692	0.314414
Up	TAF9B	95	0.010672	30201684	0.315954
Up	ENAH	93	0.005535	11011272	0.334152
Up	RASSF8	85	0.005775	8281018	0.329922
Up	NT5E	83	0.005924	8457918	0.344862
Up	MMP2	80	0.007291	6784648	0.331068
Up	DKK3	80	0.008204	17387242	0.318371
Up	ADAM33	79	0.008159	12989774	0.311004
Up	SYNC	70	0.004661	5519042	0.323939
Up	IGFBP3	9	8.10E-04	2690902	0.337213
Up	NUPR1	9	4.66E-04	2088352	0.330698
Up	RAB3B	7	3.06E-04	950270	0.284317
Up	DCN	6	1.75E-04	560894	0.331927
Up	KIRREL1	5	1.10E-04	275782	0.306414
Up	PTPN14	5	1.32E-04	1329820	0.323487
Up	TIMP3	5	2.54E-04	448596	0.27282
Up	LOX	5	9.26E-05	180020	0.298666
Up	SH3BP4	5	1.81E-04	512628	0.303561
Up	MMP14	5	9.61E-04	1915706	0.323036
Up	RND3	5	2.94E-05	194548	0.317111
Up	HSPB2	4	1.71E-04	394832	0.290216
Up	HTRA1	4	1.74E-04	346798	0.2859
Up	KRT10	4	8.62E-05	779084	0.325934
Up	IGFBP5	4	1.00E-04	240296	0.297919
Up	FBLIM1	3	2.55E-05	64124	0.276079
Up	COL1A2	3	0	0	0.31976
Up	COL5A1	3	0	0	0.289813
Up	MPDZ	3	6.23E-06	12558	0.283059
Up	WNT5A	3	6.41E-05	162430	0.260567
Up	FGF2	3	8.78E-05	110622	0.261768
Up	GDF5	3	9.29E-05	175082	0.256983
Up	CACNA2D1	3	1.43E-04	474286	0.283837
Up	HSPB8	3	3.94E-05	92946	0.259165
Up	NQO1	3	8.74E-05	666902	0.306699
Up	CSPG4	3	6.46E-05	110864	0.286732
Up	GPC1	3	1.96E-05	78784	0.287597
Up	SLC1A1	3	8.76E-05	132234	0.265472
Up	DHCR24	3	4.77E-04	1250390	0.314448
Up	TFAP2C	3	4.59E-05	211728	0.29126

Up	ADGRL2	3	6.52E-05	605850	0.307491
Up	DKK2	3	1.54E-04	143978	0.265217
Up	GPM6A	3	7.44E-06	44776	0.256391
Up	TUSC3	3	4.76E-05	138146	0.253563
Up	MAGI1	3	5.88E-05	204300	0.286167
Up	PTX3	3	4.42E-05	191210	0.237186
Up	GAS6	2	4.39E-05	57518	0.265867
Up	FBLN1	2	3.69E-05	179400	0.290176
Up	TNC	2	0	0	0.31869
Up	HSPG2	2	0	0	0.295221
Up	FBLN2	2	3.69E-05	179400	0.290176
Up	PRELP	2	0	0	0.289325
Up	SERPINE1	2	2.16E-05	14554	0.264456
Up	HSPB6	2	0	0	0.25495
Up	CERCAM	2	7.84E-05	123654	0.24889
Up	COLEC12	2	1.35E-05	31742	0.250834
Up	TMEM97	2	3.82E-05	117056	0.303615
Up	MGARP	2	8.66E-05	201970	0.30979
Up	CCN2	2	0	0	0.31869
Up	JAM2	2	1.16E-05	47856	0.286349
Up	L1CAM	2	0	0	0.303895
Up	CXCL12	2	0	0	0.288614
Up	FAT1	2	4.57E-05	35704	0.257137
Up	MEOX1	2	1.96E-05	73070	0.244741
Up	DLC1	2	2.94E-05	99244	0.279125
Up	FBLN5	2	4.53E-05	50002	0.246734
Up	SYNPO2	2	1.48E-05	72408	0.268615
Up	OSMR	2	1.07E-04	136252	0.30578
Up	FMN2	2	2.21E-05	129376	0.289412
Up	FIBIN	2	3.06E-06	14838	0.252935
Up	TMEM126A	2	1.09E-05	4870	0.243
Up	DZIP1	2	0	0	0.291756
Up	CREB3L1	2	5.71E-05	113772	0.237285
Up	ROBO2	2	0	0	0.291756
Up	SCD	2	2.14E-04	616616	0.309031
Up	FARP1	2	5.27E-06	18376	0.285529
Up	SPRY4	2	0	0	0.291756
Up	GNG12	2	1.20E-05	45730	0.28678
Up	GPX8	2	3.99E-05	47738	0.25904
Up	LRIG3	2	0	0	0.316013
Up	MGST1	2	0	0	0.310441
Up	COL8A1	2	0	0	0.266644
Up	FKBP10	2	2.33E-05	31460	0.271301
Up	CGNL1	2	0	0	0.288925
Up	C1S	2	0	0	0.295221
Up	PLPP3	2	3.48E-05	330906	0.295914
Up	AHNAK2	2	3.41E-04	797944	0.278789
Up	CAP2	2	0	0	0.308987
Up	LIMCH1	2	3.74E-05	206946	0.288594
Up	CDH13	2	2.06E-05	106022	0.270505
Up	GLO1	2	1.55E-05	60598	0.283405
Up	ENPP1	2	7.79E-05	193952	0.282017
Up	LOXL4	2	7.79E-06	30586	0.240001
Up	LAMB1	2	6.51E-05	289844	0.278989
Up	PARVA	2	8.08E-06	18296	0.281314
Up	NTF3	1	0	0	0.242567
Up	TEAD1	1	0	0	0.281019
Up	GRIA1	1	0	0	0.255604
Up	FRMD6	1	0	0	0.248083
Up	GPR161	1	0	0	0.256001
Up	DNAJC12	1	0	0	0.255436
Up	GPR183	1	0	0	0.232827
Up	SLC16A2	1	0	0	0.256437
Up	GPM6B	1	0	0	0.303529
Up	FRAS1	1	0	0	0.234507
Up	S100A16	1	0	0	0.240817
Up	SELENOP	1	0	0	0.303529
Up	COL12A1	1	0	0	0.248731
Up	HSPB7	1	0	0	0.265078
Up	COL6A1	1	0	0	0.248731

Up	RGPD3	1	0	0	0.244399
Up	EDNRB	1	0	0	0.278545
Up	PTPN21	1	0	0	0.281019
Up	THBS2	1	0	0	0.248731
Up	F3	1	0	0	0.251821
Up	GPNMB	1	0	0	0.303529
Up	F10	1	0	0	0.251821
Up	PTGIS	1	0	0	0.278545
Up	HEYL	1	0	0	0.253886
Up	MAL2	1	0	0	0.234104
Up	C11orf87	1	0	0	0.253886
Up	CCBE1	1	0	0	0.261576
Up	PDLIM4	1	0	0	0.253886
Up	MYOM2	1	0	0	0.248486
Up	ALDH1A3	1	0	0	0.278545
Up	COL5A2	1	0	0	0.246203
Up	FAP	1	0	0	0.278545
Up	TBX5	1	0	0	0.281019
Up	PAPPA	1	0	0	0.251821
Up	CYP51A1	1	0	0	0.250212
Up	SH3D19	1	0	0	0.275343
Up	C1QTNF1	1	0	0	0.2881
Up	PMP22	1	0	0	0.265078
Up	EFS	1	0	0	0.278771
Up	CCN1	1	0	0	0.278771
Up	DDAH1	1	0	0	0.262948
Up	NDNF	1	0	0	0.248644
Up	INSYN1	1	0	0	0.269892
Up	TYRO3	1	0	0	0.260607
Up	CPE	1	0	0	0.243249
Up	PDE1C	1	0	0	0.303529
Up	HOXC8	1	0	0	0.253886
Up	NFATC4	1	0	0	0.261433
Up	SIX4	1	0	0	0.242808
Up	TENM3	1	0	0	0.243249
Up	SYDE1	1	0	0	0.257879
Up	SV2B	1	0	0	0.281019
Up	TBX15	1	0	0	0.231776
Up	CSRP2	1	0	0	0.278771
Up	PLS3	1	0	0	0.303529
Up	STC2	1	0	0	0.243249
Up	STMN2	1	0	0	0.243428
Up	PXDN	1	0	0	0.243249
Up	CCL2	1	0	0	0.222669
Up	ZFHX4	1	0	0	0.237482
Up	MFAP4	1	0	0	0.24868
Up	RNF182	1	0	0	0.255436
Up	KDELR3	1	0	0	0.254655
Up	ALDH1L2	1	0	0	0.278771
Up	MYRIP	1	0	0	0.278545
Up	SIK1	1	0	0	0.239211
Up	FBXL7	1	0	0	0.278771
Up	MXRA8	1	0	0	0.265078
Up	CTHRC1	1	0	0	0.239773
Up	DCLK1	1	0	0	0.257879
Up	MSMO1	1	0	0	0.229327
Up	GLRB	1	0	0	0.250212
Up	RNASE4	1	0	0	0.239773
Up	EHD2	1	0	0	0.225985
Up	SULF1	1	0	0	0.243249
Up	SERPINE2	1	0	0	0.283424
Up	BRINP1	1	0	0	0.249949
Up	VGLL3	1	0	0	0.253886
Up	MOXD1	1	0	0	0.243249
Up	GABRE	1	0	0	0.242513
Up	SPATA18	1	0	0	0.278771
Up	FGF7	1	0	0	0.264611
Up	LYPD6	1	0	0	0.233887
Up	SHROOM3	1	0	0	0.20535
Up	EPAS1	1	0	0	0.246656

Up	CORO2B	1	0	0	0.274708
Up	ELN	1	0	0	0.254338
Up	FST	1	0	0	0.2881
Up	FBN1	1	0	0	0.2881
Up	IGFBP4	1	0	0	0.256468
Up	COL6A3	1	0	0	0.248731
Up	DDR2	1	0	0	0.264611
Up	COMP	1	0	0	0.2881
Up	TNFRSF11B	1	0	0	0.2881
Up	FOSL1	1	0	0	0.239331
Up	CRMP1	1	0	0	0.251238
Down	POU5F1	337	0.031615	1.33E+08	0.341947
Down	TTYH1	301	0.038422	50091836	0.333697
Down	ACTA1	297	0.032044	49797326	0.378738
Down	GPR17	281	0.030766	67201082	0.341647
Down	TF	187	0.021112	32975666	0.344918
Down	ACTN2	170	0.016466	45608564	0.330634
Down	CDC25C	148	0.011959	18386638	0.347475
Down	ANOS1	146	0.009068	16642448	0.330915
Down	SOX15	129	0.008672	20832648	0.320657
Down	CTNNA3	127	0.015201	28821768	0.321739
Down	SLC6A15	126	0.005636	13383702	0.337466
Down	TMEM132A	120	0.014064	17227190	0.330979
Down	LLCFC1	119	0.013504	21828900	0.321426
Down	NCAPG	116	0.012125	15240656	0.350272
Down	HNRNPA1L2	116	0.009768	11848452	0.353959
Down	CNTNAP3	115	0.010836	17490008	0.315385
Down	CCDC140	114	0.003785	34105842	0.299972
Down	GRIN2C	113	0.014484	31550902	0.314621
Down	SCARNA22	113	0.003559	24353256	0.315188
Down	HRNR	112	0.005503	9562614	0.360007
Down	PRKCG	108	0.006972	15178164	0.335013
Down	PLG	104	0.008701	12345418	0.336565
Down	FGF8	104	0.004798	27422758	0.30528
Down	CHRNB2	102	0.008851	17815822	0.30528
Down	SCN2B	90	0.003079	9858196	0.313907
Down	GPR21	82	0.005833	6935358	0.313299
Down	TENT5B	82	0.00574	16230452	0.309656
Down	NTRK3	81	0.004018	16244994	0.320238
Down	PAX2	81	0.006853	9100722	0.311433
Down	TCP10L	72	0.005243	7955386	0.315513
Down	FOXD4L6	70	0.006258	9934396	0.318028
Down	ESRP1	67	0.004713	9762444	0.323438
Down	MLNR	67	0.003767	14767070	0.304013
Down	IQCN	66	0.005665	10906426	0.310621
Down	GRIN2B	64	0.004015	4454140	0.338558
Down	RCCD1	64	0.006974	21362344	0.303852
Down	RPL3L	61	9.99E-04	3680128	0.323097
Down	PCDHA4	55	0.005377	11704920	0.306787
Down	ASIC1	54	0.004226	10341314	0.309723
Down	TUBAL3	54	0.002254	4239766	0.323866
Down	ADAMTS2	52	0.004777	6481510	0.289149
Down	SLC39A5	51	0.002853	15305650	0.277087
Down	SAXO1	51	0.005224	4011246	0.311331
Down	TRIM50	50	0.003451	8450288	0.301036
Down	POLE2	49	0.004783	9370288	0.301692
Down	CNTN2	48	0.002964	2583556	0.334974
Down	ST8SIA5	47	0.00393	3277438	0.297227
Down	CPNE4	45	0.002897	11333786	0.294239
Down	PKLR	45	0.004452	3855808	0.324491
Down	AMHR2	44	0.001696	3400478	0.307337
Down	ZDHHC19	43	0.004468	3217626	0.3059
Down	MND1	41	0.003103	7965954	0.299511
Down	FGF17	41	0.001178	5649674	0.292233
Down	MGAT4C	37	0.002884	2544600	0.306338
Down	TMEFF1	36	0.002362	5565412	0.303475
Down	PCDH17	36	0.002121	18059538	0.295986
Down	PAGE1	36	0.003763	8857476	0.287347
Down	ARHGAP44	35	0.003102	10753564	0.296057
Down	NUP62CL	35	0.00258	6466622	0.30383

Down	GPR52	34	0.002208	2379410	0.297557
Down	DRD4	34	0.002397	10979846	0.296119
Down	LRRC73	34	0.002725	5993076	0.297598
Down	GAD1	34	0.001392	4081726	0.30565
Down	PPM1E	33	0.001685	3956794	0.30516
Down	CSPG5	31	0.0028	10036266	0.2913
Down	SGK2	30	5.78E-04	3299462	0.298989
Down	PCLO	30	0.001186	3681300	0.309399
Down	ZFPM2	29	0.001198	2984992	0.299501
Down	RAPSN	29	0.00106	3254242	0.303561
Down	MAB21L3	29	0.002945	8747740	0.284468
Down	ENPP7	28	0.001638	1993646	0.293644
Down	RBFOX3	28	0.002179	7629378	0.297795
Down	SLC22A1	27	0.002875	11454010	0.286444
Down	GABRG2	26	0.001859	5831690	0.283069
Down	NEU4	26	0.00157	1335940	0.301438
Down	PPIAL4G	26	0.002515	9288904	0.291955
Down	HUS1B	25	0.001585	6645416	0.292682
Down	POLR3G	24	0.002539	1614384	0.288264
Down	SNTG2	24	0.001976	4990106	0.290757
Down	CDH3	24	0.00108	969852	0.320106
Down	RAB26	24	0.001535	2529524	0.293233
Down	TRHR	23	0.002611	5070952	0.267309
Down	GRK7	23	0.00112	4146306	0.28999
Down	KRT74	23	0.001434	1161178	0.308887
Down	RASEF	22	0.002151	8486914	0.292343
Down	SLC13A5	22	0.001269	1070702	0.319712
Down	ACP7	22	0.001071	5260776	0.28394
Down	HSD17B1	20	9.72E-04	3469268	0.279398
Down	RNU12	20	0.001472	5758912	0.282351
Down	TRPV6	19	8.59E-04	3467682	0.279699
Down	CNDP1	19	6.59E-04	1279762	0.296939
Down	RCVRN	19	0.001124	884206	0.308342
Down	TAS2R41	19	0.001379	3994650	0.278717
Down	ELAVL3	18	3.71E-04	1203626	0.29432
Down	NYX	18	0.001617	7690832	0.280926
Down	LRRTM2	18	0.001283	4605450	0.274374
Down	OR52B2	18	0.001942	4232370	0.263643
Down	CARD14	17	0.001264	3726976	0.275237
Down	RANBP17	16	9.03E-04	2044174	0.293152
Down	RSPO4	16	0.001534	3795350	0.268851
Down	FOXD4L3	16	0.001179	1674454	0.28112
Down	DOC2A	15	0.001899	9985344	0.252362
Down	PTPRT	15	8.49E-04	638576	0.32007
Down	CDHR2	15	0.001261	5322022	0.273133
Down	PRB3	15	0.001026	2844334	0.272768
Down	COL23A1	15	2.86E-04	1012922	0.283274
Down	NANOS3	15	5.85E-04	2057386	0.284458
Down	SLC28A2	15	0.001511	3337422	0.27059
Down	TG	14	4.88E-04	1974452	0.286148
Down	OMP	14	0.001495	3909438	0.247575
Down	RAB40AL	14	0.001736	1259766	0.263174
Down	TCHH	14	0.00116	1178286	0.301554
Down	ANKRD2	13	6.05E-04	1460610	0.284355
Down	ASPG	13	9.66E-04	2839696	0.267326
Down	SPIN2A	13	5.45E-04	1766010	0.283321
Down	MATN1	12	7.16E-04	2084470	0.249433
Down	MUC4	12	3.28E-04	298454	0.316257
Down	LIMS3	12	4.99E-04	1446072	0.260638
Down	RN7SK	11	2.55E-04	1393846	0.28066
Down	SLC8A2	11	5.05E-04	2838808	0.279052
Down	AQP7	11	9.40E-04	3678260	0.258408
Down	ADGRG2	11	4.83E-04	1544946	0.254421
Down	PRODH	10	7.20E-04	1944738	0.283387
Down	PDE4C	10	7.32E-04	1253358	0.244427
Down	RNU4ATAC	10	4.77E-04	1557620	0.261856
Down	LENEP	10	4.74E-04	2696142	0.247168
Down	DCLK3	9	0.001182	3196594	0.255163
Down	VWA5B2	9	7.59E-04	1734106	0.266197
Down	CD164L2	9	8.36E-04	1564926	0.265102

Down	RN7SL1	9	2.82E-04	1418894	0.249049
Down	PTTG2	9	5.09E-04	1076380	0.282985
Down	MADCAM1	8	2.19E-05	62448	0.264025
Down	ABCB11	8	7.12E-04	1241966	0.255558
Down	BICDL2	8	5.25E-04	345760	0.27591
Down	DNAAF1	8	4.77E-04	1405604	0.272646
Down	NDST3	8	5.26E-04	1187390	0.27275
Down	SEZ6	8	5.99E-04	1741950	0.28395
Down	IFNL1	7	7.43E-04	1694514	0.270795
Down	CYP4F8	7	5.18E-04	1321144	0.250285
Down	PRLHR	7	7.16E-04	2862922	0.216858
Down	PRR36	7	2.66E-04	431044	0.278256
Down	ABCC9	7	4.90E-04	1194174	0.267551
Down	NKAIN3	7	5.01E-04	1456116	0.252429
Down	KCNQ4	7	2.35E-04	996048	0.285567
Down	TBX1	6	2.88E-05	43934	0.257214
Down	IHH	6	7.62E-04	2978072	0.254262
Down	CNIH2	6	4.70E-04	749124	0.210895
Down	C1QTNF4	6	2.52E-04	728828	0.252258
Down	FN3K	6	4.84E-04	1416598	0.258798
Down	BAIAP2L2	6	3.20E-04	153024	0.241257
Down	UBQLN3	6	4.69E-04	998944	0.26018
Down	NRG2	5	2.38E-04	603524	0.27927
Down	EPHA10	5	1.22E-05	29080	0.263053
Down	CTAGE6	5	2.92E-04	773042	0.230635
Down	SLC5A11	5	1.11E-04	68094	0.279334
Down	SLC25A2	5	7.06E-04	1250394	0.238871
Down	RP1L1	5	4.67E-04	1662652	0.26822
Down	PAPPA2	5	2.39E-04	491834	0.266337
Down	SNORA7A	5	1.76E-06	13900	0.263927
Down	B4GALNT2	5	2.49E-04	459332	0.267417
Down	SLC10A4	5	2.84E-04	615956	0.239171
Down	NXNL2	5	2.53E-04	742150	0.265332
Down	STPG2	4	2.72E-04	389476	0.258727
Down	SLC9A4	4	4.70E-04	1012054	0.195188
Down	SPDYE2	4	4.98E-06	8532	0.237996
Down	TDRD6	4	1.66E-06	9256	0.261043
Down	B3GNT4	4	1.76E-04	465034	0.253721
Down	ABHD16B	4	2.46E-05	35960	0.280687
Down	ATP5MGL	4	4.71E-04	876472	0.244958
Down	SLC22A13	3	4.66E-04	589362	0.195705
Down	LEFTY2	3	4.66E-04	773442	0.232921
Down	MUC12	3	5.10E-07	4322	0.278653
Down	OVCH1	3	1.32E-06	6186	0.260543
Down	ABCC11	3	2.34E-04	669032	0.262008
Down	ERICH6	3	2.33E-04	512848	0.279516
Down	TAS2R60	3	2.58E-05	66986	0.24287
Down	DLL4	3	2.34E-04	627684	0.233753
Down	ESPNL	3	2.35E-04	319400	0.198831
Down	ZSCAN10	3	2.37E-04	604314	0.228618
Down	P2RY4	3	1.19E-06	3970	0.235655
Down	NPIPB13	3	8.20E-07	3466	0.256545
Down	OR52K2	3	2.41E-04	995144	0.220914
Down	KRTAP5-9	2	3.21E-06	4920	0.249869
Down	DUX4	1	0	0	0.259557
Down	EYS	1	0	0	0.303529
Down	PPIAL4E	1	0	0	0.225985
Down	KRTAP10-3	1	0	0	0.218572
Down	SLC3A1	1	0	0	0.303529

Table 5 MiRNA - hub gene and TF – hub gene topology table

Regulation	Hub Genes	Degree	MicroRNA	Regulation	Hub Genes	Degree	TF
Up	CCND1	543	hsa-miR-6874-5p	Up	BCAR1	28	GATA2
Up	FN1	366	hsa-miR-1307-3p	Up	CAV1	16	SREBF1
Up	TJP1	346	hsa-miR-153-3p	Up	FN1	14	RELA
Up	YAP1	315	hsa-miR-92b-3p	Up	FLNC	12	GATA3
Up	IGF2BP1	295	hsa-miR-7160-3p	Up	IGF2BP1	12	MAX
Up	CAV1	257	hsa-miR-301a-3p	Up	GJA1	9	ARID3A
Up	EGFR	241	hsa-miR-4446-3p	Up	TJP1	9	STAT1
Up	FLNC	211	hsa-miR-218-5p	Up	YAP1	9	ELK4
Up	CEP55	187	hsa-miR-942-5p	Up	EGFR	8	TEAD1
Up	GJA1	170	hsa-miR-100-3p	Up	CCND1	8	HOXA5
Up	LDHB	156	hsa-miR-23b-3p	Up	CEP55	7	POU2F2
Up	RPL23A	133	hsa-miR-3936	Up	LDHB	6	NFYA
Up	BCAR1	129	hsa-miR-19b-3p	Up	NIFK	6	FOXC1
Up	NIFK	107	hsa-miR-519d-5p	Up	RBPMS	4	TFAP2A
Up	RBPMS	82	hsa-miR-582-5p	Up	RPL23A	4	FOXA1
Down	NCAPG	172	hsa-miR-561-5p	Down	SLC6A15	16	SRF
Down	TMEM132A	122	hsa-miR-23a-3p	Down	POU5F1	11	IRF2
Down	ACTN2	117	hsa-miR-6887-3p	Down	HNRNPA1L2	11	MEF2A
Down	HNRNPA1L2	112	hsa-miR-7157-3p	Down	ACTN2	11	USF2
Down	TF	110	hsa-miR-152-3p	Down	CTNNA3	10	YY1
Down	SLC6A15	109	hsa-miR-196a-5p	Down	TF	8	ESR1
Down	CTNNA3	84	hsa-miR-4717-5p	Down	CDC25C	8	NFIC
Down	ANOS1	72	hsa-miR-1250-5p	Down	GPR17	7	PRRX2
Down	TTYH1	60	hsa-miR-6830-3p	Down	TTYH1	7	ZNF354C
Down	ACTA1	57	hsa-miR-1252-3p	Down	ACTA1	7	NRF1
Down	CDC25C	49	hsa-miR-107	Down	CCDC140	7	RUNX2
Down	GPR17	33	hsa-miR-642a-5p	Down	TMEM132A	6	CEBPB
Down	POU5F1	17	hsa-miR-6734-3p	Down	CNTNAP3	5	KLF5
Down	SOX15	2	hsa-miR-520c-3p	Down	SOX15	4	JUN
Down	LLCFC1	1	hsa-miR-27a-3p	Down	NCAPG	2	TFAP2C

Table 6 Drug- hub gene topology table

Regulations	Gene	Degree	Drug (One Example)
Up	GABRE	76	Lormetazepam
Up	F10	70	Lonoctocog alfa
Up	MET	34	Capmatinib
Up	PDGFRB	28	Becaplermin
Up	GRIA1	19	Perampanel
Up	MMP2	17	Incyclinide
Up	SERPINE1	12	Troglitazone
Up	GLRB	11	Thiocolchicoside
Up	GLO1	10	Baicalein
Up	FGF2	9	Sucralfate
Up	NT5E	9	Quemliclustat
Up	EDNRB	9	Sitaxentan
Up	F3	7	Tisotumabvedotin
Up	FN1	6	Ocriplasmin
Up	COL1A1	6	Vonicog alfa
Up	CCND1	6	Navitoclax
Up	LDHB	5	Oxamic Acid

Up	MMP14	5	Marimastat
Up	SELENOP	4	Zinc chloride
Up	ASS1	4	Arginine
Up	RPL23A	4	Puromycin
Up	CCL2	4	Mimosine
Up	SERPINB2	3	Urokinase
Up	KRT10	3	Zinc acetate
Up	DDR2	3	Imatinib
Up	PTGIS	3	Phenylbutazone
Up	EPAS1	3	Vadadustat
Up	S100A16	3	Calcium phosphate dihydrate
Up	MGST1	2	Glutathione
Up	HSPG2	2	Palifermin
Up	SLC1A1	2	Aspartic acid
Up	TMEM97	2	Roluperidone
Up	ENPP1	2	Taribavirin
Up	GJA1	2	Carvedilol
Up	IGFBP3	2	Alitretinoin
Up	CXCL12	2	Tinzaparin
Up	L1CAM	1	Ethanol
Up	MSMO1	1	NADH
Up	DCLK1	1	Fostamatinib
Up	COL1A2	1	PR-15
Up	PAPPA	1	Phenethyl Isothiocyanate
Up	UCHL1	1	Phenethyl Isothiocyanate
Down	GABRG2	86	Medazepam
Down	DRD4	40	Cabergoline
Down	GRIN2B	39	Taurine
Down	CHRNB2	26	Physostigmine
Down	TF	17	Ferrous succinate
Down	PLG	16	Alteplase
Down	ACTA1	13	Kabiramide C
Down	PDE4C	12	Roflumilast
Down	SCN2B	8	Brivaracetam
Down	PRKCG	7	Staurosporine
Down	ABCC9	6	Glimepiride
Down	KCNQ4	5	Ezogabine
Down	PKLR	4	2-Phosphoglycolic Acid
Down	P2RY4	3	Uridine 5'-triphosphate
Down	MLNR	3	Erythromycin
Down	GPR17	3	Uridine diphosphate glucose
Down	HRNR	2	Zinc
Down	GAD1	2	Pyridoxal phosphat

Down	POLE2	2	Brincidofovir
Down	ABCB11	2	Glyburide
Down	DCLK3	1	Fostamatinib
Down	AMHR2	1	ATP

Table 7. Novel biomarkers for ALS

Regulation	Novel biomarkers
Up regulated genes	COL1A2, GREM1, DCN, STC2, COL12A1, THBS2, TNFRSF11B, COL1A1, COL8A1, CCN1, COL3A1, SVEP1, PRELP, CDH11, LUM, KIRREL1, THY1, TNC, ITGA11, SULF1, FN1, PAPPA, LAMA4, PSG5, TENM2, KCNK2, SOD3, FBLN1, EFEMP1, FST, AMOTL2, LAMB1, ANTXR1, COL16A1, HAS2, SNAI2, SLIT3, FLRT2, ABI3BP, STC1, COL11A1, PRRX1, SRPX2, DKK1, IL13RA2, GRIA1, FGF5, ATP8B1, CDH13, CACNA2D1, HSPB7, GFRA1, CREB3L1, PTGIS, OSR2, CLDN11, BMPER, TWIST2, TEAD1, ADAMTS12, ASS1, CEMIP, TWIST1, SLIT2, EMX2, BRINP1, CSPG4, ELN, POSTN, COL6A1, GPR176, NUPR1, NFASC, FHOD3, LRIG3, SSTR1, DKK2, ROBO2, GLRB, F3, FGF7, OSR1, PTPN14, TFAP2C, JPH2, F10, HOXC6, NR2F2, CHST3, COMP, TENM3, PDLIM4, CPE, TBX3, RARRES2, MFAP2, LSAMP, ZIC1, CCND1, PDPN, INSYN1, COL5A2, NFATC4, CCBE1, DZIP1, PCDH18, FAP, ALDH1A3, TAFA5, RSPO3, DCLK1, SIX2, SEMA3D, CD276, MFAP5, HOXC8, MGARP, MXRA8, FJX1, AKR1C2, NES, PLA2R1, HOXA11, CLMP, TBX5, DDR2, DKK3, NR2F1, FBN1, SIM1, TBX18, SERPINE2, GREB1L, SYDE1, NTF3, GPC1, FKBP10, CTHRC1, VSTM4, PLPPR4, COL5A1, FARP1, DDAH1, HSPB6, EMP2, GDF5, TBX15, BDKRB2, BICC1, SLC2A10, VASN, TUSC3, SLC1A1, TJP1, IGF2BP1, FRAS1, SHROOM3, SIX4, MET, GABRE, VIT, PARVA, SPRY4, FAT1, EML1, PXDN, PLPP3, ARNT2, MID1, HMCN1, JAM2, TMEM98, MAMDC2, HLA-DQB2, CLSTN2, SERPINE1, C1QTNF1, EDNRB, OGN, SIK1, PTX3, UPK3A, CHODL, ENAH, MMP14, TM4SF1, GPM6B, LMCD1, CD248, FERMT2, ADAMTS5, PMP22, HEYL, NCS1, BMP3, LRRN3, NT5E, TMEM126A, ENPP1, CXCL10, SERPINB2, GPR15, PDGFRB, SLC16A2, HSPG2, SMARCA1, PIERCE2, MYOM2, DACT1, STAC, MAL2, GPR183, CELA1, SEMA5A, CCR6, CD3G, CYP51A1, AKR1C3, PLA2G7, EPAS1, LOXL1, PRKACB, GPR161, ALPK2, DLC1, MACROD2, JCHAIN, LAMC1, MEOX1, FOSL1, COL15A1, WNT5B, DHCR24, NPR3, RSC1A1, RND3, CCDC80, TMEM47, MXRA5, FLNC, ITGBL1, LOXL4, MFAP4, ANGPTL2, CCN5, AHNAK2, DPT, GNG12, MRGPRF, RAB3B, PRSS12, FMN2, THSD4, STEAP2, GABBR2, LRRC15, CNTN3, S100A16, CSPG4, IGKV1D-17, LRIG3, SRPX, KCNJ6, JPH2, SYNC, GRIA3, ADGRL2, FBLIM1, C1QTNF5, FRMD6, ACKR4, KCNIP3, CAP2, STEAP1, EFS, MYRIP, KCNK15, ECM2, MPDZ, CAVIN1, RPL36A-HNRNPH2, ADGRL4, TRBV11-3, NALF2, LYPD6, SLC2A10, FBLN2, EVA1A, MAGI1, ENOX1, IGKV1D-8, EMP1, PLPP3, ADAMDEC1, TRDV3, PACSIN3, GPR85, TRDV2, TRBV13, IGKV1-37, EHD2, SV2B, TRBV7-7, SH3D19, IGHV4-28, TRAV12-2, PODN, COLEC12, EPB41L1, IGLV8-61, TRBV14, KLRB1, TRAV25, CEP55, IGKV1-9, MGST1, IGHV3-11, FBLN5, CERCAM, GAS1, COL6A3, TRAV24, KRT10, TRBV7-9, RGS1, IGKV5-2, TRAV29DV5, TSPAN13, FPR3, IGHV3-21, TRBV12-5, TRBV7-2, GLO1, TMEM97, MSMO1, IGHV4-30-2, HSPA13, TRAV1-2, TRAV10 and IGHV1-2
Down regulated genes	RNU5A-1, RNU5B-1, RNU5E-1, SNORA67, RNU4ATAC, SNORA44, SNORD14C, SNORA22, SNORD46, SNORA71C, SNORA47, SNORA60, SNORA3A, SNORD67, SNORA64, SNORA24, SNORD89, SNORA10, SNORD118, SNORA20, RNU6ATAC, SNORA26, SNORA61, SNORD55, SNORD104, SNORA14B, SNORA22C, RNU12, SNORA78, SCARNA20, SNORA37, SNORD99, SNORA52, SCARNA22, SNORD57, SNORA77B, SNORD21, RNU4-1, SNORD8, RNU2-1, SNORD13, SNORA68, SNORD110, SNORA79B, SNORA38, SNORD105B, PPIAL4G, SNORA38B, SNORD95, SNORA80D, SNORA9, RNU1-1, RNU4-2, RNU6-7, SNORA50B, RNVU1-7, SNORA49, SNORD100, SNORD116-15, SNORD9, SNORA65, SNORA71A, SNORD56, SNORD116-17, SNORA66, SCARNA3, SNORA84, RNVU1-28, SNORD14D, SNORA40B, SCARNA21, SNORA80E, SNORD35A, SNORA8, SNORD14A, SCARNA18, SNORA12, SNORD117, SNORA33, SNORA2C, SNORA71E, SNORA7B, SNORA74B, SNORA71D, SNORD97, SNORA57, SNORA13, SNORA2A, SNORA7A, SNORA21, SNORD116-16, SNORD94, SNORD10, SNORA80B, SNORA48, SNORA73B, SNORA73A, SNORD116-2, RNVU1-31, SCARNA1, SNORD116-3, SNORA23, SNORA11B, SNORA46, MND1, RMRP, SNORD88C, SNORA80A, SNORD116-22, SNORD41, SNORA14A, MT-ND3, SNORD71, SNORA54, SNORA5A, HNRNPA1L2, RNF225, RNVU1-4, MT-ATP8, TMEM132A, RPPH1, RNU5F-1, B4GALNT2, SNORA11F, H1-7, SNORA3B, ZFPM2, ACTN2, RNVU1-26, RNVU1-15, SNORA31, IHO1, RNVU1-2A, PTPRT, EPHA10, RAB40AL, IHH, RNVU1-2, FOXD4L3, RNVU1-27, FBXO39, PRODH, ZSCAN10, AMHR2, A3GALT2, TCP10L, MGAT4C, SNORA50C, PAPPA2, SLC39A5, TDRD6, MT-ND1, SLC3A1, GRIN2C, SPDYE2, MT-ATP6, MT-ND6, SCARNA7, MT-ND4, MT-ND2, MT-ND4L, CYP4F8, SCARNA5, RNVU1-6, SCARNA17, SLC28A2, ASPG, UBQLN3, RPL3L, CNDP1, SGK2, DCLK3, FGF22, CARD14, NTRK3, MT-ND5, PAX2, PKLR, HSD17B1, TAF11L5, OVCH1, ADAMTS2, SOX15, MMP21, GRK7, SNORA74A, POLE2, H1-6, SCARNA6, TBX1, IFNL1, POU5F1, ZDHHC19, B3GNT4, PPM1E, SLC8A2, TF, ADAM20, RNVU1-33, ESRP1, CDC25C, PPIAL4H, ABHD16B, SCARNA10, SLC22A13, FOXD4L4, ST8SIA5, NKX6-3, SCARNA2, FOXD4L6, HUS1B, NEU4, TENT5B, POLR3G, GALNTL6, KASH5, PPIAL4E, NANOS3, ENPP7, TRIM50, NME9, SNORA5C, FN3K, SPIN2A, SLC25A2, ABCB11, ANKRD2, TAF11L2, RBFOX3, DRD4, ATP5MGL, BCO2, RNA5S1, RCCD1, RP1L1, KRT74, PCLO, TCHH, RSPH10B, AQP7, ACTA1, KRTAP10-3, CEP295NL, KRTAP16-1, NPHP3-ACAD11, CFAP157, KRTAP10-2, RAPSN, GRIN2B, KRTAP5-9, SNTG2, TUBAL3, NCAPG, H3-5, DNAI7, FOXD4L4, NKX6-3, SAXO1, EYS, DOC2A, ANKRD2, SLC9A4, GABRG2, SLC13A5, SLC6A15, AQP7, SLC28A1, TTYH1, MT-CO2, SLC10A4, KCNS1, SLC4A9, SLC5A11, ASIC1, ABCC11, KCNQ4, SCN2B, NHERF4, SLC22A1, TRPV6, OR52H1, OR2L3,

PCLO, TAS2R41, OR52B2, OR4F17, OR5B21, OR2L8, ESPNL, RCVRN, OR52K2, OR2L2, GRK7, OR2T11, OR5AN1, OR2B6, TAS2R3, OR56A4, TAS2R30 and STRC